

Aus dem Neurologischen Institut (Edinger-Institut),  
Frankfurt am Main

**Angiopoietin-2 induced blood-brain barrier compromise  
and increased stroke size is rescued by targeting  
vascular endothelial protein tyrosine phosphatase**

Dissertation  
zur Erlangung des Doktorgrades  
der Naturwissenschaften

vorgelegt beim Fachbereich der Biowissenschaften  
der Johann Wolfgang Goethe-Universität  
in Frankfurt am Main

von Stefanie Gurnik  
aus Nürnberg

Frankfurt am Main, 2015  
(D30)



Vom Fachbereich Biowissenschaften der  
Johann Wolfgang Goethe-Universität als Dissertation angenommen.

Dekan:.....  
(Prof. Dr. M. Piepenbring)

Gutachter:.....  
(Prof. Dr. A. Starzinski-Powitz)

.....  
(Prof. Dr. K.H. Plate)

Datum der Disputation:.....

**TABLE OF CONTENTS**

<b>LIST OF FIGURES</b>	<b>7</b>
<b>LIST OF TABLES</b>	<b>8</b>
<b>ABBREVIATION</b>	<b>9</b>
<b>SUMMARY</b>	<b>13</b>
<b>ZUSAMMENFASSUNG</b>	<b>16</b>
<b>1. INTRODUCTION</b>	<b>22</b>
<b>1.1 The blood-brain barrier (BBB)</b>	<b>23</b>
1.1.1 Endothelial cells – component of the NVU	24
1.1.2 Other components of the NVU	27
1.1.3 Regulation of the BBB by Wnt / $\beta$ -Catenin and Sonic Hedgehog signaling	29
<b>1.2 Angiogenesis / Vasculogenesis</b>	<b>30</b>
<b>1.3 The Angiopoietin / Tie signaling pathway</b>	<b>32</b>
1.3.1 The tyrosine kinase receptors Tie1 and Tie2	32
1.3.2 Angiopoietins	33
1.3.3 Regulation of Angiopoietin expression	35
1.3.4 Activation of Tie2 receptors	36
1.3.5 Tie2 downstream signaling	36
1.3.6 Tie receptor independent pathways for Angiopoietins	39
<b>1.4 Breakdown of the BBB in correlation to diseases</b>	<b>39</b>
1.4.1 BBB dysfunction in ischemic stroke	41
1.4.2 Angiopoietins in BBB maintenance and breakdown	44
<b>1.5 Aim of the study</b>	<b>44</b>
<b>2. METHODS</b>	<b>46</b>
<b>2.1 Animals</b>	<b>46</b>
2.1.1 Breeding	46
2.1.2 Genotyping	46
2.1.3 Collection of blood serum and enzyme-linked immunosorbent assay (ELISA)	48
2.1.4 Anesthesia	48
2.1.5 Perfusion	48
<b>2.2 Isolation of mouse brain microvascular endothelial cells (MBMECs)</b>	<b>48</b>
<b>2.3 Isolation of mouse brain microvessels (MBMVs)</b>	<b>49</b>
<b>2.4 Culture of mammalian cells</b>	<b>49</b>
2.4.1 Freezing and thawing of mammalian cells	49
2.4.2 Cell counting using a hemacytometer	50
2.4.3 Transendothelial electrical resistance (TEER) measurement	50
2.4.4 <i>In vitro</i> permeability assay	50
<b>2.5 <i>In vivo</i> studies / animal models</b>	<b>51</b>
2.5.1 Permeability assay using small tracers	51
2.5.2 Permeability assay using Evans Blue	52
2.5.3 Electron microscopy (EM)	52
2.5.4 Staining of the glycocalyx	52
2.5.5 Animal models for ischemic stroke	53

---

2.5.5.1 Permanent stroke model	53
2.5.5.2 Transient stroke model	53
2.5.6 VE-PTP treatment	54
<b>2.6 RNA isolation and analysis</b>	<b>54</b>
2.6.1 RNA isolation	54
2.6.2 Determination of RNA concentration (Experion)	54
2.6.3 Determination of RNA concentration (Photometer)	55
2.6.4 cDNA synthesis	55
2.6.5 Quantitative Real Time PCR (qPCR)	56
<b>2.7 Protein analysis</b>	<b>57</b>
2.7.1 Protein extraction from cultured cells	57
2.7.2 Protein extraction from tissues	57
2.7.3 Determination of protein concentration	57
2.7.4 Protein solubilization and denaturation	58
2.7.5 Immunoblotting	58
2.7.5.1 SDS – polyacrylamide gel electrophoresis (PAGE)	58
2.7.5.2 Protein blotting	58
2.7.5.3 Immunodetection of blotted proteins	59
<b>2.8 Histology procedures</b>	<b>59</b>
2.8.1 Tissue embedding and sectioning	59
2.8.2 Staining procedures	60
2.8.2.1 Giemsa staining	60
2.8.2.2 Light microscopic staining	60
2.8.2.3 Immunofluorescence staining (desmin, aquaporin-4)	60
2.8.2.4 Immunofluorescence staining (VE-Cadherin, ZO-1, Claudin-5)	61
2.8.3 Slide preparation for tissues with water soluble tracers (Evans Blue)	61
2.8.4 Image acquisition and analysis	61
<b>2.9 FACS (Fluorescence activated cell sorting)</b>	<b>61</b>
<b>2.10 Contribution of Collaborators</b>	<b>62</b>
<b>2.11 Statistical analysis</b>	<b>62</b>
<b>3. RESULTS</b>	<b>63</b>
<b>3.1 Determination of hAng-2 expression in transgenic mice</b>	<b>63</b>
3.1.1 Ang-2 DT mice overexpress hAng-2 in a doxycycline regulated manner	63
3.1.2 Mouse brain microvessels of Ang-2 DT mice express high levels of Ang-2	64
<b>3.2 Ang-2 is associated with increased permeability of brain microvessels <i>in vitro</i> and <i>in vivo</i></b>	<b>65</b>
3.2.1 Increase in permeability of MBMECs with hAng-2 treatment and in mice overexpressing Ang-2	65
3.2.2 Ang-2 overexpression increases brain permeability to small tracers <i>in vivo</i>	67
<b>3.3 Ang-2 modifies components of the neurovascular unit</b>	<b>68</b>
3.3.1 Overexpression of Ang-2 leads to loss of pericytes in the brain	69
3.3.2 Ultrastructural analyses reveal permeability features in Ang-2 DT mice	70
3.3.3 The expression of junctional molecules and components of the transcytotic pathway are modified by the overexpression of Ang-2	72
3.3.4 Number of infiltrating macrophages increases in Ang-2 DT mice	73
3.3.5 Ang-2 mediated brain permeability does not result in gross edema formation	74
<b>3.4 Continuous Ang-2 expression does not interfere with intrinsic Ang-1 levels</b>	<b>75</b>

---

<b>3.5 Tightening of the BBB upon long-term overexpression in Ang-2 DT mice</b>	<b>76</b>
<b>3.6 Ang-2 overexpression leads to increased stroke sizes and increased permeability in infarct areas, effects partly reversed in therapeutic treatments targeting the Tie2 signaling pathway</b>	<b>77</b>
3.6.1 Ang-2 levels correlate with stroke stages in human patients	77
3.6.2 Overexpression of Ang-2 results in increased infarct size and permeability	78
3.6.3 Therapeutics activating Tie2 signaling show improved outcome in infarct sizes and brain permeability	79
<b>4. DISCUSSION</b>	<b>84</b>
<b>4.1 Ang-2 increases the permeability of brain endothelial cells <i>in vitro</i></b>	<b>84</b>
<b>4.2 Modifications of the neurovascular unit mediated by Ang-2</b>	<b>86</b>
<b>4.3 Inflammatory response due to Ang-2 mediated permeability</b>	<b>88</b>
<b>4.4 Angiopoietins and Wnt / Sonic hedgehog pathways</b>	<b>89</b>
<b>4.5 The impact of Ang-2 in pathophysiology</b>	<b>90</b>
<b>4.6 Therapeutic targeting of Tie2 signaling in stroke</b>	<b>90</b>
<b>4.7 A potential role of Ang-2 in aging</b>	<b>92</b>
<b>4.8 Conclusion and perspectives</b>	<b>93</b>
<b>5. REFERENCES</b>	<b>97</b>
<b>6. APPENDIX</b>	<b>116</b>
<b>6.1 Instruments</b>	<b>116</b>
<b>6.2 Reagents</b>	<b>117</b>
<b>6.3 Buffers and solutions</b>	<b>119</b>
6.3.1 Medium for cell culture	119
6.3.2 Agarose gel electrophoresis	119
6.3.3 Buffers for MBMVs	120
6.3.4 Buffers for MBMECs	122
6.3.5 Buffers and solutions for SDS PAGE	122
6.3.6 Buffers for Immunohistochemistry	124
<b>6.4 Primers</b>	<b>126</b>
6.4.1 Primers for PCR	126
6.4.2 Primers for qPCR	126
<b>6.5 Antibodies</b>	<b>127</b>
6.5.1 Primary antibodies	127
6.5.2 Secondary antibodies	128
<b>6.6 Recombinant proteins</b>	<b>128</b>
<b>6.7 Kits</b>	<b>129</b>
<b>6.8 Software</b>	<b>129</b>
<b>DANKSAGUNG</b>	<b>130</b>
<b>ERKLÄRUNG</b>	<b>132</b>
<b>CURRICULUM VITAE</b>	<b>133</b>

---

**LIST OF FIGURES**

Figure 1-1: The neurovascular unit (NVU) (Obermeier et al., 2013)	24
Figure 1-2: Composition of junction proteins in endothelial cells of the NVU (Abbott et al., 2006)	25
Figure 1-3: The canonical Wnt / $\beta$ -Catenin pathway (Nusse, 2005)	30
Figure 1-4: Angiogenesis (modified from Heinke et al., 2012)	31
Figure 1-5: Structures of the tyrosine kinase receptors Tie1 and Tie2 and its ligands Ang-1 and Ang-2 (Augustin et al., 2009)	34
Figure 1-6: Tie2 downstream signaling for maintaining endothelial quiescence (Thomas and Augustin, 2009)	37
Figure 1-7: The BBB in health and disease (Daneman and Prat, 2015)	40
Figure 1-8: The BBB permeability and cerebral blood flow during ischemia and reperfusion (Sandoval and Witt, 2008)	42
Figure 3-1: Doxycycline based Ang-2 expression	64
Figure 3-2: Overexpression of hAng-2 was verified in Ang-2 DT mice	65
Figure 3-3: Ang-2 mediated decrease in brain endothelial resistance	66
Figure 3-4: Lucifer Yellow (0.45 kD) crosses the brain endothelium of Ang-2 DT mice	68
Figure 3-5: Ang-2 overexpressing mice possess decreased number of pericytes in brain sections	69
Figure 3-6: Ultrastructural analysis demonstrate permeability features in Ang-2 DT mice	71
Figure 3-7: Junction proteins and a transcellular transport protein show different expression level in Ang-2 DT mice	73
Figure 3-8: Macrophages and myeloid derived suppressor cells infiltrate into brain tissue of Ang-2 DT mice	74
Figure 3-9: No edema formation in mice overexpressing Ang-2	74
Figure 3-10: No compensatory effect of endogenous Ang-1 detectable in Ang-2 DT mice	75
Figure 3-11: Tightening effect of the BBB in 6-12 months old Ang-2 DT mice	76
Figure 3-12: Ang-2 expression increases in higher stroke grades	78
Figure 3-13: Stroke size and permeability increase in Ang-2 DT mice subjected to permanent MCAO	79
Figure 3-14: The VE-PTP Inhibitor induces the activation of the Tie2 signaling pathway and decreases pVE-Cadherin in vitro	80
Figure 3-15: The VE-PTP Inhibitor decreases stroke volumes and permeability in WT CD1 mice 24 h after occlusion	82
Figure 3-16: The inhibitor of VE-PTP induces the Akt and Tie2 activation also in vivo	83
Figure 4-1: The influence of Ang-2 on brain permeability	96

## LIST OF TABLES

Table 2-1: Reaction mixture for PCR	47
Table 2-2: PCR program	47
Table 2-3: Wavelengths of different tracers	51
Table 2-4: The reaction mixture for reverse transcription	55
Table 2-5: The reaction mixture for qPCR	56
Table 2-6: qPCR program	56
Table 6-1: MCDB131 medium	119
Table 6-2: Ingredients for TBE buffer (10 x)	119
Table 6-3: Preparation of Blue Juice (5 x)	120
Table 6-4: Tail lysis buffer (pH 8.0)	120
Table 6-5: MVB buffer (1 x; pH 7.4)	120
Table 6-6: Salt Solution (10 x)	121
Table 6-7: HES buffer	121
Table 6-8: PBS for 25 % BSA	121
Table 6-9: Buffer A (pH 7.4)	122
Table 6-10: Final concentration of UREA / SDS buffer used for Western Blot analysis	122
Table 6-11: 4x Tris-CI Upper buffer (pH 6.8)	122
Table 6-12: 4x Tris-CI Lower buffer (pH 8.8)	123
Table 6-13: Running buffer (10 x)	123
Table 6-14: Transfer buffer (10 x)	123
Table 6-15: TBS (20 x; pH 7.6-7.7)	124
Table 6-16: Ingredients for stacking and separating gels	124
Table 6-17: 4 % Paraformaldehyde in PBS (pH 7.4)	124
Table 6-18: PBS (20 x)	125
Table 6-19: PBSA solution (pH 7.5):	125
Table 6-20: Antibody incubation buffer (pH 7.2)	125
Table 6-21: Permeabilization / blocking buffer (pH 7.4-7.6):	126
Table 6-22: Primers used for qPCR analysis	126
Table 6-23: Antibodies for immunohistochemical analysis	127
Table 6-24: Antibodies for Western Blot analysis	127
Table 6-25: Antibodies for FACS analysis	128
Table 6-26: Secondary antibodies	128
Table 6-27: Kits used during this study	129
Table 6-28: Softwares which were used for analysis and quantitation	129



**ABBREVIATION**

°C	degree Celsius
AD	Alzheimer's disease
AEF	astrocytic endfeet
Ang-1 / -2	Angiopoietin-1 / -2
Ang-2 DT	Angiopoietin-2 double transgenic
APC	adenomatous polyposis coli
ATP	adenosine triphosphate
BBB	blood-brain barrier
BCA	bicinchoninic acid
bEND	brain endothelioma
BL	basal lamina
BSA	bovine serum albumin
cDNA	complementary desoxyribonucleic acid
CNS	central nervous system
DAPI	4',6-diamidino-2-phenylindole
DEPC	diethylpyrocarbonate
dH <sub>2</sub> O	distilled water
ddH <sub>2</sub> O	double distilled water
DMSO	dimethyl sulfoxide
DNA	desoxyribonucleic acid
Dok	docking protein
Dox	doxycycline
Dsh	Dishevelled
EC	endothelial cell
ECGS	endothelial cell growth supplement
ECL	enhanced chemoluminescence
EDTA	ethylene-diamine-tetra-acetic acid
EGF	endothelial growth factor
ELISA	enzyme-linked immunosorbent assay
EM	electron microscopy

eNOS	endothelial nitric oxide synthase
ERK	extracellular signal-regulated kinases 1/2
FACS	fluorescence activated cell sorting
FAK	focal adhesion kinase
FBS	fetal bovine serum
FKHR	forkhead transcription factor Foxo1
g	gramm
GAGs	glucosaminoglycans
Glut-1	glucose transporter-1
Gr-1	granulocyte antigen-1
GRB2	growth factor receptor-bound protein 2
GSK	glycogen synthase kinase
h	hour(s)
HB-EGF	heparin binding EGF-like growth factor
HBSS	Hank's balanced salt solution
H&E	hematoxylin and eosin
HRP	horseradish peroxidase
HSCs	hematopoietic stem cells
ICAM-1	intercellular adhesion molecule-1
IgG	immunoglobulin G
IHC	immunohistochemistry
JAMs	junction adhesion molecules
kD	kilo Dalton
kg	kilogramm
KLF-2	kruppel-like factor 2
l	liter
LAM	leukocyte adhesion molecule
LY	Lucifer Yellow
MBMECs	mouse brain microvascular endothelial cells
MBMVs	mouse brain microvessels
MCA	middle cerebral artery
MCAO	middle cerebral artery occlusion

mDia	mammalian diaphanous
MDSC	myeloid derived suppressor cells
mg	milligramm
MHC	major histocompatibility complex
min	minute(s)
ml	milliliter
mM	millimolar
MMPs	matrix metalloproteinases
mRNA	messenger ribonucleic acid
µg	mikrogramm
µl	mikroliter
µM	mikromolar
NF-κB	nuclear factor kappa B
nm	nanometer
NVU	neurovascular unit
ON	over night
PBS	phosphate buffered saline
PC	pericyte
PCR	polymerase chain reaction
PDGF	platelet-derived growth factor
PFA	paraformaldehyde
pH	pondus Hydrogenii
PI3K	phosphatidylinositol-3-OH kinase
PVDF	polyvinylidene difluoride
qPCR	quantitative polymerase chain reaction
RBCs	red blood cells
RNA	ribonucleic acid
ROS	reactive oxygen species
RT	room temperature
RFUs	relative fluorescence units
sec	seconds
SDS	sodium dodecyl sulfate

SDS-PAGE	sodium dodecyl sulfate polyacrylamide gel electrophoresis
SEM	standard error of the mean
SHH	sonic hedgehog
SFM	serum-free medium
SMC	smooth muscle cell
SMO	smoothened
TCF	T-cell factor
TEER	transendothelial electrical resistance
TGF	transforming growth factor
Tie2	tyrosine kinase with immunoglobulin and epidermal growth factor homology receptor 2
TMR	tetramethylrhodamine
TNF	tumor necrosis factor
tTA	tetracycline-controlled transactivator
TTC	triphenyl tetrazolium chloride
TXR	TexasRed
V	voltage
VCAM-1	vascular cell adhesion molecule-1
VE-Cadherin	vascular endothelial Cadherin
VEGF	vascular endothelial growth factor
VE-PTP	vascular endothelial protein tyrosine phosphatase
WT	wild type
ZNS	Zentrales Nervensystem
ZO	zona occludens

## SUMMARY

The brain vascular system is composed of specialized endothelial cells, which regulate the movement of ions, molecules and cells from the blood lumen to the central nervous system (CNS). Endothelial cells in the brain form the blood-brain barrier (BBB) that is essential to maintain the brain homeostasis and protect the CNS from pathogens and toxins for a proper neurological function. Endothelium together with other cellular components such as pericytes, astrocytes and the basement membrane, forms the neurovascular unit (NVU), the structural unit of the BBB. Breakdown of the BBB occurs in various neurological disorders, leading to edema and neuronal damage. Therapeutic strategies focusing on factors that regulate the permeability of the BBB may help to improve neurological disorders and facilitate drug delivery to the brain.

Angiopoietins (Ang) are potential candidates for therapeutic targeting the BBB due to their role in regulating the vascular permeability in periphery. They are key growth factors that control angiogenesis and vessel maturation. Ang-1 and Ang-2 possess similar binding affinities to the Tie2 receptor tyrosine kinase, which is almost exclusively expressed on endothelial cells. Ang-1 is expressed in smooth muscle cells and pericytes, and binds in a paracrine manner to Tie2. This results in phosphorylation of the receptor and induction of downstream signaling pathways leading to vessel maturation via pericyte recruitment and blood vessel stabilization. Ang-2, on the other hand, is stored in Weibel-Palade bodies in endothelial cells and is released upon inflammatory or angiogenic stimuli. Therefore, in mature, stabilized blood vessels, Ang-2 expression is low. Increased level of Ang-2 is only observed during development or in pathology such as ischemia, cancer and inflammation. When Ang-2 is released, it acts in an autocrine manner and interferes with Tie2 phosphorylation in a context-dependent way. Antagonizing the receptor results in de-stabilization of the vessels, often accompanied by reduced numbers of pericytes leading to myeloid cell infiltration. In conjunction with the vascular endothelial growth factor (VEGF), Ang-2 contributes to blood vessel sprouting, whereupon in absence of VEGF it promotes vessel regression.

While Ang-1 has been reported to prevent vascular leakage, Ang-2 has been shown to increase vascular permeability in non-brain endothelial cells *in vitro* and *in vivo*. However, the role of Ang-2 / Tie2 signaling on BBB remains unclear. Furthermore, it has been demonstrated that pericytes regulate the BBB integrity, which collectively suggests a possible role of Ang-2 on modulating BBB properties. Therefore, it was hypothesized

that Ang-2 induces breakdown of the BBB accompanied by increased permeability in the brain. As high Ang-2 levels correlate with neuro-pathological disorders that are associated with the dysfunction of the BBB, the impact of Ang-2 under pathological conditions was investigated.

To evaluate the role of Ang-2 on permeability of BBB endothelium, a gain-of-function mouse model with the tetracycline-controlled (Tet-Off) gene expression system was used. This model is based on withdrawal of doxycycline induced endothelial cell-specific expression of Ang-2 driven by a Tie-1 promoter. In transendothelial electrical resistance (TEER) measurements on primary cultures of mouse brain microvascular endothelial cells (MBMECs) isolated from wild type and transgenic mice, a decrease in TEER and increase in permeability upon Ang-2 treatment was observed. This was confirmed by *in vitro* experiments with different molecular weight tracers. *In vivo* analysis with Ang-2 overexpressing mice resulted in increased permeability to a low molecular (0.45 kD Lucifer Yellow) but not to a high molecular weight tracer (70 kD Evans blue which binds to albumin) indicating a size-dependent permeability mediated by Ang-2. This permeability effect *in vivo* is based on decrease of junctional proteins identified by Western Blot analysis (Claudin-5, VE-Cadherin) that was confirmed in ultrastructural levels with defective inter-endothelial junctions. Moreover, immunohistochemistry revealed a reduction of pericytes in brain microvessels that was supported by degenerating pericytes shown by EM in Ang-2 transgenic animals. In addition to that images at ultrastructural level showed signs of swollen astrocytic endfeet with increased numbers of vesicles in endothelial cells that is apparently mediated by decreased numbers of pericytes. Furthermore, an increase of infiltrating macrophages in brain samples of mutants was observed. Similar phenotypes have been reported in pathologies in correlation with BBB breakdown. These results altogether demonstrate that increased Ang-2 levels lead to dysfunction of the BBB.

It has previously been shown that Ang-2 is upregulated in pathological disorders of the brain such as stroke, which was validated in the current study using samples from human stroke patients. These patients revealed increased Ang-2 levels in the brain vasculature as well as in blood serum. Moreover, increased permeability and enlarged stroke sizes were observed in a permanent middle cerebral artery occlusion (MCAO) model of mice overexpressing Ang-2 suggesting Ang-2 as a risk factor for stroke.

As Ang-2 increased endothelial permeability in the brain potentially by blocking Ang1 / Tie2 signaling, as this is the instance in peripheral blood vessels, it was investigated if restoring the Tie2 receptor activation could alleviate the stroke phenotype caused by increased Ang-2 levels in a pre-clinical mouse stroke model (transient MCAO). Vascular endothelial protein tyrosine phosphatase (VE-PTP) regulates the activation of the Tie2 receptor. It is also associated with the adherens junction molecule VE-Cadherin, regulating its activity. In this study it was shown that a VE-PTP inhibitor, resulted in a significant activation of Tie2 and the downstream kinase Akt in isolated MBMECs and bEnd5 cells. Additionally, there was a trend towards a decrease in phosphorylation of VE-Cadherin, which essentially indicates a tightening of blood vessels. Based on this, it was investigated whether the VE-PTP inhibitor could alleviate the stroke pathology in a transient MCAO model. A treatment with the inhibitor before and after the induction of transient stroke resulted in decreased infarct sizes and an improved post-stroke behavior. Furthermore, the endothelial permeability of treated mice demonstrated with IgG staining was lower compared to control groups, indicating improved barrier properties with VE-PTP inhibitor treatment.

In conclusion, these findings demonstrate that Ang-2 increases permeability of the BBB by downregulating endothelial junction proteins, allowing the transfer of molecules by paracellular transport. In addition, it increases the vesicle-mediated transcellular transport. The BBB breakdown caused by increased levels of Ang-2 exacerbated the stroke symptoms, which was partially rescued by therapeutic activation of the Tie2 pathway, suggesting that Angiotensin / Tie2 signaling axis may play a key role in modulating the BBB integrity.

Taken together, Angiotensins appear to be essential regulators of the BBB and seem to be potential therapeutic targets for neurological disorders that are accompanied by a compromised BBB.

A scientific manuscript entitled “Angiotensin-2 increases vascular permeability at the blood-brain barrier” has been submitted in January 2015 and was re-submitted as “Angiotensin-2 induced blood-brain barrier compromise and increased stroke size is rescued by targeting vascular endothelial protein tyrosine phosphatase” in May 2015.

## ZUSAMMENFASSUNG

Das vaskuläre System des Gehirns besteht aus Endothelzellen, die den Transport von Ionen, Molekülen und verschiedenen zellulären Komponenten vom Lumen der Blutgefäße zum zentralen Nervensystem (ZNS) regulieren. Endothelzellen im Gehirn besitzen im Vergleich zu peripheren Endothelzellen mehr Verbindungsproteine, die deren Zell-Zell Kontakt verstärken. Zusammen mit anderen zellulären Bestandteilen, wie Perizyten, Astrozyten, Basallamina und Neuronen formen sie die neurovaskuläre Einheit (neurovascular unit, NVU), die zur Barriereeigenschaft der Blut-Hirn-Schranke beiträgt. Sie ist essentiell, um die Homöostase im Gehirn aufrechtzuerhalten, das ZNS vor Pathogenen und Toxinen zu schützen und die neurologische Aktivität zu bewahren. Die Beschädigung der Blut-Hirn-Schranke tritt in verschiedenen neurologischen Krankheiten auf, die zur Ödembildung führen können und die neuronale Aktivität zerstören. Dies führt zu phänotypischen Veränderungen der Endothelzellen mit verringerten Verbindungsmolekülen und einer erhöhten Anzahl an Leukozyten-Adhäsionsmolekülen, die die Infiltration von Leukozyten fördern. Damit assoziiert werden zusätzlich erhöhte Transzytose-Werte und veränderte Transportsysteme, die alle zusammen zur Degenerierung von Neuronen beitragen. Therapeutische Ansätze setzen daher auf Faktoren, die die Blut-Hirn-Schranke wieder verdichten, um neurologische Defekte zu verbessern, oder um die Medikamentenzufuhr ins Gehirn zu erleichtern, da ca. 98 % der Neuropharmaka nicht ohne Hilfsmittel die Barriere im Gehirn passieren können.

Angiopoietine (Ang) stellen potentielle Kandidaten zur therapeutischen Intervention dar, da sie die vaskuläre Permeabilität in peripheren Blutgefäßsystemen beeinflussen. Es ist bekannt, dass sie wichtige Faktoren in der Entwicklung der Angiogenese sind und darüber hinaus bei der Gefäßstabilisierung eine Rolle spielen. Ang-1 und Ang-2 besitzen eine sehr ähnliche Bindungsaffinität zu ihrem Rezeptor Tie2, der fast ausschließlich auf Endothelzellen exprimiert ist. Ang-1 ist auf glatten Muskelzellen und Perizyten lokalisiert und bindet auf parakrine Weise an den Rezeptor Tie2. Dies resultiert in der Phosphorylierung des Rezeptors und induziert dabei weitere Signalwege die zur Gefäßstabilisierung durch Verbindungsproteine beitragen und über Anlagerungen von Perizyten stabilisieren. Darüber hinaus wirkt Ang-1 anti-apoptotisch und anti-inflammatorisch. Ang-2 wiederum ist in Weibel-Palade bodies gespeichert, die sich in Endothelzellen befinden. Durch inflammatorische oder angiogene Stimuli wird Ang-2 schnell freigesetzt. Dadurch ist die Ang-2 Expression in gereiften, stabilisierten Gefäßen sehr gering und hohe Ang-2 Werte werden nur während der Entwicklung oder



Remodelierung von Blutgefäßen oder in der Pathologie erreicht, was mit erhöhten Inflammationsraten zusammenhängt. Wenn Ang-2 aus den Weibel-Palade bodies freigesetzt wird, wirkt es im Gegensatz zu Ang-1 auf autokrine Weise auf den Rezeptor und inhibiert dabei Tie2, was jedoch Kontext-abhängig ist. Das Inhibieren der Rezeptoraktivität führt zur Destabilisierung der Blutgefäße, bedingt durch die Reduzierung von Perizyten, was die myeloide Zellinfiltration fördert. Zusammen mit dem vaskulären endothelalem Wachstumsfaktor (VEGF) induziert Ang-2 das Wachstum von Blutgefäßen, wobei es die Rückbildung der Blutgefäße fördert, wenn VEGF nicht präsent ist.

Während Ang-1 das Blutgefäßsystem vor Permeabilität schützt, konnte mit Ang-2 gezeigt werden, dass es die vaskuläre Permeabilität *in vitro* und *in vivo* in peripheren Endothelzellen erhöht. Jedoch bleibt die Rolle des Ang-2 / Tie2 Signalweges in der Blut-Hirn-Schranke mit seinen speziellen Endothelzellen unklar. Darüber hinaus zeigten Studien, dass Perizyten den Zusammenhalt der Blut-Hirn-Schranke regulieren, während Ang-2 mit der Reduzierung von Perizyten assoziiert wird. In diesem Zusammenhang liegt die Vermutung nahe, dass Ang-2 die Blut-Hirn-Schranke beeinflusst. Daher wurde zu Beginn dieser Arbeit die Hypothese aufgestellt, dass Ang-2 zu einer Beschädigung der Blut-Hirn-Schranke führt, die mit erhöhter Permeabilität im Gehirn assoziiert wird. Da erhöhte Ang-2 Werte mit neuro-pathologischen Bedingungen in Verbindung stehen, die zu einer Beschädigung der Blut-Hirn-Schranke führen, wurde zusätzlich der Einfluss von Ang-2 auf pathologischer Ebene im Gehirn untersucht.

Um die Wirkung von Ang-2 auf die Permeabilität der speziellen Endothelzellen im Gehirn zu untersuchen, wurde ein Überexpressionsmodell (Gain-of-function) an Mäusen mit einem Tetrazyklin-kontrollierten (Tet-Off) Genexpressionssystem verwendet. Dieses System wurde schon erfolgreich im Hindlimb Modell an Mäusen und bei Untersuchungen von inflammatorischen Prozessen eingesetzt. In diesem Modell induziert das Absetzen von Doxyzyklin die endothel-spezifische Expression von Ang-2, welches vom Tie1 Promotor kontrolliert wird. Die Expression von Ang-2 wird bei Geburt der Mäuse induziert und erstreckt sich über einen Zeitraum von 8 bis 12 Wochen. Um im Rahmen dieser Studie sicherzustellen, dass eine Überexpression von Ang-2 erfolgte, wurde bereits vor den Versuchen Blut von den Tieren entnommen, was mit Hilfe eines antikörper-basierten Nachweisverfahrens (enzyme-linked immunosorbent assay, ELISA) überprüft wurde.

Innerhalb dieser Arbeit wurde die Permeabilität an der Blut-Hirn-Schranke der Ang-2 überexprimierenden Mäuse zunächst mit Hilfe von elektrischen Resistenzmessungen von primären mikrovaskulären Endothelzellen aus dem Gehirn untersucht (transendothelial electrical resistance, TEER), die aus Wildtypen und transgenen Mäusen isoliert wurden. Es stellte sich heraus, dass Ang-2 die Resistenz der Zellen verringerte und dabei die Permeabilität erhöhte. Ein ähnlich signifikantes Ergebnis konnte erzielt werden, als rekombinantes hAng-2 Protein für 24 Stunden zu den Wildtyp Zellen hinzugefügt wurde. Die erhöhte Permeabilität wurde zusätzlich durch fluoreszierende Tracer *in vitro* bestätigt. *In vivo* Studien ermittelten eine signifikant erhöhte Durchlässigkeit für kleine molekulare Tracer (0,45 kD Lucifer Yellow) in Ang-2 überexprimierenden Mäusen, während größere molekulare Tracer (70 kD Evans Blue, das an Albumin bindet) nicht die Blut-Hirn-Schranke passieren konnten. Da erhöhte Permeabilitätsraten in transgenen Mäusen detektiert wurden, konnten im nächsten Schritt die einzelnen Komponenten der NVU untersucht werden. Zunächst wurden die Verbindungsproteine zwischen den Endothelzellen überprüft. Obwohl immunhistochemische Färbungen keine erkennbaren strukturellen oder expressionsbasierten Unterschiede von den Tight- und Adhäsionsverbindungsmarkern VE-Cadherin, Claudin-5 oder ZO-1 erbrachte, zeigten Western Blot Analysen aus isolierten Mikrogefäßen von Ang-2 transgenen Mäusen eine Herunterregulierung von Claudin-5 und VE-Cadherin. qPCR Daten wiesen darüber hinaus eine starke Verminderung von Claudin-3 auf. Diese Veränderungen der Verbindungsproteine bestätigten sich auch auf ultrastruktureller Ebene. Elektronenmikroskopische Aufnahmen erbrachten Erkenntnisse über unterbrochene Zell-Zell Verbindungen zwischen den anliegenden Endothelzellen in transgenen Mäusen. Dies fördert den parazellulären Durchtritt zwischen den Endothelzellen.

Durch immunhistochemische Färbungen von Hirnproben in Ang-2 überexprimierenden Mäusen wurde eine verminderte Anzahl an Perizyten ermittelt, was mit zuvor publizierten Daten korreliert. Sie zeigten, dass Ang-2 in peripheren Blutgefäßsystemen für eine verminderte Anzahl an Perizyten verantwortlich ist. Dies bestätigte sich auch auf ultrastruktureller Ebene, die degenerierte Perizyten detektierte. Zusätzlich zeigten diese Aufnahmen Hinweise von Ödembildungen in Astrozyten mit erhöhter Anzahl an Vesikeln in Endothelzellen. Die erhöhte Menge an Vesikeln ist vermutlich durch die verringerte Anzahl an Perizyten zurückzuführen, die die Caveolae vermittelte Transzytose fördert, was in einer vorherigen Arbeit belegt wurde. Außerdem weist ein Protokoll zur Detektierung der negativ geladenen Glykokalyx eine von ca. 300 nm - 400 nm auf ca. 100 nm verkürzte und weniger verdichtete Glykokalyx in Ang-2 transgenen Mäusen auf.

Auch das kann zur erhöhten Permeabilität an der Blut-Hirn-Schranke beitragen. Einzelne Partikel des Färbemittels für die Glykokalyx konnten innerhalb der Endothelzellen und in der Basallamina detektiert werden, was wiederum auf transzellulären Transport durch das Endothel hinweist.

Eine eigene Publikation aus dem Jahr 2011 dokumentierte, dass Ang-2 die Infiltration von myeloiden Zellen aus dem Blut in das umliegende Gewebe fördert. Diese Untersuchung war auch Teil dieser Studie. In diesem Zusammenhang wurde festgestellt, dass eine erhöhte Menge von Makrophagen im Gehirn der Mutanten infiltriert sind, was durch Durchflusszytometrie ermittelt wurde. Ähnliche Phänotypen wurden im Zusammenhang mit der Beschädigung der Blut-Hirn-Schranke in pathologischen Modellen beschrieben. Diese Ergebnisse weisen darauf hin, dass erhöhte Ang-2 Werte zur Dysfunktion der Blut-Hirn-Schranke beigetragen haben.

In bereits veröffentlichten eigenen Publikationen konnte nachgewiesen werden, dass Ang-2 in pathologischen Modellen des Gehirns, wie z.B. beim Schlaganfall, hochreguliert ist. Im Rahmen dieser Arbeit konnte ich zeigen, dass menschliche Biopsien von Schlaganfallpatienten eine erhöhte Expression von Ang-2 in Blutgefäßen des Gehirns, sowie auch zwei bis fünfzehn Tage nach dem Schlaganfall im Blutserum aufwiesen. Darüber hinaus stelle ich vor, dass Ang-2 überexprimierende Mäuse eine erhöhte Permeabilität und vergrößerte Infarktareale entwickelten, nachdem sie einer Okklusion der mittleren Zerebralarterie (MCAO) für 24 Stunden ausgesetzt waren.

In dieser Arbeit konnte ich nachweisen, dass Ang-2 ein induzierender Faktor der endothelialen Hirn-Permeabilität ist, deren Regulation womöglich über den Tie2 Signalweg stattfindet, wie es in peripheren Blutgefäßen der Fall ist. Des Weiteren wurde untersucht, ob die Reaktivierung des Rezeptors Tie2 in einem prä-klinischen transienten MCAO-Modell die Folgen des Schlaganfalls (bedingt durch hohe Ang-2 Werte) mindern könnte. Die vaskuläre endotheliale Protein Tyrosin Phosphatase (VE-PTP) reguliert die Aktivität des Rezeptors Tie2. Zudem reguliert es zusätzlich die Wirkung des Adhäsionsverbindungs-moleküls VE-Cadherin, was normalerweise durch Dephosphorylierung die Verbindungen der anliegenden Endothelzellen verstärkt. Im Zuge meiner Arbeit demonstriere ich, dass ein VE-PTP Inhibitor zu einer signifikant erhöhten Aktivität von Tie2 und deren Anschluss-signalweg Akt in isolierten Gehirndothelzellen und in Schlaganfallproben von Ang-2 überexprimierenden Mäusen führte. Des Weiteren verringerte sich in der Tendenz die Phosphorylierung von VE-Cadherin, das entsprechend Blutgefäße stabilisiert, obwohl durch Inaktivierung von

VE-PTP erhöhte phosphorylierte VE-Cadherin Werte zu erwarten gewesen wären. Es ist bekannt, dass die Aktivierung von Tie2 Rho induziert, welches die Src Kinase inhibiert, die ansonsten zur Phosphorylierung von VE-Cadherin und dementsprechend zur Destabilisierung der Endothelzellen beiträgt. Die in dieser Arbeit durchgeführten Western Blot Analysen suggerierten, dass der stark aktivierte Tie2 Signalweg die Phosphorylierung von VE-Cadherin verringert, obwohl der Inhibitor die Wirkung der Phosphatase mindert, was durch verringerte pVE-Cadherin Expression dargestellt wurde. Dies erklärt mechanistisch den Prozess, der *in vivo* erzielt wurde. Der VE-PTP Inhibitor verbesserte die Folgen des Schlaganfalls im transienten MCAO-Modell, der 30 Minuten andauerte und nach 24 Stunden untersucht wurde. Die Behandlung von Wildtyp Mäusen vor und nach Induzieren des transienten Schlaganfalls mit dem Inhibitor bewirkte verkleinerte Infarktvolumen und verbesserte neurologische Reaktionen bei Mäusen. Darüber hinaus war die Permeabilität im Bereich des Infarkts geringer als bei den Kontroll-Gruppen, was auf eine verbesserte Stabilität der Blut-Hirn-Schranke mit der Behandlung vom VE-PTP Inhibitor hindeutet.

Zusätzlich wurden in dieser Arbeit Experimente an länger exprimierenden Ang-2 transgenen Mäusen (Ang-2 Überexpression von 6 bis 12 Monaten) erläutert. Sie zeigten auf, dass Ang-2 interessanterweise die Permeabilität im Gehirn nach einer Langzeit-Expression nicht nur wieder herstellt, sondern auch die Barriereeigenschaft von Blutgefäßen im Gehirn verstärkt. Dies wurde durch Resistenzmessung (TEER) der isolierten mikrovaskulären Endothelzellen aus dem Gehirn bestimmt und mit Hilfe von Tracer-Studien *in vivo* bestätigt. Auch die zuvor erhöhte Anzahl an Makrophagen, die in den 8 bis 12 Wochen alten transgenen Mäusen festgestellt wurde, konnte nicht in länger exprimierenden Ang-2 transgenen Mäusen bestätigt werden. Es wird angenommen, dass ein kompensatorischer Effekt gegen die zuvor entdeckte Ang-2 vermittelte Beschädigung der Blut-Hirn-Schranke erfolgte, um diese auszugleichen. Welche Proteine dabei hochreguliert werden und somit einen essentiellen Beitrag zum kompensatorischen Effekt leisten, ist bisher nicht bekannt. Ang-1 ist der agonistische Ligand beider Proteine, der zur Aktivierung des Tie2 Rezeptors führt. Daher könnte Ang-1 ein potentielles Protein sein, das für den kompensatorischen Effekt in länger exprimierenden Ang-2 transgenen Mäusen verantwortlich ist. Darüber hinaus könnten mRNA Screenings von isolierten mikrovaskulären Endothelzellen Aufschluss über weitere Proteine geben, die möglicherweise hochreguliert sind, um den Ang-2 basierten Effekt auf die Blut-Hirn-Schranke zu kompensieren.

Zusammenfassend deuten diese Erkenntnisse darauf hin, dass Ang-2 die Permeabilität an der Blut-Hirn-Schranke durch Verminderung von endothelialen Verbindungsproteinen erhöht und somit den parazellulären Transport fördert. Zusätzlich erhöht sich mit Ang-2 die Anzahl an Vesikeln, was den transzellulären Transport begünstigt. Ob dieses Ereignis in Zusammenhang mit anderen Signalwegen stattfindet als dem Angiopoietin / Tie Weg, ist bisher nicht bekannt.

Die Beschädigung der Blut-Hirn-Schranke, bedingt durch hohe Ang-2 Werte, verstärkt die Symptome des Schlaganfalls. Dies wird durch die Aktivierung des Tie2 / Akt Signalweges wieder verbessert. Diese Ergebnisse weisen darauf hin, dass das Angiopoietin / Tie2 Signal womöglich eine Schlüsselrolle bei der Regulierung der Blut-Hirn-Schranke spielt. Somit stellen Angiopoietine potenzielle therapeutische Targets zur Behandlung von neurologischen Krankheiten dar, die mit einer beeinträchtigten Blut-Hirn-Schranke Aktivität einhergehen.

## **1. INTRODUCTION**

The cardiovascular system is responsible for the transport of essential molecules throughout the body and supplies the surrounding tissue with oxygen, nutrients and immune cells, respectively. The inner layer of blood vessels is composed of endothelial cells. The blood vessels in the brain comprise specialized endothelial cells, which form a tight barrier, called the blood-brain barrier (BBB), to protect the sensitive central nervous system (CNS) from toxins and pathogens and maintaining its homeostasis (Zlokovic, 2008; Daneman, 2012). On the other hand, BBB is also responsible for negligible bioavailability of many CNS drugs via efflux transporters expressed at the BBB (Obermeier et al., 2013). It has previously been shown that canonical Wnt signaling is a crucial pathway in the induction and maintenance of the BBB properties (Liebner et al., 2008; Stenman et al., 2008; Daneman et al., 2009). More recently sonic hedgehog signaling has been demonstrated to be involved in regulating BBB function (Wang et al., 2008). However, it is unclear if the above pathways regulate the BBB properties alone or with other additional signaling mechanisms, e.g. with the Ang / Tie signaling pathway.

Abnormal changes and network formation of the vascular system contribute to cancer, ischemia and inflammatory diseases. Therapeutic approaches focus on stimulation or inhibition of angiogenic pathways to balance the network formation of blood vessels (Daneman, 2012). Among those angiogenic factors are Angiopoietins (Ang) which regulate the initiation of angiogenesis and maturation of new blood vessels. Ang-1 and Ang-2 bind to its receptor tyrosine kinase Tie2 (Suri et al., 1996; Maisonpierre et al., 1997), which is predominantly expressed on endothelial cells (Dumont et al., 1992). Ang-1 activates the receptor by autophosphorylation and induces downstream signaling cascades that promote the recruitment of pericytes, prevent inflammatory processes as well as apoptosis (Davis et al., 1996; Papapetropoulos et al., 2000; Jeon et al., 2003; Cai et al., 2008). Ang-1 has been reported to prevent vascular leakage through the inhibition of NF- $\kappa$ B (Jeon et al., 2003) and specifically at the BBB, it has been shown to protect VEGF induced BBB dysfunction (Valable et al., 2005). In contrary, Ang-2 competes with Ang-1 and inactivates the Tie2 receptor leading to inhibition of downstream signaling pathways (Maisonpierre et al., 1997; Yuan et al., 2009). Ang-2 contributes to vessel destabilization via pericyte regression in the retina (Hammes et al., 2004; Augustin et al., 2009; Eklund and Saharinen, 2013). In the CNS, pericytes are known to regulate the neurovascular permeability (Armulik et al., 2010) suggesting a role of Ang-2 on BBB permeability. In non-brain endothelial cells it has previously been shown

that Ang-2 increases vascular permeability *in vitro* and *in vivo* (Benest et al., 2013; Ziegler et al., 2013). However, whether Ang-2 / Tie2 signaling influences the specialized endothelial cells of the brain, which form the BBB remains unsolved.

Ang-1 is expressed in pericytes and smooth muscle cells and is constitutively released (Suri et al., 1996; Maisonpierre et al., 1997) whereas Ang-2 is stored in endothelial cells and only delivered upon inflammatory or angiogenic stimuli (Oh et al., 1999; Kim et al., 2000; Fiedler et al., 2004; Augustin et al., 2009). Ang-2 is therefore only highly expressed during development and in pathogenesis such as inflammatory diseases and tumor environments (Stratmann et al., 1998; Holash et al., 1999; Zhang et al., 2003). Additionally, we have shown that Ang-2 is associated with myeloid cell infiltration (Coffelt et al., 2010; Scholz et al., 2011). This was supported by data from human inflamed tissues where Ang-2 was expressed at highest levels in the brain (Scholz et al., 2011). Stroke is another cerebrovascular disease, which is associated with BBB breakdown and increased permeability (Beck et al., 2000; Nourhaghighi et al., 2003; Knowland et al., 2014). Previous and own reports indicated overexpression of Ang-2 in stroke (Beck et al., 2000; Zhang et al., 2002). All together these data suggest a role of Ang-2 on brain permeability. Better understanding of the signaling pathways controlling the BBB function is critical for developing novel therapeutics that either open the BBB for CNS drug delivery or tighten the BBB in neurological disorders associated with vascular leakage and brain edema.

### **1.1 The blood-brain barrier (BBB)**

The BBB is a specialized multicellular vascular structure of the central nervous system (CNS) which tightly regulates the transport of molecules and ions from the blood circulation to the CNS. One cellular component of the BBB is the endothelium, which is supported by astrocytes and pericytes in the barrier function. The BBB is responsible for brain homeostasis. It protects the CNS from toxins and pathogens, inflammation, injury and diseases (Liebner et al., 2011; Daneman and Prat, 2015).

Transporter proteins expressed at the BBB coordinate the delivery of nutrients into the brain and discharge waste products and potential pathogens (Mittapalli et al., 2010). At the same time, drug delivery to the CNS is also hampered by the BBB due to the presence of drug efflux transporters (Löscher and Potschka, 2005). Cellular and non-cellular components of the BBB such as astrocytes, pericytes, the basement membrane and interacting neurons with microglial cells cooperate together with endothelial cells

forming the neurovascular unit (NVU) (Hawkins and Davis, 2005) (Figure 1-1). This formation maintains the microenvironment in the brain, which is essential for proper neuronal function.

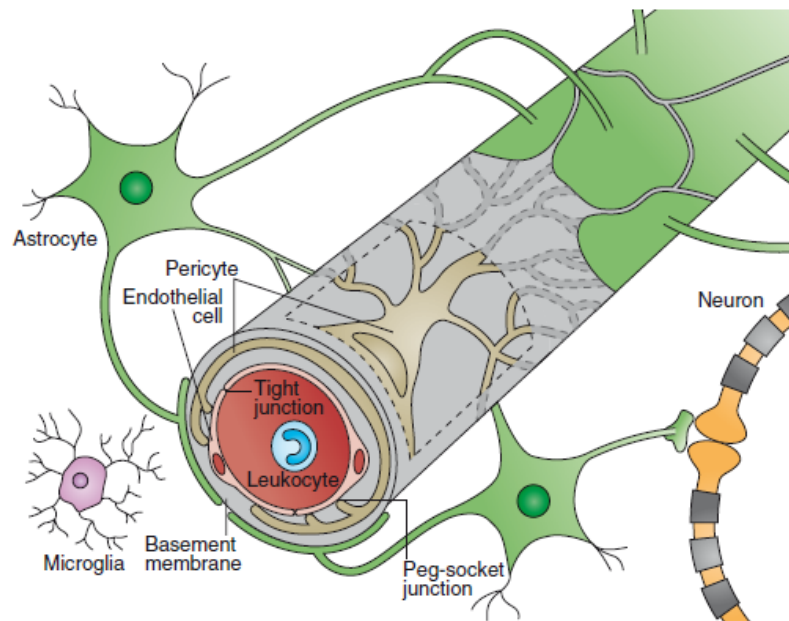


**Figure 1-1: The neurovascular unit (NVU) (Obermeier et al., 2013)**

The NVU is important for proper barrier function at the BBB. It is composed of neural cells and peripheral cells that interplay and mediate crosstalks to neurons. Endothelial cells possess more tight junction proteins compared to peripheral endothelial cells for tightening the barrier and minimize leukocyte infiltration. Pericytes reside in the basement membrane and are connected to endothelial cells. Astrocytes in the neuronal tissue exhibit foot processes, which almost completely ensheath endothelial cells. Additionally, they are connected to neurons and are important linkers for proper neuronal functioning.

### 1.1.1 Endothelial cells – component of the NVU

Endothelial cells in the CNS are linked together by high numbers of tight junctions compared to the peripheral blood vessels, which provide a high-resistance paracellular barrier to ions and other molecules from the blood (Bazzoni and Dejana, 2004). Tight junctions are transmembrane molecules that are linked to the cytoskeleton with cytoplasmic adaptors (Figure 1-2). Members of these tight junction transmembrane molecules in the brain are Claudins, Occludin and junction adhesion molecules (JAMs) (Del Maschio et al., 1999; Lippoldt et al., 2000; Nitta et al., 2003). Brain endothelial cells predominantly express Claudin-5, which is essential for barrier formation. Claudin-5 deficient mice exhibit a size-selective permeability at the BBB (Nitta et al., 2003). Additionally, other Claudins such as Claudin-3 and Claudin-12 have been identified at the BBB (Nitta et al., 2003; Liebner et al., 2008; Daneman et al., 2010a). One of the first



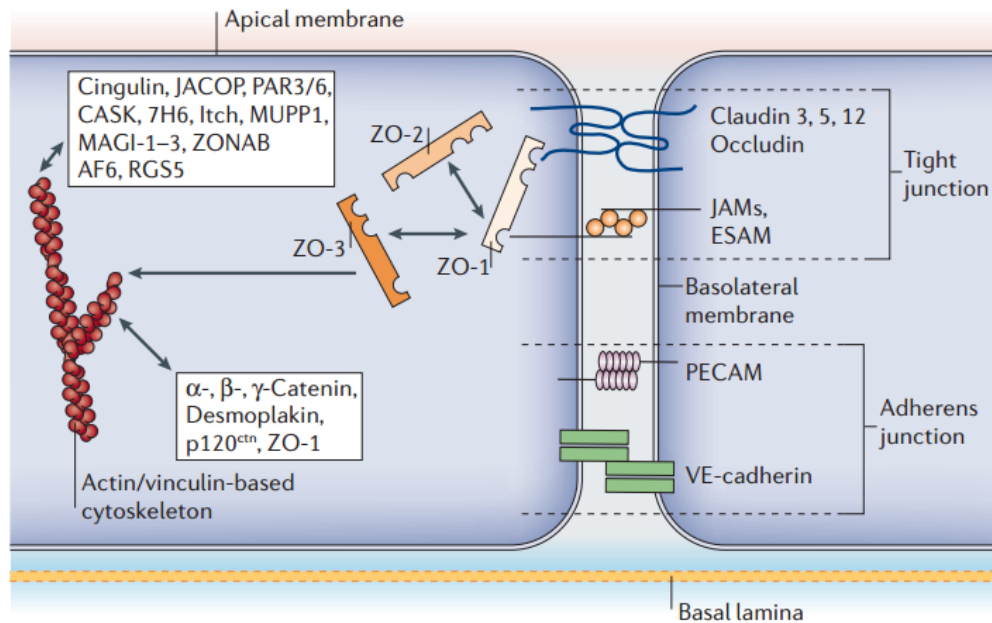


**Figure 1-2: Composition of junction proteins in endothelial cells of the NVU (Abbott et al., 2006)**

Endothelial cells are linked together by tight and adherens junctions. Occludin, Claudin-3, -5 and -12, junctional adhesion molecules (JAMs) and endothelial selective adhesion molecule (ESAM) are connected to the cytoskeleton by the adaptor proteins zonula occludens (ZO)-1, -2 and -3. Vascular endothelial (VE)-Cadherin and the platelet-endothelial adhesion molecule (PECAM) modulate counterbalanced adhesion. All these adaptor proteins regulate the interaction of membrane proteins with the actin or vinculin-based cytoskeleton.

described BBB endothelial transmembrane proteins is Occludin which is highly expressed in the brain and known to regulate the calcium flux across the BBB (Saitou et al., 2000) and are therefore important for the resistance of the barrier. JAM, a member of the immunoglobulin superfamily has also been identified to regulate paracellular permeability and leukocyte extravasation (Johnson-Léger et al., 2002; Ludwig et al., 2005).

Cytoplasmic adaptors of tight junctions are zona occludens (ZO)-1, ZO-2, Cingulin, Jacop, membrane associated guanylate kinase inverted (MAGIs), and membrane palmitoylated protein (MPPs) (Van Itallie and Anderson, 2013), which link tight junctions to cytoskeletal proteins like F-actin. The main transmembrane adherens junction protein is vascular endothelial Cadherin (VE-Cadherin) which interacts in the presence of calcium. Together with Catenins ( $\alpha$ ,  $\beta$ ,  $\gamma$ , p120) it forms a complex which is linked to the actin-filament network (Brieher, 2013).

Brain endothelial cells undergo extremely low rates of transcytosis compared to endothelial cells in the rest of the organism, thereby restricting the transcellular transport of molecules (Coomber and Stewart, 1985). A major transcytosis pathway is mediated by Caveolin-1 expressing plasmalemmal vesicles called caveolae. Caveolin-1 has been shown to be upregulated at the BBB in brain injuries (Zhao et al., 2011; Gu et al., 2012) indicating an increase in permeability mediated by caveolae.

The BBB endothelium is highly polarized into luminal and abluminal membrane compartments in order to achieve the paracellular / transcellular transport regulation (Betz and Goldstein, 1978). Efflux transporters are located at the luminal surface of the endothelial cell which transport small lipophilic molecules and other substrates including CNS drugs against their concentration gradient by usage of ATP (Löscher and Potschka, 2005), thus conferring drug-resistance. High numbers of mitochondria in the CNS compared to other organs provide the required ATP levels (Oldendorf et al., 1977). Mdr1, BCRP and MRPs are prominent members of the efflux transporters (Ha et al., 2007). Nutrient transporters carry nutrients and specific waste products down their concentration gradient through endothelial cells. Glut-1 (Slc2a1) is highly enriched in the CNS capillary endothelium and transports glucose down its gradient across the BBB (Cornford et al., 1994). Glut-1 deficiency leads to an epileptic syndrome (De Vivo et al., 2002). Ager, a receptor-mediated transporter is important to remove waste products from the CNS (Mittapalli et al., 2010).

Compared to peripheral endothelial cells the CNS possess extremely low levels of immune surveillance due to the low levels of leukocyte adhesion molecule (LAM) expression (Henninger et al., 1997; Daneman et al., 2010a, 2010b) whereby ICAM-1 and VCAM-1 influence the extravasation of T-cells across the BBB (Vajkoczy et al., 2001; Abadier et al., 2015).

The glycocalyx is embedded into the luminal side of endothelial cells. It is composed of proteoglycans and glycoproteins which form a network to soluble plasma molecules. Glycosaminoglycans (GAGs) are attached to proteoglycans. Together with other components of the glycocalyx such as glycoproteins, glycolipids and plasma proteins they are modified by glycosylation regulating the binding of ligands to endothelial cells like immune cells (Sperandio et al., 2009). Because of the polyanionic structure of the glycocalyx it is negatively charged which forms a mechanic barrier for particles from the luminal side to access to the endothelium (Curry and Adamson, 2012). The glycocalyx

is highly dynamic and endothelial cells regulate the biochemical properties of the GAGs to adapt to the local environment, dependent on the microenvironment, cation content, concentration and the pH of soluble proteins (Arisaka et al., 1995; Paka et al., 1999). The glycocalyx is an endothelial barrier which limits the access of certain proteins but increases the permeability of small molecules (van Haaren et al., 2003). The enzymatic removal and the neutralization of the negatively charged surface of the glycocalyx increase the permeability (van den Berg et al., 2003; Ueda et al., 2004). Stimuli which reduce the glycocalyx like enzymes, cytokines, ischemia or reperfusion seem to uncover the adhesion molecules on the endothelial cells (Henry and Duling, 2000; Vink et al., 2000; Mulivor and Lipowsky, 2004). In line with this is that the breakdown of the glycocalyx contributes to an increase in leukocyte adhesion to the endothelium (Constantinescu et al., 2003) suggesting increased leukocyte infiltration.

Therefore, the glycocalyx exerts a function of limiting the entry of certain blood cells to the endothelium for maintaining CNS homeostasis.

The composition of a physical barrier with non-fenestrated, tightly connected blood vessels, low rate of transcytosis for the regulation of molecular transport, and low levels of LAMs allow the endothelial cells to tightly regulate CNS homeostasis.

#### 1.1.2 Other components of the NVU

Additional components of the NVU are pericytes, astrocytes, the basement membrane and neurons (Daneman and Prat, 2015). Pericytes surround the microvascular endothelial blood vessels and are located at the abluminal surface embedded in the basal membrane (Sims, 1986). Brain blood vessels exhibit the highest pericyte coverage with endothelial to pericyte ratio of 1:1 or 1:3 compared to peripheral capillaries (e.g. muscle - 100:1) suggesting an important role in BBB maintenance (Shepro and Morel, 1993). Specific markers to detect pericytes are still not available because of their heterogeneity. CNS pericytes are positive for platelet-derived growth factor (PDGF) receptor  $\beta$  and NG2 but desmin is also used to detect pericytes (Armulik et al., 2011). Mice lacking PDGFR- $\beta$  or its ligand PDGF-b have increased permeability features with altered distribution of tight junctions. These mice die at birth due to hemorrhages in the brain (Lindahl et al., 1997; Hellström et al., 2001; Armulik et al., 2010), which indicate that pericytes are also required for the formation of the BBB during embryogenesis. Lack of pericytes leads to increase transcytosis rates and significantly higher expression of LAMs, which results in inflammatory response (Armulik et al., 2010; Daneman et al., 2010b). In addition to that, Armulik and colleagues suggested the role of pericytes in

guidance of astrocytic endfeet to the endothelial layer for proper astrocytic endfeet polarization (Armulik et al., 2010).

Astrocytes are glial cells, which supply nutrients from circulation to neurons, regulate ion concentration and control immune reactions for maintaining brain homeostasis. Astrocytic endfeet almost completely ensheath endothelial cells. (Abbott et al., 2006). Astrocytes have been shown to induce barrier properties in co-culture studies with endothelial cells *in vitro* (Abbott et al., 2006). Astrocytic conditioned medium contains factors secreted by astrocytes that modulate and maintain the barrier properties by inducing the expression of transporter proteins, metabolic enzymes, and increased tight junction formation (Hayashi et al., 1997). They also secrete VEGF, which is required for remodeling processes and the formation of blood vessels. VEGF is therefore very important during embryogenesis whereas it is associated with BBB breakdown in adulthood during inflammatory processes (Argaw et al., 2009). Aquaporin-4, a water channel and Kir 4.1, an ATP-sensitive potassium channel are expressed on astrocytic endfeet for regulating water homeostasis (Neuhaus, 1990). Aquaporin-4 channels increase the water uptake during ischemic stroke and edema (Kleffner et al., 2008). Taken together, astrocytes provide a cellular link from endothelial cells to neurons for regulating blood flow and neuronal activity (Attwell et al., 2010; Gordon et al., 2011).

The NVU is composed of two different basement membranes, the inner vascular endothelial membrane and the outer parenchymal membrane. Endothelial cells and pericytes secrete the vascular basement membrane to interact and adhere to blood vessels (Del Zoppo et al., 2006) whereas astrocytes secrete the extracellular matrix of the parenchymal basement membrane, which supports protein interactions of dystroglycans to astrocytic endfeet (Agrawal et al., 2006). The basement membrane comprises type IV collagens, laminin, nidogen, heparin sulfate proteoglycans and other glycoproteins (Wu et al., 2009; Sorokin, 2010). It is a compartment for different signaling processes to maintain the anchor of the NVU and to induce survival, differentiation and migration during BBB development in addition of being a physical barrier for leukocyte infiltration. BBB dysfunction is often associated with breakdown of the basement membrane by activation of matrix metalloproteases (Daneman and Prat, 2015).

Neurons also have an impact on the whole function of the NVU through interactions with endothelium and the astrocytes (Abbott et al., 2006). The primary communication route occurs between astrocytes and neurons (Koehler et al., 2006), although also direct

interaction to the endothelium has been demonstrated (Hamel, 2006). Glia cells and neurons can act in both directions. Induction of synapses with enhanced synaptic efficacy has been shown in co-culture experiments of astrocytes and neurons suggesting a role for astrocytes in promoting the development of new functional synapses (Pfrieger and Barres, 1997; Ullian et al., 2001). Each cell type of the NVU contributes to CNS barrier properties thus protecting neuronal functioning and maintaining homeostasis.

### 1.1.3 Regulation of the BBB by Wnt / $\beta$ -Catenin and Sonic Hedgehog signaling

The Wnt /  $\beta$ -Catenin signaling pathway plays a certain role during embryogenesis specifically in the CNS. It is responsible for cell fate specification, cell proliferation and cell migration. (Liebner et al., 2008; Stenman et al., 2008; Daneman et al., 2009). Neural stem cells and neural progenitors secrete Wnt7a and Wnt7b in the forebrain of the ventral region whereas Wnt1, Wnt3, Wnt3a and Wnt4 are expressed in the dorsal region and the hindbrain (Stenman et al., 2008; Daneman et al., 2009). The canonical Wnt pathway implies binding of the Wnt ligands to a Frizzled receptor on the endothelium. This leads to stabilization of  $\beta$ -Catenin, which is normally degraded in the proteasome (Figure 1-3).  $\beta$ -catenin translocates to the nucleus and induces the transcription of several target genes (Logan and Nusse, 2004), such as Lef1, Apcdd1, Axin2, Stra6 and Glut-1. These regulated proteins are enriched in the CNS (Daneman et al., 2009, 2010a). Conditional knockout mice of  $\beta$ -Catenin showed normal vascularization in all organs but displayed angiogenic defects with a thickened vascular plexus and capillary beds inducing hemorrhages in the brain (Stenman et al., 2008; Daneman et al., 2009). A similar phenotype has been observed by deleting Wnt7a / Wnt7b indicating the importance of Wnt /  $\beta$ -Catenin pathway for BBB formation in the CNS. The role of Wnt pathway in postnatal BBB maintenance has also been demonstrated by the transcriptional regulation of glucose-transporter Glut-1 and the tight junction protein Claudin-3 (Liebner et al., 2008; Stenman et al., 2008; Daneman et al., 2009). Apart from Wnts other ligands like Norrin, a member of the TGF- $\beta$  family, can bind to the Frizzled receptors and activate the Wnt signaling. Norrin based Wnt signaling has been shown to induce the formation of retinal blood vessels and the deletion of the receptor or the ligand leads to leakiness of the blood-retinal barrier and vascular malformations (Xu et al., 2004; Wang et al., 2012).

More recently, the Sonic Hedgehog pathway has also been indicated in BBB maintenance. Sonic Hedgehog is a factor secreted by astrocytes that acts on Patched-1 receptor expressed on endothelial cells to activate the signaling pathway during

embryonic development, neuronal guidance and angiogenesis (Wang et al., 2008). The Hedgehog signaling pathway induces the signal transducer Smoothed and the transcription factor Gli to regulate the expression of junctional proteins to promote the BBB phenotype. Mice that lack the signal transducer Smoothed decrease the expression of junctional proteins, increase BBB permeability and disturb the basal lamina (Alvarez et al., 2011).

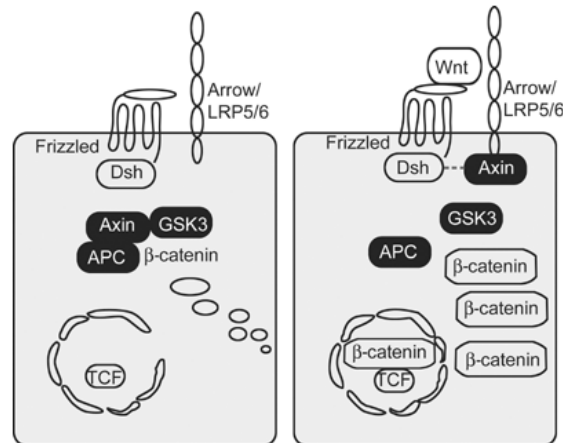


**Figure 1-3: The canonical Wnt /  $\beta$ -Catenin pathway (Nusse, 2005)**

Without the Wnt ligand a complex of Axin, APC and GSK3 actively phosphorylate  $\beta$ -Catenin for targeting ubiquitination and translocation to the proteasome for digestion. When Wnt is present it binds to the Frizzled receptor. Dsh induces binding of Axin to the cytoplasmic tail of LRP5/6 which destroys the destruction complex for  $\beta$ -Catenin. Subsequently,  $\beta$ -Catenin accumulates in the cytoplasm and translocates into the nucleus for targeting the transcription of genes which belong to the TCF family.

## 1.2 Angiogenesis / Vasculogenesis

Angiogenesis implicates the proliferation, sprouting and remodeling process of pre-existing blood vessels. (Risau, 1997; Swift and Weinstein, 2009). It comprises a precise balance between angiogenic growth and inhibitory factors to control angiogenesis throughout the body (Reiss et al. 2015). Disturbed balances contribute to abnormal growth of blood vessels leading to vascular diseases (Risau, 1997). Vascular endothelial growth factor (VEGF) was identified as a major regulator of endothelial sprouting and the formation of the primary plexus (Gerhardt et al., 2003).

During embryogenesis the vascular system is the first developing organ system. It implies the de novo vessel formation of mesodermal-derived precursor cells, called vasculogenesis (Figure 1-4). Mesodermal cells differentiate to haemangioblasts which form together to blood islands composed of angioblasts in the periphery and hematopoietic stem cells in the center (Flamme and Risau, 1992). Blood islands arise by in situ differentiation in mice around embryonic day (E) 7.0-7.5 (Poole and Coffin,

1989; Coffin and Poole, 1991). They assemble and fuse together in embryonic developmental stages to form a primary capillary plexus. VEGF signaling is important during vasculogenesis. It has been reported that mice lacking VEGF receptor-2 (*flk-1<sup>-/-</sup>*) fail to develop blood islands which leads to embryonic lethality at E8.5-E9.5 (Shalaby et al., 1995; Carmeliet et al., 1996; Ferrara, 1996). Angiogenic sprouting occurs around E8.5 (Adams and Alitalo, 2007).

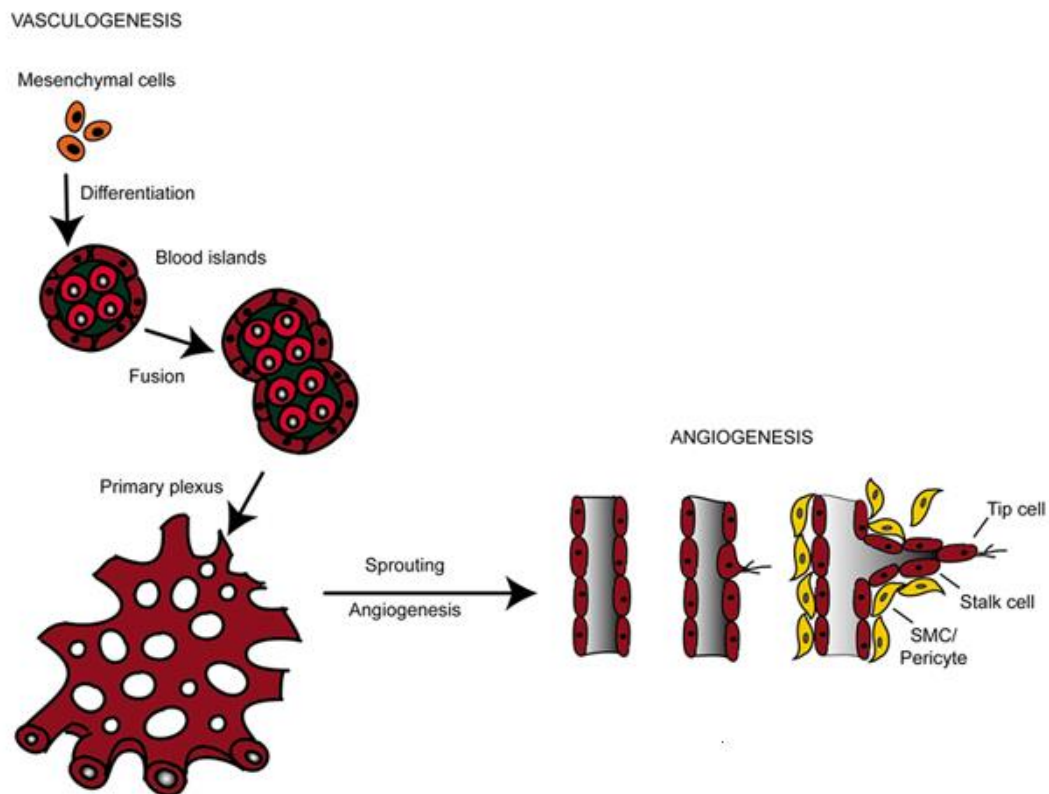


**Figure 1-4: Angiogenesis (modified from Heinke et al., 2012)**

Vasculogenesis is the de novo formation of precursor cells forming a primary plexus via blood islands. Angiogenic sprouting is based on sprouting from tip cells towards an angiogenic stimulus whereas stalk cells proliferate to elongate towards the growth factors. Pericytes / Smooth muscle cells (SMC) stabilize newly formed vessels.

The angiogenic process is initiated by insufficient supply of oxygen (hypoxia) to the tissue. This triggers the upregulation of pro-angiogenic factors like VEGF (Breier and Risau, 1996; Gerhardt, 2008). The basement membrane is then degenerated by matrix metalloproteases and mural cells detach from endothelial cells. VEGF-A is originated in different cell types, such as macrophages and smooth muscle cells. They regulate the survival by differentiation and proliferation of endothelial cells (Klagsbrun and D'Amore, 1996). VEGF via the Notch signaling pathway stimulates tip cells and induce the

formation of filopodia to migrate towards the angiogenic stimulus (Hellström et al., 2007; Lobov et al., 2007). At the same time stalk cells proliferate to support the sprout elongation and form a vascular lumen. Macrophages promote the fusion of tip cells that are stabilized by VE-Cadherin, an adherens junction (Schmidt and Carmeliet, 2010). Endothelial cells then undergo maturation through alignment of smooth muscle cells on the vessel wall followed by the formation of a new basement membrane (Gerhardt et al., 2003).

Angiopoietins are growth factors which modulate angiogenesis by angiogenic sprouting and subsequent vessel maturation in correlation with pericyte recruitment and vessel regression (Reiss et al., 2015, Scholz et al., 2015), that is discussed in detail in the next section.

### **1.3 The Angiopoietin / Tie signaling pathway**

#### **1.3.1 The tyrosine kinase receptors Tie1 and Tie2**

Tie1 and Tie2 are endothelial-specific tyrosine kinase receptors discovered in early 1990s that are expressed by vascular and lymphatic endothelial cells. Structurally they exhibit 76 % sequence identity in the cytoplasmic region (Schnürch and Risau, 1993; Dumont et al., 1994; Sato et al., 1995). The extracellular part shows only 33 % similarity between Tie receptors, which consists of two immunoglobulin – like domains, followed by epidermal growth factor– like repeats and finally composed of three fibronectin type III domains (Barton et al., 2006) (Figure 1-5). Tie1 is almost exclusively expressed by endothelial cells in differentiating angioblasts during vasculogenesis, in the dorsal aorta of embryos and in migrating endothelial cells of the developing heart (Korhonen et al., 1994). Tie1 is upregulated in hypoxic conditions upon VEGF stimulation, in wound healing processes, tumor growth and development (Korhonen et al., 1992; McCarthy et al., 1998). The second receptor of the Angiopoietin ligands is Tie2. It is expressed by endothelial cells and also by hematopoietic and precursor cells which exerts a critical role for hematopoiesis. Tie2 mediates the adherence and the aggregation of hematopoietic stem cells (HSCs) (Dumont et al., 1992; Takakura et al., 1998). It is also expressed within a population of monocytes, which are involved in the recruitment of tumor-associated macrophages (De Palma et al., 2005), and is additionally upregulated in tumor angiogenesis (Peters et al., 1998). Tie2 deficient mice die around embryonic day (E) 9.5 and E10.5 due to remodeling failure in the vasculature and severe heart defects. 30 to 70 % less endothelial cells were observed in E8.5 and E9.5 stages and



vessels exhibited less branches and fewer pericytes compared to wild type embryos (Dumont et al., 1994; Sato et al., 1995; Patan, 1998). It has been shown that loss of Tie2 induces apoptosis of endothelial cells which results in hemorrhages (Jones et al., 2001).

In contrast, mice lacking Tie1 die later during development around E13.5 and postnatal day (P) 1. These mice lose the structural vessel integrity, resulting in edema formation (Sato et al., 1995), the hematopoietic system is however unaffected (Rodewald and Sato, 1996). Mice lacking both Tie1 and Tie2 receptors die around E10.5 similar to Tie2-deficient mice due to cardiovascular defects. Additionally, the vascular system itself is severely affected. On the other hand vasculogenesis was normal suggesting that both receptors are dispensable for the developmental angiogenic sprouting but are essential for maintaining the integrity of the mature vasculature (Puri et al., 1999).

### 1.3.2 Angiopoietins

Angiopoietins are secreted glycoproteins belonging to the family of growth factors. They are essential for blood vessel development and maturation (Augustin et al., 2009; Eklund and Saharinen, 2013, Reiss et al. 2015). The Angiopoietins consist of mainly two domains. The fibrinogen homology domain is required for receptor binding whereas the coiled-coil domain is responsible for dimerization or oligomerization (Kim et al., 2005; Barton et al., 2006) (Figure 1-5).

The 70 kD Ang-1 was discovered by a secretion-trap expression cloning in 1996 (Davis et al., 1996). It is highly expressed in the myocardium during development and at later stages expressed in smooth muscle cells, perivascular cells and fibroblasts (Suri et al., 1996; Maisonpierre et al., 1997). The phenotype of Ang-1 deficient mice is reminiscent of the phenotype of Tie2 deficient mice (Dumont et al., 1994; Sato et al., 1995). They are embryonically lethal at E11-E12.5 due to an immature primary plexus and a deficient heart growth based on the retraction of endocardium from the myocardial wall (Suri et al., 1996). A myocardial overexpression of Ang-1 results in heart hemorrhages in 90 % of cases leading to embryonic lethality between E12.5 and E15.5. Although the remaining 10 % survive, they develop cardiac hypertrophy (Ward et al., 2004). However, mice overexpressing Ang-1 under the control of a keratin 14 promoter do survive and are generally healthy. Their skin shows signs of erythema due to larger vessels compared to wild type mice. The cell-cell contacts are not affected and the vasculature is largely intact (Suri et al., 1998).

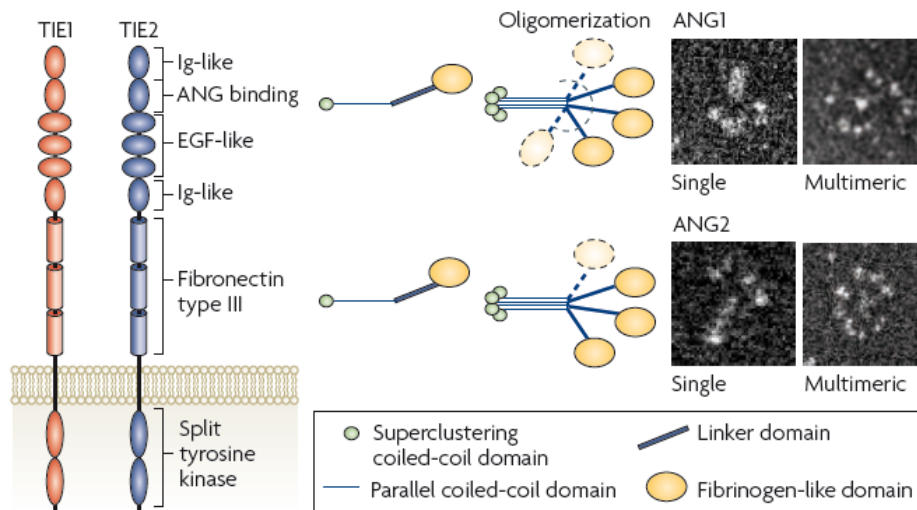


**Figure 1-5: Structures of the tyrosine kinase receptors Tie1 and Tie2 and its ligands Ang-1 and Ang-2 (Augustin et al., 2009)**

The receptors Tie1 and Tie2 share very similar structures. Intracellularly they are composed of a split tyrosine kinase domain whereas the extracellular domain consists of three fibronectin type III domains, two immunoglobulin (IgG)-like domains which are located in between three endothelial growth factor (EGF)-domains and an angiopoietin (ANG)-binding domain. Angiopoietin-1 (ANG1) and Angiopoietin-2 (ANG2) are the soluble ligands for these receptors. They polymerize to oligomers through a parallel coiled-coil domain and the superclustering coiled-coil domain.

Different studies verified that Ang-1 / Tie2 signaling promotes the formation of quiescent and mature blood vessels via the recruitment of smooth muscle cells and pericytes (Suri et al., 1998; Cai et al., 2008). Ang-2, Ang-3 and Ang-4 were found subsequently by homology screening (Maisonpierre et al., 1997; Valenzuela et al., 1999). In contrast to Ang-1, Ang-2 which shares approximately 60 % sequence homology to Ang-1, is not expressed in the developing heart. Its transcription pattern is localized to the dorsal aorta and in aortic branches. In later developmental stages, Ang-2 is mainly downregulated and only expressed in regions undergoing vascular remodeling such as ovary, placenta or uterus (Maisonpierre et al., 1997). 90 % of Ang-2 deficient mice in C57 / B16 background survive and show minor vascular defects. However, milky fluid termed chylous ascites is secreted in the peritoneal cavity after birth in these mice, which contains fat indicating defects in the lymphatic system (Fiedler et al., 2006). However, in the 129 / J genetic background Ang-2 deficient mice die at P14 due to severe chylous ascites (Gale et al., 2002). In the retina, the hyaloid vessels that normally regress during development, were still detectable in Ang-2 deficient mice (Gale et al., 2002; Hackett et al., 2002). This reflects a role of Ang-2 in remodeling and regression of the vasculature

and a specific role in lymphangiogenesis although Ang-2 is not essential in embryonic development. However, mice overexpressing Ang-2 exhibit disruption of vessel integrity and embryonic lethality similar to Ang-1 and Tie2 deficient mice (Suri et al., 1996; Maisonpierre et al., 1997). This suggests that Ang-1 acts as a stimulating factor on the Tie2 receptor whereas Ang-2 is the antagonistic part to the Ang-1 / Tie2 signaling pathway. Indeed, Ang-2 induces vessel regression through subsequent induction of apoptosis in the absence of VEGF while it induces angiogenesis together with VEGF (Holash et al., 1999; Lobov et al., 2002).

Ang-3 and Ang-4 have a consensus amino acid sequence of 65 % and are mouse and human orthologues. Ang-3 was identified as an antagonist of Tie2 whereas Ang-4 possessed agonistic functions on Tie2 (Valenzuela et al., 1999). Little is reported about these glycoproteins.

### 1.3.3 Regulation of Angiopoietin expression

In later developmental stages Ang-1 is not strongly regulated (Davis et al., 1996). It acts in a paracrine manner on the Tie2 receptor on the endothelium. Ang-1 binds to the extracellular matrix through its linker peptide region (Xu and Yu, 2001). It is expressed by tumor cells and in neuronal cells in the brain (Stratmann et al., 1998; Zagzag et al., 1999) and is overexpressed during angiogenesis (Augustin et al., 2009). Ang-2 is almost exclusively expressed by endothelial cells and stored in the Weibel-Palade bodies, where it colocalizes with the homeostasis glycoprotein von Willebrand factor (Fiedler et al., 2004). Under the control of cytokine activation e.g. histamine, thrombine or vasopressin Ang-2 is released from the endothelium (Fiedler et al., 2004) and acts in an autocrine manner on the Tie2 receptor (Scharpfenecker et al., 2005). Ang-2 is highly expressed in regions of vascular remodeling such as the placenta during the first trimester of women's pregnancy (Wang et al., 2007). Ang-2 is also upregulated under pathological conditions (Stratmann et al., 1998; Zagzag et al., 1999; Zhang et al., 2003; Oliner et al., 2004). The upregulation of Ang-2 occurs by hypoxia, shear stress and VEGF (Oh et al., 1999; Mandriota et al., 2000). Transcription factor FOXO1 (also called FKHR1) leads also to an increase in Ang-2 expression (Daly et al., 2004). On the other hand the transcription factor Kruppel-like factor 2 (KLF2) which is regulated by shear stress downregulates the production of Ang-2 while it upregulates Tie2 expression (Parmar et al., 2006). Ang-2 is also upregulated in inflammatory disorders (Scholz et al., 2011, 2015).

#### 1.3.4 Activation of Tie2 receptors

Ang-1 and Ang-2 act on the Tie2 receptor in tetrameric or higher-oligomeric forms. The molecules oligomerize through the parallel coiled-coil domain and bind with the same binding affinity to Tie2 via the fibrinogen-like domain (Procopio et al., 1999; Davis et al., 2003; Fiedler et al., 2003), although both ligands induce different signaling cascades. Ang-1 is known to induce Tie2 via autophosphorylation due to multimeric clustering (Kim et al., 2005). The effects of Ang-2 on the vasculature seem to be context-dependent. The Ang-1 antagonistic effect of Ang-2 is reported under vascular remodeling and inflammatory conditions where the constitutively released Ang-1 decreases in ratio to higher Ang-2 expression (Augustin et al., 2009; Scholz et al., 2015). Ang-2 competes with Ang-1 for Tie2 binding and destabilizes vessels and operates as a pro-inflammatory factor while blocking Tie2 phosphorylation (Yuan et al., 2009; Reiss, 2010). However, Ang-2 also can act as a Tie2 agonistic but has much lower activity compared to Ang-1 (Bogdanovic et al., 2006; Yuan et al., 2009). It is reported that Ang-2 can operate as a stimulator of Tie2 on already activated endothelium (Daly et al., 2006). In cultured endothelial cells high concentration of Ang-2 leads to phosphatidylinositol-3 kinase (PI3K) - Akt activation (Kim et al., 2000; Harfouche and Hussain, 2006). Differences in ligand structures or oligomerization may change the agonistic and antagonistic function on the Tie2 receptor (Barton et al., 2006; Augustin et al., 2009). It has been shown that oligomers function as activators whereas dimers can antagonize the activation of the Tie2 receptor (Davis et al., 2003; Kim et al., 2005; Barton et al., 2006). Recent evidence suggest that three residues in the fibrinogen domain of Angiopoietins lead to divergent ligand activity (Yu et al., 2013).

The Tie1 receptor also influences the receptor activation of Tie2. Tie1 heterodimerizes with Tie2 and inhibits the clustering of Tie2. This limits the activation of Ang-1 on the Tie2 receptor (Marron et al., 2007). Tie1 undergoes ectodomain cleavage by stimulation with VEGF and tumor necrosis factor (TNF) (Yabkowitz et al., 1999; Tsiamis et al., 2002), which induces increased responsiveness of Ang-1 activation on Tie2 (Marron et al., 2007).

#### 1.3.5 Tie2 downstream signaling

Ang-1 induces autophosphorylation of the Tie2 receptor which is blocked by Ang-2 (Augustin et al., 2009; Eklund and Saharinen, 2013, Reiss et al. 2015). Activated Tie2 induces several signaling pathways. It leads to maintenance of vascular quiescence on

resting endothelial cells whereas it influences migration, permeability, inflammation and vascular maturation on activated endothelial cells.

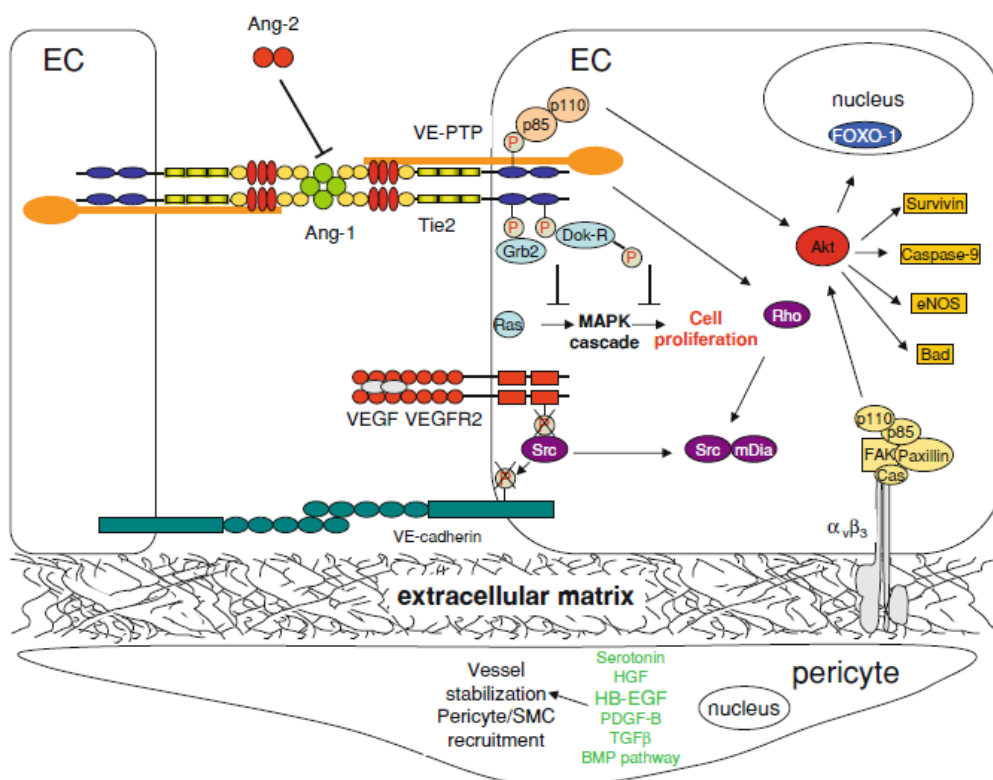


**Figure 1-6: Tie2 downstream signaling for maintaining endothelial quiescence (Thomas and Augustin, 2009)**

When Ang-1 binds to the Tie2 receptor on quiescent endothelial cells it induces autophosphorylation. Tie2 translocates in a trans-complex to other Tie2 receptors from adjacent cells. This complex additionally contains a vascular endothelial protein tyrosine phosphatase (VE-PTP) which regulates the phosphorylation rates of Tie2. Phosphorylation of Tie2 activates the Akt pathway which induces survival and blocks apoptosis through Survivin, Caspase-9, eNOS or BAD. Activation of Grb2 and Dok-R inhibits the MAP-Kinase cascade, which normally promotes cell proliferation. Activated Tie2 induces Rho for sequestering Src through mDia which is normally activated by vascular endothelial growth factor (VEGF) signaling. Src normally phosphorylates VE-Cadherin which leads to internalization of this adherens junction and increased permeability. The Forkhead transcription factor FOXO-1 gets phosphorylated, translocates to the nucleus and induces the expression of target genes. Several factors are included in the scheme, which are important for vessel stabilization and pericyte recruitment such as PDGF-B, TGF- $\beta$  and Serotonin in pericytes.  $\alpha_v\beta_3$  integrins are expressed in the extracellular matrix which also contribute to the Akt pathway.

Tie2 activation leads to phosphorylation of the p85 subunit of the PI3K and to the recruitment of growth factor receptor-bound protein 2 (GRB2), which induces the activation of Akt (Figure 1-6). This leads to the activation of several survival related pathways such as nitric oxide synthase (eNOS) and Survivin and inhibition of pro-

apoptotic proteins like BAD and Caspase 9 leading to cell survival (Papapetropoulos et al., 2000; Kontos et al., 2002; DeBusk et al., 2004). In quiescent endothelial cells Tie2 is translocated to cell-cell junctions, where it complexes with Tie2 molecules on adjacent endothelial cells and interacts with vascular endothelial protein tyrosine phosphatase (VE-PTP), a molecule that regulates Tie2 phosphorylation (Saharinen et al., 2008).

In activated endothelial cells Ang-1 / Tie2 signaling pathway induces endothelial cell migration. Tie2 expressed in a polarized manner translocates to the extracellular matrix, where it binds to matrix immobilized Ang-1 (Saharinen et al., 2008). Adaptor proteins - GRB14 and SHP2 are then activated and recruited to the Tie2 receptor for induction of PI3K. Thus activated docking protein (Dok)-R interacts with rasGAP, Nck and Crk that are associated with migration and proliferation (Jones and Dumont, 1998). Ang-1 can also induce migration via its action on the focal adhesion kinase (FAK), which leads to phosphorylation of paxillin leading to the activation of MAP kinase ERK for induction of migration (Tournaire et al., 2004).

The Ang-2 expression is associated with pericyte dropout in a diabetic retinopathy (Hammes et al., 2004). Ang-1 on the other hand induces the expression of heparin binding EGF-like growth factor (HB-EGF) which induces SMC migration in a paracrine manner (Iivanainen et al., 2003). In addition to that hepatocyte growth factor (HGF) and platelet-derived growth factor-B (PDGF-B) that are both expressed in endothelial cells are also associated with the recruitment of SMCs to endothelial cells (Lindahl et al., 1997; Kobayashi et al., 2006). PDGF receptor- $\beta$  (PDGFR- $\beta$ ) is expressed on pericytes and acts via the ligand PDGF-B. Blocking experiments of PDGFR- $\beta$  inhibit the recruitment of pericytes leading to retinal hemorrhages, which could almost completely be rescued by recombinant Ang-1 treatment (Uemura et al., 2002). In addition to that, researchers evidenced also in tumor environments the recruitment of pericytes by Ang-1 whereas Ang-2 induces pericyte dropout (Machein et al., 2004; Cao et al., 2007). Activated Tie2 therefore induces quiescence and maturation of blood vessels. Additionally, it decreases endothelial cell permeability by dephosphorylation of VE-Cadherin, an adherens junction molecule stabilizing endothelial cells. Ang-1 / Tie2 sequesters the non-tyrosine kinase Src, which is normally mediated by VEGF / VEGF receptor 2 signaling to induce cell permeability, through mammalian diaphanous (mDia). Hence, VE-Cadherin is not phosphorylated and does not internalize leading to vessel stabilization (London et al., 2009).

Ang-1 is furthermore known as an anti-inflammatory cytokine. It protects against lipopolysaccharide induced sepsis and prevents vascular leakage (Witzenbichler et al., 2005). The effect of Ang-1 on permeability was initially shown by Thurston et al. in 1999. Experiments of dermal microvessels from mice overexpressing Ang-1 (K14 promotor) reveal decreased permeability which is still prevented by the VEGF-induced leakage in the skin (Thurston, 1999). Tie2 activation induces the recruitment of ABIN2 with NF- $\kappa$ B to block its pathway for preventing apoptosis and the induction of inflammation (Tadros et al., 2003).

#### 1.3.6 Tie receptor independent pathways for Angiopoietins

Angiopoietins are also known to bind in a Tie2-independent manner in cells that do not express Tie2 but which express integrins such as  $\alpha$ 2 $\beta$ 1,  $\alpha$ 5 $\beta$ 1,  $\alpha$ v $\beta$ 3 and  $\alpha$ v $\beta$ 5 (Carlson et al., 2001; Cascone et al., 2005; Weber et al., 2005). It has been reported that Ang-1 acts on Tie2 negative cardiac and skeletal myocytes while binding to integrins leading to their survival (Dallabrida et al., 2005). Neuronal cells are Tie2 negative but they are still protected from apoptosis by Ang-1 signaling via integrin binding (Valable et al., 2003). Ang-1 is presented in osteoblasts and binds to integrins which leads to adhesion of hematopoietic stem cells (HSCs) to osteoblasts whereas Ang-1 / Tie2 controls the maintenance of the bone marrow stem cell niche (Arai et al., 2004). Ang-2 on the other hand binds to  $\alpha$ 5 $\beta$ 1 integrins, and via the Akt pathway, and stimulates breast cancer metastasis and induces glioma invasion by induction of matrix metalloprotease-2 through  $\alpha$ v $\beta$ 1 integrin signaling and simultaneous expression of focal adhesion kinase (FAK) (Hu et al., 2006; Imanishi et al., 2007). FAK also plays a role in integrin-dependent binding of Ang-2 in angiogenic processes. The expression of Tie2 becomes decreased in angiogenic tip cells leading to an active confirmation of integrins. Ang-2 binds to integrins that activates the phosphorylation of FAK at Tyr397 for endothelial sprouting and migration (Felcht et al., 2012). In addition, our laboratory identified the role of Ang-2 in inflammation in which Ang-2 overexpressing mice promote myeloid cell-infiltration via  $\beta$ 2-integrins (Scholz et al., 2011).

#### 1.4 Breakdown of the BBB in correlation to diseases

The disruption of the BBB is associated with many pathological diseases of the CNS including multiple sclerosis, stroke, Alzheimer's disease, epilepsy and brain cancer. This dysfunction of the barrier in the brain is indicated by alterations of the endothelial phenotype by decreasing tight junctions and increasing LAMs, increase in transcytosis,

changes in transport systems and increased leukocyte infiltration. This leads to neuronal dysregulation and degeneration (Daneman and Prat, 2015). Continuous BBB disruption induces vasogenic edema resulting from increased import of water and plasma proteins to the CNS. The edema can be slightly reduced by diminishing blood volume and the cerebrospinal fluid in the ventricles. However, the consequence of severe BBB disruption is still an increase in intracranial pressure, damaging of the CNS tissue including death (Stamatovic et al., 2006; Nag et al., 2009). The molecular mechanisms that are involved in BBB disruption are the induction of VEGF, matrix metalloproteases, cytokines and reactive oxygen species (ROS) (Daneman and Prat, 2015) (Figure 1-7).

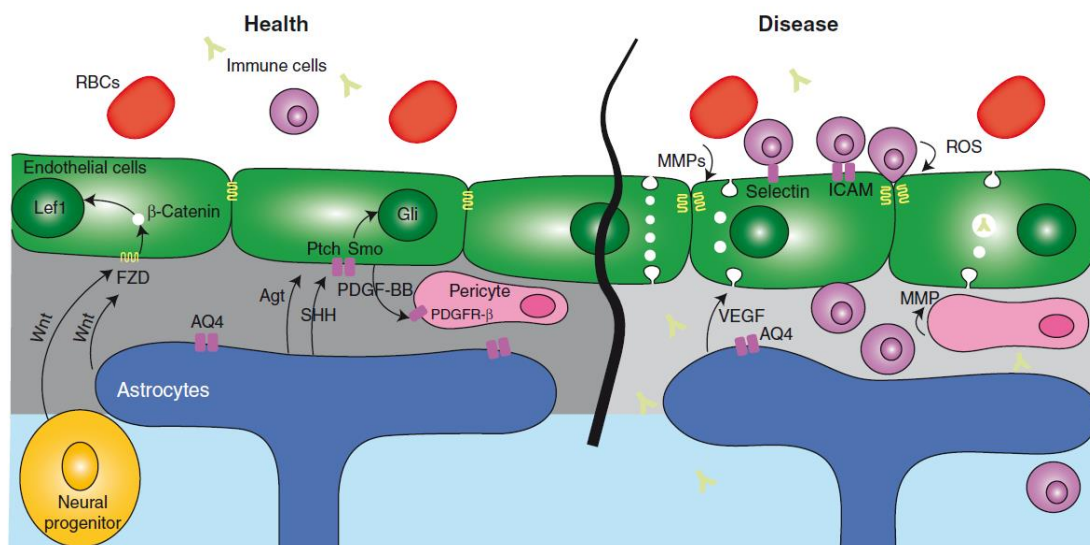


**Figure 1-7: The BBB in health and disease (Daneman and Prat, 2015)**

Under healthy conditions neuronal progenitor cells secrete Wnt proteins which bind to the Frizzled receptor (FZD) for stabilizing  $\beta$ -Catenin. It induces the expression of several target genes for maintaining BBB properties. Astrocytes produce Sonic hedgehog (SHH) which acts on the Patched-1 receptor (Ptch). The signal transducer Smoothed (Smo) and Gli are activated to induce the expression of junctional proteins. PDGF-B produced by endothelial cells function on the PDGFR- $\beta$  to recruit pericytes to endothelial cells for vessel maturation. Therefore immune cells and red blood cells (RBCs) from the lumen cannot enter to the neural compartment.

Several brain diseases are associated with BBB breakdown. The vascular endothelial growth factor (VEGF) produced by astrocytes increase the permeability of endothelial cells. Matrix metalloproteases (MMP) and reactive oxygen species (ROS) destroy tight junction complexes to increase paracellular permeability. MMPs additionally act on parts of the basement membrane. During BBB breakdown an increase of transcytosis occurs which leads to an upregulation of transcellular transports. Endothelial cells activate the expression of adhesion molecules such as Selectin and ICAM for adhesion of leukocytes and infiltration into the neuronal compartment of the CNS.



In some diseases the breakdown of the BBB is the primary event which leads to brain injury such as in stroke or traumatic injuries. In other cases the disease has been suggested for the onset of BBB dysfunction such as in multiple sclerosis (MS), epilepsy and Alzheimer's disease (AD) (Kermode et al., 1990; Huang, 2006; Oby and Janigro, 2006; Correale and Villa, 2007).

AD is a disorder in which neurons are degenerated resulting in loss of memory and eventually dementia. Disease causing amyloid  $\beta$  clearance from the brain across BBB seem to be altered leading to accumulation of amyloid  $\beta$  in perivascular space. Amyloid  $\beta$  activates the transmigration of monocytes and induces the secretion of inflammatory cytokines. Epilepsy is a neurologic disorder with recurrent seizures that are often followed by BBB disruption and changing ionic balance in the neuronal tissue. The deficiency of Glut-1 can lead to epilepsy which can be treated by altering the energy source circumventing the demand of Glut-1 (De Vivo et al., 2002). Increased Pgp and Mrd1 expression are accompanied with refractory epileptic brains (Marchi et al., 2004).

Glioblastoma is classified as a grade IV tumor with a very poor prognosis (Ohgaki and Kleihues, 2005). The most malignant brain tumor is characterized by hypercellularity, exaggerated vascularization, several necrosis areas and high numbers of fenestrated endothelial cells. Alterations in tight junctions and caveolae expression increases the permeability (Wolburg et al., 2012). Human glioblastoma possess decreased expression of Claudin-3 with a diminished network formation of tight junction molecules (Liebner et al., 2000; Wolburg et al., 2003). The disruption of the basal lamina impair the BBB integrity (Candelario-Jalil et al., 2009). Moreover, Aquaporin-4 is described to be upregulated in glioblastoma (Warth et al., 2004) which is associated with astrocyte migration suggesting a promoting role of Aquaporin-4 in infiltration of malignant cells (Wolburg et al., 2012).

Another example for the breakdown of the BBB in a cerebrovascular disorder is the ischemic stroke which will be described in detail in the next section.

#### 1.4.1 BBB dysfunction in ischemic stroke

Stroke is a cerebrovascular disease associated with BBB breakdown. It is a severe CNS disorder and occurs by a loss of cerebral blood flow due to mechanical plugging of a blood vessel, mostly via a thrombus or emboli (Daneman, 2012). This leads to shortage of oxygen and nutrients in the epicenter of the core ischemic zone (infarct) and to the surrounding tissue (penumbra). The ischemic stroke can be divided into two periods of

pathological impacts, the ischemia itself and its reperfusion which is indicated by time-dependent biochemical and cellular changes leading to a bimodal increase in BBB permeability (Figure 1-8) (Sandoval and Witt, 2008). There is a rapid opening of the BBB occurring within minutes to hours, following a refractory phase which results in a protracted opening for days (Belayev et al., 1996; Huang et al., 1999).

The blockade of blood supply depletes the production of ATP, resulting in accumulation of lactic acid by anaerobic metabolism, which contributes to swelling of endothelial cells. Neuronal excitotoxicity is associated with an excessive release of glutamate from neurons. A massive number of neurons die during this event in the initial phase of ischemia (Broughton and Partridge, 2009). This also results in an imbalance of ions by increased intracellular calcium and potassium influx inducing shrinking of neurons, swelling of astrocytic endfeet and cell damage.

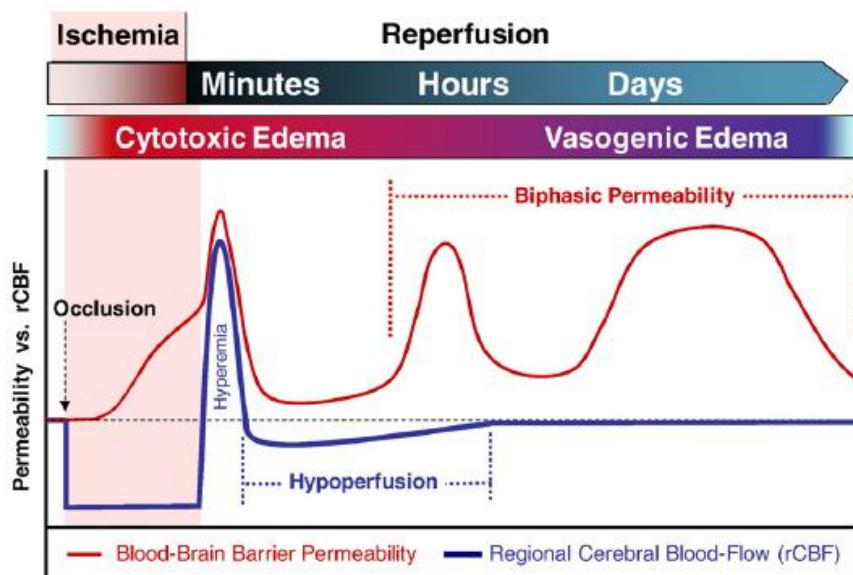


**Figure 1-8: The BBB permeability and cerebral blood flow during ischemia and reperfusion (Sandoval and Witt, 2008)**

The incidents during ischemic stroke can be categorized into ischemia and reperfusion phases. During ischemia the cerebral blood flow is blocked which increases the vascular permeability. Once blood starts to flow again the reperfusion phase begins which initially induces hyperemia with simultaneous induction of permeability. Hypoperfusion follows hyperemia until the blood flows normally usually within hours after ischemic stroke. The biphasic permeability is initiated during the hypoperfusion stage, which can persist for days. Edema is subdivided into cytotoxic edema and vasogenic edema. Cytotoxic edema appears during ischemia and lasts during reperfusion after hours. The vasogenic edema begins during the phase of reperfusion.

The initial breakdown of the BBB in stroke is accompanied by oxidative stress due to calcium dependent activation of enzymes. The oxidative stress indicates an excessive upregulation of reactive oxygen species (ROS) which damages cellular molecules like proteins and DNA and modulate tight junction proteins (Schreibelt et al., 2007). ROS also activate matrix metalloproteases, which cleave dystroglycan, an important anchor between astrocytic endfeet and the parenchymal membrane (Agrawal et al., 2006). The concentration of MMP-9 correlates with ischemic stroke (Pun et al., 2009) and the infarct volume is reduced in MMP-9 knockout mice or with an MMP-9 inhibitor (Asahi et al., 2000). This is followed by an inflammatory response activating local microglia and infiltration of leukocytes into the damaged tissue.

Reperfusion is the restoration of cerebral blood flow in the ischemic brain, which is necessary for the brain survival but also induces tissue damage during the process. As cerebral blood flow is restored it induces an initial permeability which is followed by a biphasic permeability due to increased tight junction modulation. The first permeability process goes along with the hyperemia followed by a hypoperfusion till it results in normal blood flow (Sandoval and Witt, 2008). Animal models identified these events to occur time-dependently from hours to days depending on severity of stroke (Huang et al., 1999; Witt et al., 2008). The hyperemia during the initial reperfusion leads to increased blood-pressure with enormous opening of the BBB by modulation of tight junctions (Spengos et al., 2006). The subsequent hypoperfusion implicates failing nutrition supply, which would be necessary for the recovery of the infarct region and the penumbra, which also results in endothelial and astrocytic swelling (Iadecola, 1998). This edema can cause death and can be separated in cytotoxic and vasogenic edema. Cytotoxic edema develops right after ischemic incidence because of the inappropriate water and ion regulation leading to swelling of different cell types (Betz et al., 1989). In contrary to that, vasogenic edema directly changes the assembly of tight junctions at endothelial cells, which allows macromolecules to pass through the BBB (Heo et al., 2005). The water content increases therefore overall in the brain and has the tendency to appear more in the white matter than in the grey matter (Ayata and Ropper, 2002). The remodeling of the vasculature occurs via upregulation of VEGF that induces formation of blood vessels (Hayashi et al., 1997; Plate et al., 1999; Zhang et al., 2000). This angiogenesis is initiated during vasogenic edema but fails due to the disassembly of tight junctions (Sandoval and Witt, 2008). The remodeling process of the vasculature can last for weeks after ischemic stroke (Strbian et al., 2008) including the regulation of the assembly and reassembly of tight junctions (Sandoval and Witt, 2008).

#### 1.4.2 Angiopoietins in BBB maintenance and breakdown

Ang-1 is known to be involved in BBB tightening processes. It promotes angiogenesis and decreases the permeability time-dependently in the human BBB where it upregulates junctional proteins (Prat et al., 2001). The mechanism of Ang-1 mediated decrease in vascular permeability even in the presence of the known permeability inducer VEGF was reported to occur via stabilization of VE-Cadherin by sequestering Src through mDia (Thurston, 1999; London et al., 2009) (see 1.3.5) in peripheral endothelial cells. When Ang-1 is co-expressed with VEGF it also protects against inflammatory effects in the brain (Shen et al., 2011). The Src-suppressed C-kinase substrate which decreases VEGF expression in turn induces upregulation and secretion of Ang-1 leading to increased tight junction expression and decreased barrier permeability (Lee et al., 2003). Ang-2 on the other hand is upregulated during injury and diseases and therefore suggested to be involved in early BBB breakdown (Nourhaghighi et al., 2003). The detailed mechanism how Ang-2 induces BBB breakdown and whether Ang-2 alone could be the initiator for increase in brain permeability is still unknown and needs further investigated.

Angiopoietins are regulated during and after stroke incidence. After an MCAO in mice the expression ratio of VEGF and Ang-1 changes after 2 to 4 hours, whereby VEGF increases and Ang-1 levels become low (Plate et al., 1999; Beck et al., 2000; Zhang et al., 2000). However, between day 2 and 21 after stroke, Ang-1 expression increases (Beck et al., 2000; Lin et al., 2000). In contrast, Ang-2 is upregulated initially and detectable also after 24 hours of ischemia in infarct and peri-infarct areas (Beck et al., 2000; Lin et al., 2000; Zhang et al., 2002). Ang-2 levels remain increased up to 14 days (Zhang et al., 2002). In combination with VEGF, Ang-2 initiates the sprouting of new blood vessels in infarction areas (Beck et al., 2000) which is important for the nutrient and oxygen supply in the damaged tissue (Hansen et al., 2008; Beck and Plate, 2009). A clinical study with 300 stroke patients correlates high Ang-2 serum levels with an increased risk for stroke (Chen et al., 2010). The detailed mechanism how Ang-2 influences stroke is however unknown (Hansen et al., 2008; Beck and Plate, 2009).

#### **1.5 Aim of the study**

Angiopoietins are angiogenic factors that contribute to remodeling processes of the vasculature. Ang-2 diminishes numbers of pericytes that have been demonstrated to regulate the neurovascular permeability at the NVU (Armulik et al., 2010) implying a certain role for Ang-2 in BBB permeability. In relation to permeability processes, Ang-1

has been reported to prevent vascular leakage (Thurston, 1999) while Ang-2 has been shown to increase vascular permeability in non-brain endothelial cells *in vitro* and *in vivo* (Benest et al., 2013; Ziegler et al., 2013). Ang-2 is increased in several pathological states in the brain and in particular highly expressed in inflamed brain tissues (Scholz et al., 2011). The mechanisms how Ang-2 / Tie2 signaling act on the BBB under physiological conditions and its role in brain pathogenesis remain unclear.

We therefore hypothesized that Ang-2 is a critical factor that leads to a breakdown of the BBB. In order to elucidate the role of Ang-2 in BBB permeability, a transgenic mouse model was used to specifically overexpress human Ang-2 in endothelial cells using a doxycycline TetOff system (Reiss et al., 2007). By removing doxycycline from birth mice continuously overexpress hAng-2. After an expression period of 8-12 weeks, the BBB function was investigated. Permeability analysis utilizing transendothelial electrical resistance (TEER) measurements and expression analysis of cellular junctional components were employed *in vitro* using cultured microvascular endothelial cells and *ex vivo* using freshly isolated brain microvessels. Further *in vivo* experiments using transgenic mice concentrated on tracer permeability studies and structural analysis of the NVU by immunohistochemistry and electron microscopy.

As Ang-2 is highly expressed in a number of diseases, we further aimed to study the impact of Ang-2 in brain permeability under pathological conditions. To this end, a permanent and transient mouse stroke model was employed. Therapeutic approaches for increasing the phosphorylation of Tie2 will also be tested for an improved outcome after stroke incidence.

## 2. METHODS

### 2.1 Animals

All animals were treated ethically according to the local guidelines for care and use of laboratory animals. The number of animals was kept to a minimum to obtain statistically valid results.

#### 2.1.1 Breeding

The hAng-2 gain-of-function mice (CD1 background) were obtained by using a tetracycline-controlled transcriptional activator (Tet-Off) system (Reiss et al., 2007). Double transgenic offspring derived from the cross between a mouse carrying the tTA driver transgene, driven by the endothelial-specific promoter Tie1, and a mouse carrying the responder transgene TetOS-hAng-2 have the tTA protein binding to the tetracycline-responsive element containing TetOS with minimal promoter that drives the expression of hAng-2 in endothelial-specific manner. This interaction of tTA and TetOS was prevented by supplying the tetracycline analogue, doxycycline, which was given to the animals in food pellets (100 mg/kg, ssniff Spezialdiäten GmbH). The transgenic animals were generally fed with doxycycline including pregnant mice that carry the double transgenic litters. Induction of hAng-2 overexpression at P0 was achieved by withdrawing doxycycline-containing food. Control animals were wild types of transgenic littermates which did not express hAng-2 or Tie1 validated by PCR analysis. 8 to 12 week old hAng-2 overexpressing and control mice were predominately used in this study.

8 to 10 week old wild type C57 / Bl6 mice (The Jackson laboratory) were used for an *in vitro* permeability assay, whereas Ang-2 transgenic mouse lines in C57 / Bl6 background based on the before described system were used for permanent stroke experiments. For therapeutic approaches in stroke experiments CD1 wild type mice from Charles River laboratories were applied.

#### 2.1.2 Genotyping

Genotypes of transgenic animals were determined by polymerase chain reaction (PCR). Tail biopsies from 3 to 4 week old mice were lysed with 300 µl tail lysis buffer and 3 µl of proteinase K, shaking on a dry heat block at 1,300 rpm at 55 °C over night (ON). The enzyme was inactivated by heating the samples at 99 °C for 20 min and the extracted DNA was stored at -20 °C until use. PCR was performed to amplify the specific DNA

sequence with primers designed for the tTA and the transgene containing human Ang-2 (see Appendix 6.4.1). The following reaction mixture was prepared for PCR:

Table 2-1: Reaction mixture for PCR

Components	Volume [ $\mu$ l]
ddH <sub>2</sub> O	14.7
10 x PCR buffer	2
MgCl <sub>2</sub> (10 $\mu$ M)	0.7
dNTPs (2.5 mM)	0.5
Primer fw (10 $\mu$ M)	0.5
Primer rev (10 $\mu$ M)	0.5
Taq polymerase (5 units/ $\mu$ l)	0.1
DNA	1

PCR was then performed by a thermal cycler using the following program:

Table 2-2: PCR program

Step	Temperature [ $^{\circ}$ C]	Time	Cycles
Initial denaturation	94	4 min	1
Denaturation	94	40 sec	30
Annealing	54	40 sec	30
Elongation	70	1 min	30
Final elongation	70	10 min	1

The PCR products were analyzed by agarose gel electrophoresis using a 1 % agarose gel in 0.5 x TBE buffer containing ethidium bromide. 4  $\mu$ l of 6 x loading buffer (Blue juice) was added to 20  $\mu$ l PCR products. The mixture was loaded onto the gel and subjected to electrophoresis at 80 V for 45 min. The amplified DNA was visualized by UV transilluminator.

### 2.1.3 Collection of blood serum and enzyme-linked immunosorbent assay (ELISA)

One day before experiments with mice were performed, 100 - 200  $\mu$ l of the peripheral blood was collected from the vena facialis with a 20 G needle (BD) in a Z-Gel tube. The serum was obtained from the hematocrit by centrifuging the tube at 13,000 rpm for 5 min at room temperature (RT). ELISA was performed on the serum to determine protein levels of mAng-1 and hAng-2 according to the manufacturer's instructions (R&D).

### 2.1.4 Anesthesia

For perfusion experiments, mice were anesthetized with a mixture of 10 mg/kg xylazine, 100 mg/kg ketamine in 4.5 ml 0.9 % NaCl solution. Freshly-prepared anesthesia was injected intraperitoneally at 10  $\mu$ l/body weight (g). This anesthesia protocol was predominantly used unless otherwise stated.

### 2.1.5 Perfusion

Mice were anesthetized as described in section 2.1.4. Mice inhaled Isofluran (Abbvie) contained in a 50 ml Falcon. Once mice lost consciousness the thorax was opened and a butterfly needle (23 GA) connected to a peristaltic pump was inserted into the left ventricle. 5 ml of 0.1 M PBS was infused for 1 min through the pump. Meanwhile an incision was made on the left atrium to create an outlet of the flow. Depending on the experiment, mice underwent further perfusion e.g. with fixatives.

## 2.2 Isolation of mouse brain microvascular endothelial cells (MBMECs)

A modified protocol was utilized to isolate endothelial cells for *in vitro* cell culture experiments (Czupalla 2014). The meninges of freshly isolated brains collected in buffer A (see 6.3.4) were removed by gently rolling the brain on Whatman filter membranes. 4 - 6 mouse brains were pooled and homogenized ten times in a dounce homogenizer (Wheaton, 0.025 mm clearance). Brain homogenates were centrifuged at 1,500 rpm for 10 min at 4 °C. The pellet was then digested with 0.75 % Collagenase II in buffer A (1:1:1 volume ratio) for 1 h while shaking at 37 °C. The digested pellet was centrifuged at 1,500 rpm for 5 min at RT and the supernatant was discarded. To remove myelin, the pellet was resuspended in 10 ml 25 % BSA / PBS and centrifuged at 3,000 rpm for 30 min at 4 °C. The supernatant was discarded and the pellet was further digested with Collagenase / Dispase and DNase I in buffer A for 12 min at 37 °C. After centrifugation, MBMECs resuspended in MCDB131 complete growth medium were seeded on 6 well-



---

plates, pre-coated with type 1 Collagen (150  $\mu\text{g}/\text{cm}^2$ ). After a 4 h incubation, the medium was changed to puromycin (5  $\mu\text{g}/\text{ml}$ ) containing medium, which was subsequently changed back to puromycin-free medium after 3 days.

### **2.3 Isolation of mouse brain microvessels (MBMVs)**

Two isolated brains with meninges removed by a Whatman filter membrane were pooled, homogenized in MVB buffer in a dounce homogenizer (Wheaton, 0.025 mm clearance), and centrifuged at 1,500 rpm for 10 min at 4 °C. The pellet was resuspended in 25 % BSA / PBS and centrifuged at 3,000 rpm for 30 min at 4 °C to remove the myelin. The microvessel pellet was resuspended in MVB buffer and filtered through a 40  $\mu\text{m}$  nylon mesh (BD). For protein analysis (section 2.7.3), the microvessels were resuspended in HES buffer with a protease and phosphatase inhibitor cocktail and stored at -80 °C. For mRNA expression analysis, the microvessels were lysed in 400  $\mu\text{l}$  RLTplus buffer (Qiagen) with 1:100  $\beta$ -mercaptoethanol and stored at -80 °C until use.

### **2.4 Culture of mammalian cells**

Cells were cultured in a humidified incubator at 37 °C with 5 %  $\text{CO}_2$ . Freshly isolated MBMECs and bEND5 cells were grown in MCDB131 growth medium and passaged approximately twice a week to prevent a complete confluency. For passaging, growth medium was removed by aspiration and the cells were washed twice with PBS and treated with 0.05 % Trypsin-EDTA for 5 min in the incubator to detach the cells from the culture flask. The cells were then resuspended in the growth medium for plating.

#### **2.4.1 Freezing and thawing of mammalian cells**

For a long-term storage, cells were washed and trypsinized as described in section 2.4, resuspended in fresh growth medium and transferred to a 15 ml Falcon tube. The cell suspension was centrifuged at 1,500 rpm for 5 min, and the cells were resuspended in freezing medium (MCDB131 medium containing 50 % FCS and 10% dimethyl sulfoxide (DMSO)) and aliquoted into cryo tubes. The cryo tubes were stored in a freezing container with isopentane at -80 °C refrigerator overnight before transferring into liquid nitrogen.

For thawing, the cells were resuspended in pre-warmed growth medium and centrifuged at 1,500 rpm for 5 min. The medium was aspirated to remove residual DMSO and the cells were resuspended in fresh growth medium and plated in cell culture dishes.

#### 2.4.2 Cell counting using a hemacytometer

For determining the number of cells, 10  $\mu$ l of a 1 ml cell suspension was transferred into a Neubauer hemacytometer. The number of cells in four sets of 16 corner squares of one hemacytometer grid was counted under the microscope at 20 x magnification. The total cell number was calculated with the following equation:

$$\text{Counted cell number} / 4 \times 10^4 = \text{cell number} / \text{ml}$$

#### 2.4.3 Transendothelial electrical resistance (TEER) measurement

100,000 cells /  $\text{cm}^2$  of isolated MBMECs were seeded onto 1  $\mu$ m pore 24-well PET transwell inserts (Greiner Bio One), pre-coated with 5  $\mu\text{g}/\text{cm}^2$  fibronectin. The cells were incubated in MCDB131 growth medium. The inserts were transferred to a cellZscope® device placed in a humidified incubator (37 °C, 5 %  $\text{CO}_2$ ) and impedance measurements were obtained continuously (Czupalla et al., 2014). Treatment was initiated upon reaching a plateau in TEER levels. Cells were treated with 500 ng/ml recombinant hAng-2, diluted in 0.1 % BSA / PBS, up to 72 h. The control cells were treated with the equivalent amount of 0.1 % BSA / PBS.

#### 2.4.4 *In vitro* permeability assay

MBMECs were isolated from 4-6 animals (C57 / Bl6 mice, The Jackson Laboratory) in each experiment and cultured on the apical side of the transwell inserts as described in section 2.4.3. The MBMEC monolayers were then incubated with the following tracers at a final concentration of 10  $\mu\text{M}$ : 0.45 kD Lucifer Yellow (LY, Sigma), 3 kD Texas Red-conjugated dextran (TXR, Invitrogen), 20 kD Tetramethylrhodamine-conjugated dextran (TMR, Sigma) and 70 kD FITC-conjugated dextran (FITC, Sigma) (Czupalla et al., 2014). In order to measure the permeability, 100  $\mu$ l of the medium from the bottom chamber was collected at a desired time point and the relative fluorescence unit (RFU) was measured by a fluorescence plate reader (Tecan) at the corresponding tracer excitation / emission (see the table 2-3) and normalized to the RFU of the apical chamber. The permeability flux was then obtained as a ratio of bottom to top chamber RFU. The permeability flux of the controls was set to 100%.

Table 2-3: Wavelengths of different tracers

Tracer	Excitation [nm]	Emission [nm]
LY	425	525
TXR	595	625
TMR	550	580
FITC	490	520

## 2.5 *In vivo* studies / animal models

### 2.5.1 Permeability assay using small tracers

A 1:2 mixture of Texas Red-3 kD dextran (1 mM) and 0.45 kD Lucifer Yellow (10 mM) was injected into the tail vein of mice (100  $\mu$ l per mouse) and allowed to circulate for 4 min. The control animals received the same amount of PBS instead of the tracers. The animals were anesthetized and transcardially perfused with PBS for 1 min to remove the intravascular dye. During the perfusion, the blood was collected in a Z-Gel tube by cardiac puncture. The serum was obtained according to section 2.1.3 and its RFU was measured by a fluorescence plate reader (Tecan). In order to determine paracellular permeability, the hemi-brain or a single kidney were harvested in 500  $\mu$ l PBS, homogenized and centrifuged at 13,000 rpm for 15 min at 4 °C. The supernatant was then measured in a fluorescence 384 well-plate reader (Tecan) at excitation / emission wavelength of 425 / 525 nm for Lucifer Yellow and 595 / 625 nm for Texas Red-3 kD dextran in order to obtain the RFU. The paracellular permeability index / percentage of the tissue was calculated as follows:

The paracellular permeability / diffusion flux brain fraction = tissue RFU / serum RFU / tissue weight [mg]

The remaining brain and kidneys were weighed and immediately stored in 500  $\mu$ l PBS at -80°C for the protein expression analysis by immunoblotting (Section 2.7), or frozen in Tissue TEK® O.C.T. Compound (Sakura) on dry ice for histological analysis.

### 2.5.2 Permeability assay using Evans Blue

2 % Evans Blue in PBS (70 kD when bound to albumin) was injected intravenously into the tail vein of mice and allowed to circulate for 2 h. After transcardial perfusion with PBS, the brains were weighed, minced with a scalpel and transferred into a tube containing formamide. The samples were incubated at 67 °C for 24 h, followed by centrifugation at 13,000 rpm for 1 h at 4 °C. 200 µl of the supernatant and 200 µl of formamide for background subtraction were transferred into a 96 well-plate fluorescence plate reader (Tecan). The absorbance of the supernatants was measured at 620 nm. The amount of extravasated Evans Blue was calculated using the following formula:

$(\text{absorbance of the supernatant [nm]} - \text{absorbance of formamide [nm]}) / \text{weight of the hemi-brain [g]}$

Some brain samples were not used for absorbance analysis but collected for histological experiments.

### 2.5.3 Electron microscopy (EM)

Mice were anesthetized and transcardially perfused with PBS for 1 min as described in section 2.1.5, followed by fixation with 4 % PFA / 2 % glutaraldehyde / PBS for 4 min. Isolated brains were further fixed in 1 % OsO<sub>4</sub> at RT for 2.5 h and then stained with 2 % uranyl acetate at 4 °C ON. The samples were dehydrated through an acetone gradient (15-20 min each in 30 %, 50 %, 60 %, 70 %, 80 %, 90 % and 100 % acetone). The dehydrated brains were immersed in 1:1 in acetone / Durcupan for 1 h and subsequently in Durcupan alone for 1 h at RT before polymerized at 60 °C for 72 h. The sections were analysed using Tecnai Spirit BioTWIN FEI electron microscope at 120 kV. Images were taken with an Eagle 4K CCD bottom-mount camera.

### 2.5.4 Staining of the glycocalyx

To stain for the glycocalyx, mice were anesthetized with xylazine / ketamine as described in section 2.1.4 and perfused with 2 % glutaraldehyde / 2 % saccharose / 0.1 M sodium cacodylate buffer, containing 2 % lanthanum nitrate (pH 7.4). The brains were isolated, post-fixed for 2 h in the same perfusion solution and subjected to 2 % H<sub>2</sub>O<sub>2</sub> / 2 % saccharose / 0.1 M sodiumcacodylate buffer, containing 2 % lanthanum nitrate for 12 h at 4 °C, followed by rinsing with 0.03 M NaOH and 2 % saccharose. The contrast was

increased by using a 2 % OsO<sub>4</sub> and 2 % lanthanum nitrate, followed by embedding in araldite. Analysis of the glycocalyx was performed without any contrast enhancement to rule out a non-specific precipitation of the staining solutions. The sections were analysed using Tecnai Spirit BioTWIN FEI electron microscope at 120 kV. Images were taken with an Eagle 4K CCD bottom-mount camera.

#### 2.5.5 Animal models for ischemic stroke

Both permanent and transient ischemic stroke models were used in this study. The permanent stroke was introduced by occluding the middle cerebral artery (MCA) for 24 h, whereas the transient stroke was created by occluding the MCA for 30 min, followed by a reperfusion for 24 h before sacrificing the mice.

##### 2.5.5.1 Permanent stroke model

For the permanent middle cerebral artery occlusion (MCAO) model, 8-10 week old hAng-2 overexpressing and wild type mice from transgenic littermates (both C57 / Bl6 background) were used. Animals were anesthetized intraperitoneally with a combination of 80 mg/kg ketamine and 100 mg/kg xylazine. During the procedure of occlusion, animals were placed on a heating pad to maintain the body temperature. An incision was made between the left eye and the left ear. The temporal muscles were transected to expose the skull. A 1-2 mm hole was made with a drill in the region over the MCAO. The ligation was made using a 10-0 nylon thread and a cut was made distally to the ligation point. The temporal muscles were placed back together, the wound was sutured, and the animals were returned to their cages after regaining consciousness. Sham animals were treated in the same way except performing the ligation for occlusion. Mice were sacrificed after 24 h and the brains were frozen in Tissue TEK® O.C.T. compound and stored in the -80 °C freezer. They were used for the histological analysis of the stroke.

##### 2.5.5.2 Transient stroke model

Wild type CD1 mice (Charles River) were anesthetized with 1.5 % isoflurane and 0.1 mg / kg buprenorphine (Temgesic, Essex Pharma). The surgery took place under a microscope with 16 x - 40 x magnification. The skin was cut at the right side of the thyroid gland. The muscles were retracted and the arteria carotis, vena jugularis and nervus vagus were exposed. The arteria carotis communis was proximally ligated, the arteria carotis externa was permanently ligated, and the arteria carotis interna was temporally

ligated with a clip. A small hole was made into the arteria carotis communis by a scissor and a silicone-coated 7-0 monofilament was inserted to occlude temporarily. The mouse was sutured and then re-opened after 30 min to remove the silicone-filament for reperfusion. The retracted muscles were put back together and the wound was sutured. After obtaining consciousness mice were returned to their cages and sacrificed after 24 h. The brain was isolated and cut into 2 mm slices using a stainless mouse brain slicer matrix for further analysis. Parts of the brain were frozen in Tissue TEK® O.C.T. compound for histological analysis. Other parts were incubated in TTC (2,3,5 triphenyltetrazolium chloride) for approximately 5 min in a dark chamber to determine the infarct area. The TTC-stained slices were scanned and analyzed by ImageJ.

#### 2.5.6 VE-PTP treatment

The effect of the vascular endothelial protein tyrosine phosphatase (VE-PTP) inhibitor was examined in the transient stroke model (section 2.5.5.2). Mice were pre-treated subcutaneously with 30 mg/kg VE-PTP inhibitor 14 h and 2 h before the surgery. Approximately 10 h after the surgical intervention mice were again injected with the inhibitor of VE-PTP.

## 2.6 RNA isolation and analysis

### 2.6.1 RNA isolation

RNA isolation was performed using RNeasy Plus Micro Kit (Qiagen) according to the manufacturer's instructions. Isolated microvessel fragments were homogenized by vortexing for 1 min at RT. Equal volume of 70 % ethanol was added to the samples and mixed well by pipetting. The mixture was transferred to RNeasy MinElute spin columns, placed on collection tubes, and centrifuged. After washing the columns with RW1 buffer and RPE buffer, 80 % ethanol was added and centrifuged for 5 min. The purified RNA was eluted in 14 µl RNase-free water.

### 2.6.2 Determination of RNA concentration (Experion)

The Experion is an automated electrophoresis system for determination of RNA quality and quantity. A microfluidic chip is used with a series of plastic wells, which is connected to small glass well plates. The glass plates contain microchannels, which are primed with

a gel matrix. The samples are directed through these microchannels from the electrophoresis station by controlling the voltage.

The electrodes of the Experion system were cleaned with an electrode cleaner before running the system. A provided RNA gel was filtered through an RNA spin filter tube at 1,500 x g for 10 min. 65 µl of this solution was mixed with 1 µl RNA stain. 1 µl of isolated RNA samples was used for quantitation. The RNA ladder (provided from Experion RNA StdSens Starter Kit, Bio-Rad) and the RNA samples were denatured at 70 °C for 2 min, following a cool-down for 5 min on ice. The Experion Std Sens Chip was primed with a filtered gel stain solution for 30 sec. 5 µl of the loading buffer was pipetted into each well together with 1 µl of the RNA sample. The primed chip with its samples was then placed into an electrophoresis system.

### 2.6.3 Determination of RNA concentration (Photometer)

RNA concentration was measured by a spectrophotometer (Eppendorf) at a wavelength of 260 nm. To assess RNA purity, the 260 / 280 and 260 / 230 ratios were determined (280 nm: absorption indicates protein contamination, 230 nm: absorption indicates contamination by organic compounds). The 260 / 280 ratio in the range of 1.8 - 2.0, and the 260 / 230 ratio between 2.0 and 2.2 indicated clean RNA preparations. RNase-free water was used as a blank.

### 2.6.4 cDNA synthesis

12 µl of the RNA product was used for cDNA synthesis. The reverse transcription was performed according to the manufacturer's instructions (RevertAid H Minus First Strand cDNA synthesis Kit; Thermo Scientific).

Table 2-4: The reaction mixture for reverse transcription

Ingredients	Volume [µl]
random hexamer primer	1
5x reaction buffer	4
RiboBlock™ RNase Inhibitor [20 u / µl]	1
10 mM dNTP Mix	2
RevertAid™ H Minus Reverse Transcriptase [200 u / µl]	1

The ingredients were mixed together with RNA on ice, vortexed and spun down for a few seconds. The samples were incubated at 25 °C for 5 min, followed by another incubation at 42 °C for 60 min. The reaction was inactivated by heating at 70 °C for 5 min. Subsequently, 1 µl of RNase H (1 U / µl) was added to the mixture at 37 °C for 30 min. The newly synthesized cDNA was directly used for quantitative real time PCR (section 2.6.5) or stored at -20 °C.

### 2.6.5 Quantitative Real Time PCR (qPCR)

The SYBR® Green system (Thermo Scientific) was used for qPCR analysis, which provides a non-specific dye that intercalates in DNA double-strands.

The reaction of qPCR was performed in ABgene PCR plates (Thermo Scientific), sealed with a Clear Seal Diamond Heat Sealing Film (Thermo Scientific) and run in a CFX96™ Real-Time System (Bio-Rad) according to the following protocol and procedure.

Table 2-5: The reaction mixture for qPCR

Ingredients	Volume [µl]
ddH <sub>2</sub> O	5
SYBR Green Mix	10
cDNA (150 ng/µl)	1
Primer forward (1 µM)	2
Primer reverse (1 µM)	2

Table 2-6: qPCR program

Step	Temperature [°C]	Time [min]	Cycles
Initial denaturation	95	15	1
Denaturation	95	0:30	45
Annealing	61	0:30	45
Elongation	72	0:35	45
Termination	95	1	1
Melting Curve	55-95	0:10	80



For quantitation of the target sequence the mean Ct value of a housekeeping gene (CD31) served as a reference. Using the reference gene, the relative expression of cDNA was calculated with iQ5 software (Bio-Rad).

## **2.7 Protein analysis**

### **2.7.1 Protein extraction from cultured cells**

The medium was removed and the cells were washed twice with ice-cold PBS and harvested on ice in RIPA lysis buffer with proteinase (Complete Mini EDTA free, Roche) and phosphatase inhibitors (PhosSTOP, Roche). The cell lysates were transferred into a tube and centrifuged at 13,000 rpm for 10 min at 4 °C. The supernatant was transferred to a fresh tube and the protein concentration was determined (section 2.7.3). The protein lysate was then denatured (section 2.7.4) for protein expression analysis by immunoblotting.

### **2.7.2 Protein extraction from tissues**

Tissues were snap-frozen in liquid nitrogen and stored in the -80 °C freezer until use. The frozen tissue was thawed on ice and immediately immersed in 500 µl RIPA buffer with proteinase and phosphatase inhibitors (Roche) and transferred to a Precellys Ceramic Kit tube (Peqlab). The tissue was homogenized twice by a Minilys homogenizer (Peqlab) for 30 sec at full speed, followed by centrifugation at 13,000 rpm for 10 min at 4 °C. After determining the protein concentration, the protein lysate was denatured (section 2.7.4).

### **2.7.3 Determination of protein concentration**

Isolated MBMVs in HES buffer were thawed on ice, followed by 5 x ultrasound sonication (10 cycles, 30 sec pause) for disrupting the cell membranes.

Pierce BCA Protein Assay Kit (Thermo Scientific) was used for protein concentration measurements according to the manufacturer's instructions. 1.5 µl of cell lysate was incubated at 37 °C for 30 min with the working reagent. BCA (bicinchoninic acid) forms a complex with proteins and develops a purple colour. The protein concentration was measured in duplicates at 562 nm with a spectrophotometer and calculated using a BSA standard curve.

For bEND5 cells, MBMECs and stroke brain samples the DC Protein Assay Kit (Bio-Rad) was applied. 5 µl of 1:10 diluted tissue samples or 5 µl of cell lysate were directly transferred in triplicates into a 96 well-plate. 1 ml of reagent A was mixed with 20 µl of reagent S. 25 µl of this mixture was then added to the cells. Subsequently 200 µl of reagent B was appended to the cells. After an incubation time for 15 min at RT the 96 well-plate was measured at 750 nm with a spectrophotometer. A BSA standard curve was used for determination of protein concentration.

#### 2.7.4 Protein solubilization and denaturation

MBMV samples were solubilized and denatured in a 2:1 mixture of UREA / SDS buffer while shaking on a dry heat block at 600 rpm at 30 °C for 1.5 h. Tissue and other cell lysates were denatured with 4 x SDS sample buffer (Merck Millipore) at 80 °C for 10 min.

#### 2.7.5 Immunoblotting

##### 2.7.5.1 SDS – polyacrylamide gel electrophoresis (PAGE)

For protein expression analyses, SDS polyacrylamide gel electrophoresis was used, which separates proteins according to their molecular weight.

Self-made Tris-Glycine or 4-12 % precast Bis-Tris gels (Life technologies) were used for the analyses. The percentage of the gels were determined according to the size of the proteins to be analysed. Gels were produced by polymerization of acrylamide. Protein samples were loaded on to the gel and SDS-PAGE was performed in 1 x running buffer (Tris-Glycine running buffer for Tris-Glycine gels, MOPS buffer for Bis-Tris gels) at 80 V-120 V. PageRuler Plus Prestained Protein Ladder (Thermo Scientific) was used as a protein molecular weight marker.

##### 2.7.5.2 Protein blotting

After resolving proteins by SDS-PAGE, the gel was taken out of the cassette and a filter membrane (Whatman paper), pre-soaked in 1 x Tris-Glycine transfer buffer, was placed on top of the gel. Either a nitrocellulose membrane or a PVDF membrane was placed on the other side of the gel, on top of which another pre-soaked anode filter paper was placed. Any trapped air bubbles were removed. The PVDF membrane was immersed in methanol and equilibrated in the transfer buffer prior to usage. A blotting pad, pre-soaked in the transfer buffer, was placed into the cathode side of the blotting cassette. The gel-

membrane assembly was placed on top of the pad in the same sequence so that the gel is closer to the cathode side than the membrane. Another pre-soaked pad was placed on top of the assembly before the cassette was closed. The blotting cassette was then placed into a blotting module filled with the transfer buffer.

The blotting was performed at 36 V in a cold room ON or at 100 V on ice for 1 h. The membrane was stained afterwards in Ponceau S to verify the protein transfer and protein loading.

#### 2.7.5.3 Immunodetection of blotted proteins

Following the protein transfer, non-specific protein binding sites on the membranes were blocked by incubation in 1 x Roti Block in H<sub>2</sub>O or in 5% BSA / PBS-T (0.1% Tween-20 / PBS) (for phosphorylated protein detection) for at least 1 hour at RT. The membranes were subsequently incubated with primary antibodies diluted in the blocking buffer for 2 h at RT or ON at 4 °C. Following washing the membranes 3 x 10 min with PBS-T to remove unbound antibodies, they were incubated with corresponding secondary antibodies diluted in the blocking buffer for 1 h at RT. Secondary antibodies were coupled to horseradish peroxidase (HRP) for enhanced chemoluminescence (ECL) detection or to a fluorophore. The membranes were subjected to ECL detection if necessary, after washing them 3 x 10 min with PBS-T. The secondary antibody signals were visualised by Odyssey™ imaging device (LI-COR), which detects both chemiluminescent and fluorescent signals. Quantitation was performed using Image Studio 3.1 software (LI-COR).

## 2.8 Histology procedures

### 2.8.1 Tissue embedding and sectioning

Tissue samples (brain and kidney) were isolated from mice, embedded in Tissue TEK® O.C.T. compound (Sakura) and frozen on dry ice. 10 µm cryosections were cut by Microm HM550 microtome at -20°C, placed on Superfrost Microscope slides and dried on a heating plate set at 37 °C. The sections were stored at -80 °C with Silica pellets.

## 2.8.2 Staining procedures

### 2.8.2.1 Giemsa staining

Cryosections were thawed on a heating plate at 37 °C for 10 min and incubated in hemalum solution (Merck) for 3 min, and then in PBS to develop the characteristic blue stain for the nuclei. The sections were subsequently incubated with Eosin for 1 min at RT to stain non-nuclear tissue components. They were then dehydrated through an ethanol gradient (5 min each in 70 %, 96 % and 100 % ethanol) into xylene (2 x 5 min), before mounted with Entellan mounting medium (Merck).

### 2.8.2.2 Light microscopic staining

Cryosections were thawed on a 37 °C heating plate for 10 min and washed 3 x in PBS for 5 min. After fixation with 4 % PFA / PBS for 10 min at RT and repeating the washing step with PBS, sections were blocked in 5 % BSA / PBS / 0.1 % Triton-x 100 in a humidifying chamber. The sections were blocked further with 20 % normal serum (species-matched to the host of the secondary antibody) in 0.1 % Triton-x 100 / PBS and incubated with a primary antibody in 10 % NS / PBS / 0.1 % Triton-x 100 for 1.5 h at RT or ON at 4°C. Following a washing step, they were incubated with a corresponding biotinylated-secondary antibody 1.5 h at RT. The slides were washed and incubated with avidin-biotin peroxidase complex using Vectastain Elite ABC Standard Kit (Vector Laboratories), which was prepared 30 min in advance. The slides were washed again and incubated with the chromogenic substrate AEC (Vector Laboratories), which develops red color upon reaction with the avidin-biotin-peroxidase complex. Positive chromogenic reaction was observed under the microscope and stopped by washing 3 x in PBS. The slides were counter-stained with Meyer's hemalum solution for 20 sec, washed with dH<sub>2</sub>O, and mounted with Aqua PolyMount.

### 2.8.2.3 Immunofluorescence staining (desmin, aquaporin-4)

Cryosections were thawed on a heating plate at 37 °C for 10 min. They were fixed in 95 % ice-cold ethanol at -20 °C for 5 min, followed by acetone fixation at RT for 1 min. After washing the slides for 3 x 5 min in PBSA solution, they were incubated with a primary antibody in an antibody incubation buffer for 1.5 h at RT. Following a washing step, they were incubated with an Alexa Fluor fluorescent secondary antibody for 1.5 h at RT. The sections were post-fixed in 4 % PFA / PBS for 10 min at RT and washed in dH<sub>2</sub>O before

counterstaining with DAPI (0.3  $\mu$ M) in dH<sub>2</sub>O for 10 min at RT. After washing in dH<sub>2</sub>O, the sections were mounted with Aqua PolyMount.

#### 2.8.2.4 Immunofluorescence staining (VE-Cadherin, ZO-1, Claudin-5)

Cryosections were thawed on a 37 °C heating plate for 10 min and fixed in ice-cold methanol for 5 min at -20 °C. The sections were air-dried for 5 min under a fume hood and were blocked for 1 h in a permeabilization / blocking buffer. They were incubated with a primary antibody in the same antibody incubation buffer at 4 °C ON. After 3 x 5 min washing with PBS, the sections were incubated in an Alexa Fluor fluorescence-conjugated secondary antibody for 1.5 h at RT and were washed again with PBS 3 x 5 min. The tissue was counterstained with DAPI (0.3  $\mu$ M) for 10 min at RT. Slides were mounted with Aqua PolyMount.

#### 2.8.3 Slide preparation for tissues with water soluble tracers (Evans Blue)

As Evans Blue is a water soluble tracer cryosections were mounted in a different way compared to a normal staining procedure where Aqua PolyMount was used.

Every step was kept in the dark not to bleach the samples. The thawed cryosections were incubated in ice-cold acetone for 2 min, air-dried for 1 min under a fume hood and subsequently dehydrated in xylene for 1 min at RT. Slides were then mounted in Entellan (Merck).

#### 2.8.4 Image acquisition and analysis

Light microscopic pictures were taken with an Eclipse 80i (Nikon) microscope using the NIS Elements software (Nikon). The fluorescent images were taken with a confocal laser scanning microscope (Nikon) and analyzed using the NIS Elements software (Nikon).

### **2.9 FACS (Fluorescence activated cell sorting)**

In this study mice were sacrificed and the brain was isolated. The cerebellum and the bulbous were removed and the rest of the brain was transferred into an enzyme digestion mixture as follows: Collagenase P (0.2  $\mu$ g/ $\mu$ l), Dispase II (0.8  $\mu$ g/ $\mu$ l), DNase I (0.01  $\mu$ g/ $\mu$ l), Collagenase A (0.3  $\mu$ g/ $\mu$ l) in 3 ml HBSS.

The brain was transferred in 3 ml digestion mix and incubated for 15 min at 37 °C while rolling with gentle rotation. The supernatant was collected in a fresh Falcon tube with 4 ml FCS. 3 ml of fresh digestion mix was then added to brain samples and resuspended with a stripette. The supernatants were centrifuged at 1,400 rpm for 10 min at 4 °C and the pellet was resuspended in 4 ml of 25 % BSA / PBS to remove myelin. After another centrifugation step at 3,000 rpm for 30 min at 4 °C the supernatant was discarded which contains the myelin. The sample was then resuspended in 1 ml HBSS and filtered through a 30 µm mesh (R&D), which was washed with 2 ml HBSS to centrifuge it at 1,400 rpm for 10 min at 4 °C. The pellet was resuspended in 1 ml red blood cell lysis buffer and incubated for 10 min at RT to lyse the erythrocytes. Subsequently, 2 ml of FACS buffer (PBS + 5 % FCS) was added to the cells. They were centrifuged at 1,400 rpm for 10 min at 4 °C to remove the supernatant. The cells were incubated in 100 µl FACS buffer with 1 µl of antibodies for 30 min at 4 °C in the dark, and then washed with 1 ml FACS buffer, followed by centrifugation at 1,400 rpm for 5 min at 4 °C. The supernatant was removed and the cells were resuspended in 200 µl PBS. The single-cell suspension was analyzed by FACSCanto™ II flow cytometry (BD) and FlowJo analytical software (FlowJo, LLC).

### **2.10 Contribution of Collaborators**

In collaboration with Jadranka Macas EM analysis were performed. Julia Starke performed staining in pMCAO experiments and analyzed together with Prof. Dr. Michel Mittelbronn human stroke data. Together with Rajumar Vutukuri the tMCAO surgeries were performed and analyzed. With help of Dr. Maiko Yamaji parts of immunoblotting and IHC were performed. Dr. Heike Beck performed the pMCAO surgeries.

### **2.11 Statistical analysis**

All statistical analyses were performed with GraphPad Prism software (GraphPad Software). A value of  $p < 0.05$  was considered as statistically significant. Data in graphs are represented as mean  $\pm$  SEM. The number of animals, number of experimental repeats, and the specific statistical test employed are indicated in the corresponding figure legends.

### 3. RESULTS

#### 3.1 Determination of hAng-2 expression in transgenic mice

The influence of Ang-2 on brain permeability was investigated *in vivo* by employing a transgenic mouse model which overexpress hAng-2 specifically in endothelial cells. The mouse system was already introduced in 2007 and successfully used in hindlimb and inflammatory experiments (Reiss et al., 2007; Scholz et al., 2011). The overexpression of hAng-2 in Ang-2 transgenic mice is based on withdrawal of doxycycline (Dox) from food (see 2.1.1). The functionality of this mouse system was validated by initial experiments described below.

##### 3.1.1 Ang-2 DT mice overexpress hAng-2 in a doxycycline regulated manner

In order to evaluate hAng-2 overexpression in transgenic mice initial experiments concentrated on different time points by withdrawal of doxycycline. Blood was taken from 8 weeks old Ang-2 double transgenic (Ang-2 DT), heterozygous (het) and wild type (WT) mice which received food containing doxycycline. All different mouse genotypes expressed very low levels of hAng-2 as analyzed by ELISA studies. 24 h withdrawal of doxycycline resulted in a significant overexpression which was even higher after 7 days in Ang-2 DT mice (11000 pg/ml). The re-addition of doxycycline led to decreased hAng-2 levels, comparable with the normal expression before withdrawal that continued up to 4 weeks with doxycycline (Figure 3-1 A). In order to investigate special properties of the blood-brain barrier (BBB) we aimed to study transgene expression in adult mice, during a period where already the BBB is formed. Consequently, overexpression was induced in mice from birth and hAng-2 expression was analyzed from age 8 to 12 weeks. Indeed, Ang-2 expression was dramatically increased in Ang-2 DT mice compared to wild type (Figure 3-1 B). These data validate the use of the transgenic mice for the endothelial specific expression. The following experiments were performed with 8 to 12 weeks old CD1 mice unless specified otherwise.

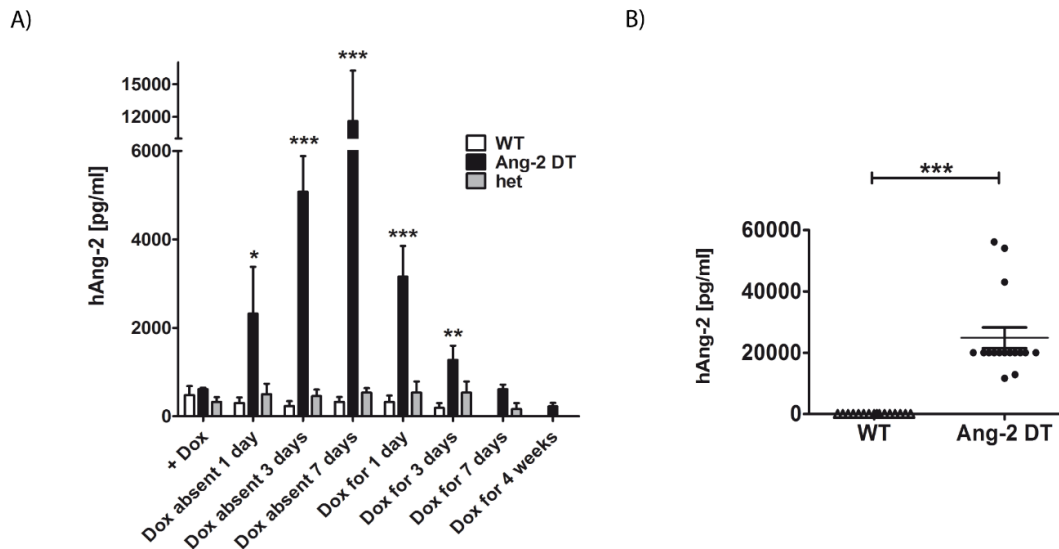


**Figure 3-1: Doxycycline based Ang-2 expression**

A) 8 weeks old Ang-2 DT, wild type and heterozygous mice were used for ELISA studies. Blood was taken from these mice and an ELISA was performed to investigate hAng-2 expression. Doxycycline was withdrawn from food up to seven days which corresponded to the highest hAng-2 expression. The opposite effect was verified by addition of doxycycline to the same mice up to 4 weeks, which brought Ang-2 to control WT levels (WT n = 6; het n = 5; Ang-2 DT n = 3; Anova by posthoc t-test; \* p < 0,05; \*\* p < 0,01; \*\*\* p < 0.001, compared to WT). B) hAng-2 was overexpressed significantly after 8 weeks of withdrawal of doxycycline from birth (n = 16 each group; 2-tailed unpaired t-test; \*\*\* p < 0.001 compared to WT).

### 3.1.2 Mouse brain microvessels of Ang-2 DT mice express high levels of Ang-2

We already evidenced that the systemic overexpression of hAng-2 in Ang-2 transgenic mice is functional in blood serum (Figure 3-1) as previously shown in another study (Scholz et al., 2011). In order to show this overexpression in the brain mRNA of mouse brain microvessels (MBMVs) were analyzed from wild type and Ang-2 DT mice. Ang-2 RNA levels significantly increased in brain microvessels of Ang-2 DT mice while the expression of its receptor tyrosine kinase Tie2 did not change compared to wild type littermates (Figure 3-2). This validates the use of these transgenic mice for investigating the effects of Ang-2 on BBB permeability.



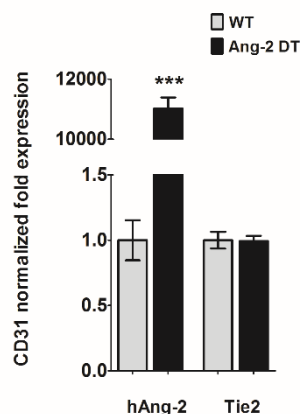


**Figure 3-2: Overexpression of hAng-2 was verified in Ang-2 DT mice**

Two brains of each genotype were used for the isolation of MBMVs in each preparation for qPCR analysis. It reveals that hAng-2 is indeed overexpressed in Ang-2 DT mice whereas Tie2 shows the same expression compared to wild type (n = 3 preparations using 2 mice / group and time point; 2-tailed unpaired t-test; \*\*\* p < 0.001 compared to WT). CD31 normalization was performed to account for the variation in vessel quality yielded in different preparations.

### 3.2 Ang-2 is associated with increased permeability of brain microvessels *in vitro* and *in vivo*

Increased permeability in the periphery of vascular endothelial cells has already been described to be associated with Ang-2 (Benest et al., 2013; Ziegler et al., 2013). In order to evaluate the role of Ang-2 in specialized endothelial cells of the brain forming the BBB, CD1 mice overexpressing hAng-2 in an endothelial specific manner were used for permeability analysis *in vitro* and *in vivo*.

#### 3.2.1 Increase in permeability of MBMECs with hAng-2 treatment and in mice overexpressing Ang-2

The effect of Ang-2 on permeability was investigated with primary mouse brain microvascular endothelial cells (MBMECs) utilizing cellZscope, a device for continuous cell monitoring that measures the transendothelial impedance of MBMEC monolayers. Cells seeded on transwell inserts (1  $\mu$ m PET) were transferred to cellZscope and grown for 2 - 3 days until confluency, indicated by a plateau in the transendothelial electrical resistance (TEER) values (Figure 3-3 A). TEER values of Ang-2 DT MBMECs were significantly decreased by 24 h and 48 h after seeding compared to wild type MBMECs (Figure 3-3 A,B), indicating an increase in paracellular permeability (Czupalla et al., 2014). These effects were also evaluated in wild type MBMECs treated with recombinant hAng-2. The pre-treatment values were set to 100 % to assess the effect of hAng-2

treatment, which resulted in a decrease after 24 h and 48 h (Figure 3-3 C) similar to MBMECs of Ang-2 overexpressing mice (Figure 3-3 B). To clarify that the Ang-2 mediated effect on permeability was not specific to MBMECs, mouse endothelioma cells (bEnd5 cells) were also studied. The outcome was comparable to the results from MBMECs (Figure 3-2 B-C) although the decrease was not significant (Figure 3-3 D).

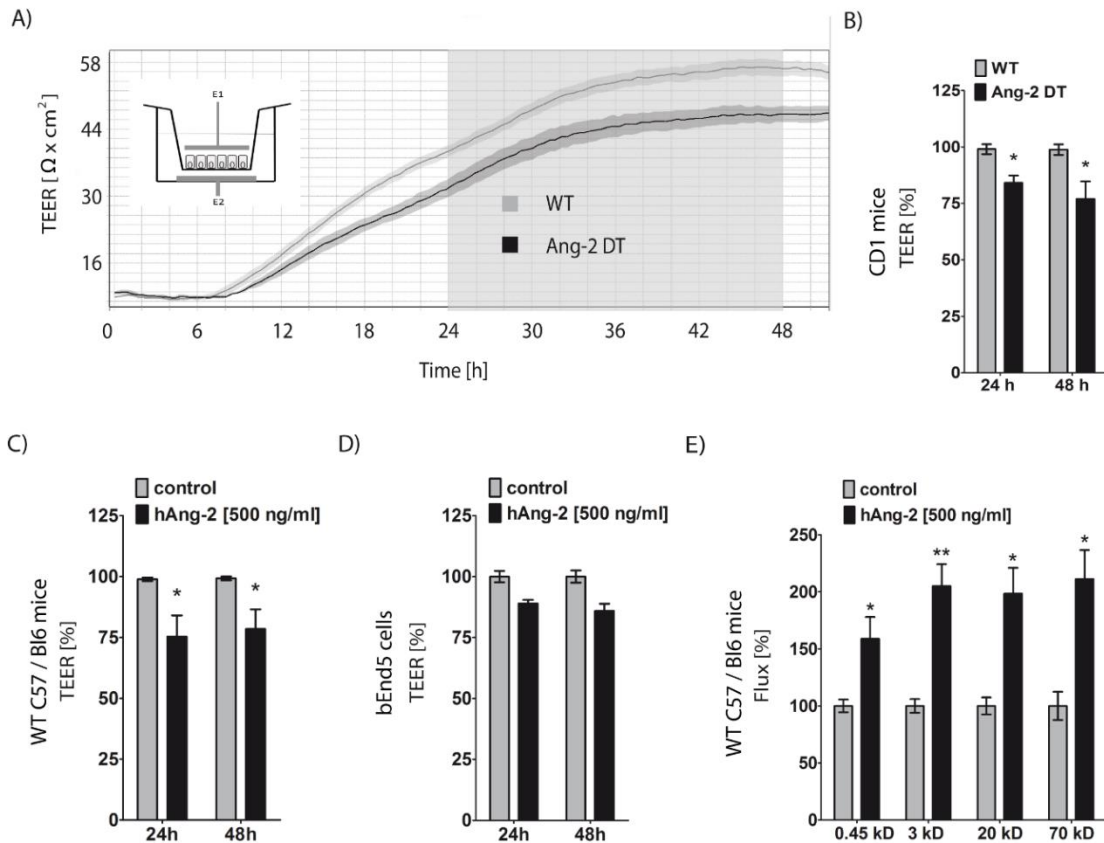


**Figure 3-3: Ang-2 mediated decrease in brain endothelial resistance**

Isolated MBMECs were grown to confluency on transwell inserts and were transferred to a cellZscope device, which measures the TEER values of the endothelial cell monolayer in a continuous fashion. A) A representative image is shown with the resistance in  $\Omega \times \text{cm}^2$  that shows the plateau in the monolayers at 48 h and a decrease in TEER of MBMECs from Ang-2 DT mice compared to wild type. B) The quantitation of the TEER measurements between wild type and Ang-2 DT mice is presented as mean  $\pm$  SEM and shown in relative % scale ( $n = 3$ , \*  $p < 0.05$  compared to WT). C) MBMECs from wild type mice were treated with recombinant hAng-2 (500 ng/ml) or with 0.1 % BSA in PBS (control). A significant decrease in the resistance was detectable after 24 h and 48 h with TEER values shown in relative % of control ( $n = 3$ , \*  $p < 0.05$ ). D) bEnd5 cells treated with recombinant hAng-2 (500 ng/ml) also showed in tendency a lower resistance compared to control (0.1 % BSA in PBS;  $n = 3$ ). E) Wild type MBMECs on transwell inserts treated for 24 h with recombinant hAng-2 (500 ng/ml) or with 0.1 % BSA in PBS (control) followed by addition of fluorescent tracers of different sizes to the top chamber (0.45 kD Lucifer Yellow, Texas Red 3 kD-dextran, Tetramethylrhodamine 20 kD-dextran, FITC 70 kD-dextran). The fluorescence of the medium in the bottom chamber was measured in a plate reader 1 h after the addition of tracers. All the tracers showed a higher flux when treated with recombinant hAng-2 ( $n = 3$ ; \*  $p < 0.05$ ; \*\*  $p < 0.01$ ). B-E statistical analysis was performed by One-way Anova to account for inter-prep variations.

The effect of Ang-2 on endothelial permeability was confirmed with an additional permeability assay using fluorescent tracers of different molecular weights and another mouse strain (C57 / Bl6) to rule out strain specific effects of Ang-2 on permeability. Wild type MBMECs were treated with recombinant hAng-2 for 24 h followed by addition of different sized fluorescent tracers (Lucifer Yellow 0.45 kD, TexasRed 3 kD-dextran, tetramethylrhodamine (TMR) 20 kD-dextran and FITC 70 kD-dextran). All tracers showed significantly higher flux in the endothelial monolayers treated with recombinant hAng-2 compared to control (Figure 3-3 E). Dextran permeability as well as the impedance data establishes a direct effect of Ang-2 on brain endothelial cells both in wild type and transgenic mice that is potentially via the intercellular junctions as both the assays measure primarily paracellular transport.

### 3.2.2 Ang-2 overexpression increases brain permeability to small tracers *in vivo*

To further determine whether Ang-2 plays a role in brain microvascular endothelial cells *in vivo*, permeability was assessed by intravenous injection of different sized tracers. Permeability to Evans Blue, a dye that binds to albumin (70 kD) that was circulated for 2 h was not different between wild type and Ang-2 transgenic mice (Figure 3-4 A-C). Neither in the immunohistochemistry sections nor in the absorbance values for Evans Blue of perfused brain homogenates differences could be detected between wild type and Ang-2 transgenic mice (Figure 3-4 A, C). Also brain tissues exhibited no blue staining indicative of extravasation of Evans Blue in Ang-2 DT mice (Figure 3-4 B). As brain permeability is tightly regulated by the BBB, the effects of Ang-2 overexpression on permeability were evaluated using smaller tracers. A combination of two different sized tracers, Lucifer Yellow (LY, 0.45 kD) and Texas Red dextran (TR 3 kD-dextran) were evaluated (circulated for 4-5 min). Images of brain sections indicated rapid clearance of tracer from circulation and therefore the permeability of brain tissue could not be detected by fluorescence microscopy (Figure 3-4 B). Accordingly, a more sensitive assay was adopted to analyze these smaller tracers. Blood was taken from mice 4 to 5 min after tracer administration followed by transcardiac perfusion. Brains and kidneys were isolated and homogenized to obtain tracer content by fluorometry normalizing to the tissue weight and serum tracer content. Analysis revealed that the permeability of TR 3 kD-dextran increased slightly, whereas the smaller tracer 0.45 kD Lucifer Yellow showed a significant increase in Ang-2 DT brains compared to wild type (Figure 3-4 E). Kidneys that served as a control for leaky endothelium did not show any differences in permeability. These assays indicate that Ang-2 mediated BBB permeability *in vivo* is size-specific to lower molecular weight tracers (0.45 kD) but not to bigger tracers.

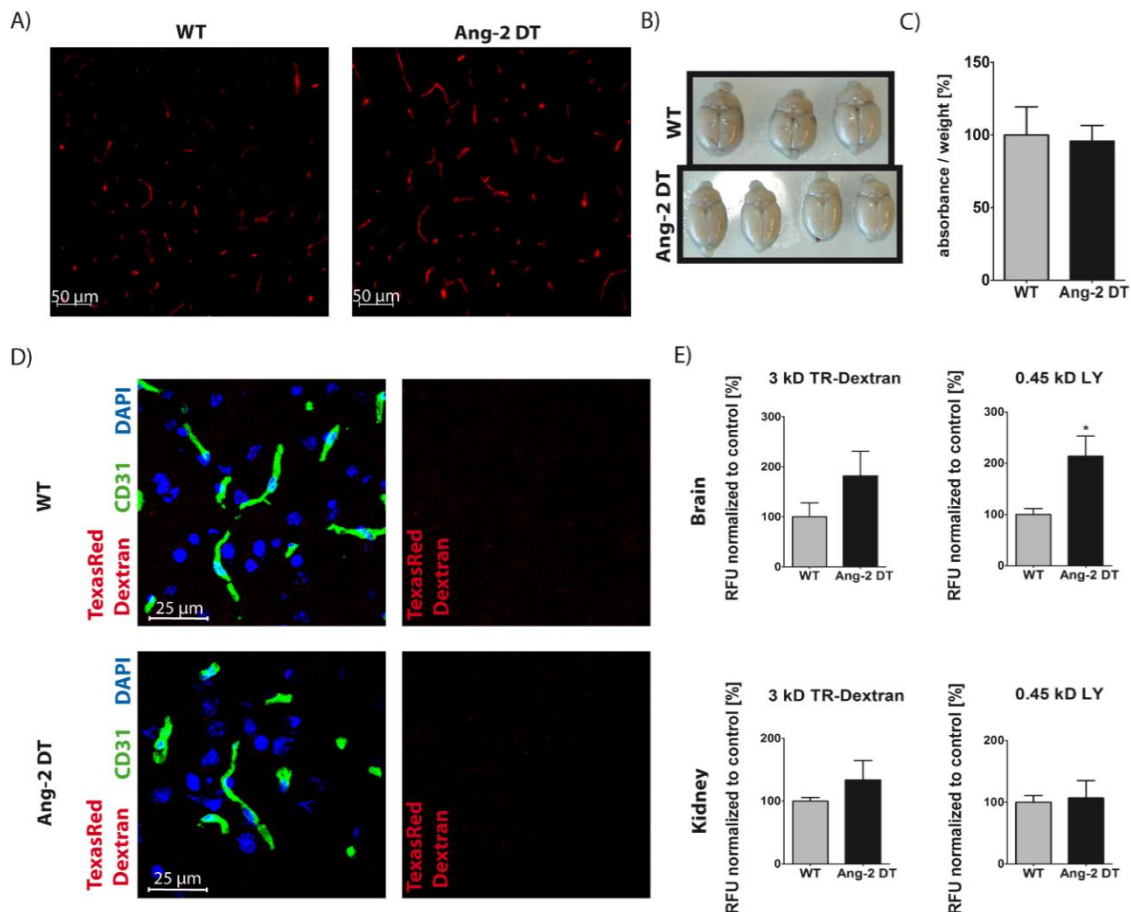


**Figure 3-4: Lucifer Yellow (0.45 kD) crosses the brain endothelium of Ang-2 DT mice**

A) 2 % Evans Blue (70 kD) was injected i.v. into the tail vein of mice and circulated for 2 h. A representative image of brain cryosections of Ang-2 DT mice is shown that indicated no change in permeability compared to wild type. B) Brain tissue of Evans Blue injected mice did not possess blue staining of the tracer. C) Homogenized brains of Evans Blue injected mice were also analyzed in a plate reader. The absorbance of brain homogenates normalized to the weight of mice did not result in any changes between wild type and Ang-2 DT (WT n = 3, Ang-2 DT n = 4; 2-tailed unpaired t-test). D) Permeability was also obtained to Texas Red 3 kD-dextran circulated for 4-5 min before PBS perfusion and sacrificing the mice. 10 μm brain cryosections with a CD31 staining (vessel marker, green) revealed no detectable Texas Red 3 kD-dextran staining in wild type and Ang-2 DT mice. E) The relative fluorescence units (RFUs) of the homogenized brain supernatant samples were measured in a fluorescence plate reader and expressed as relative % normalized to tissue weight and serum RFUs. Animals without tracer injection were used for auto-fluorescence subtraction. The fluorescence of the TR 3kD-dextran increased in tendency, whereas for the 0.45 kD LY a significant increase was detectable in the brains of Ang-2 DT mice indicating an increase in permeability to smaller tracers (n = 7; 2-tailed unpaired t-test; \* p < 0.05 compared to WT).

### 3.3 Ang-2 modifies components of the neurovascular unit

Cellular components of the neurovascular unit (NVU), which form the BBB were investigated in detail to elaborate the mechanisms behind the increase in permeability of Ang-2 DT mice across the brain endothelium.

### 3.3.1 Overexpression of Ang-2 leads to loss of pericytes in the brain

Astrocytic endfeet defects detectable by loss of localization of the endfeet at the vessels were first assessed in the transgenic mice. Cryosections of wild type and Ang-2 DT brains were stained for CD31 as a marker for endothelial cells and aquaporin-4 for astrocytic endfeet.

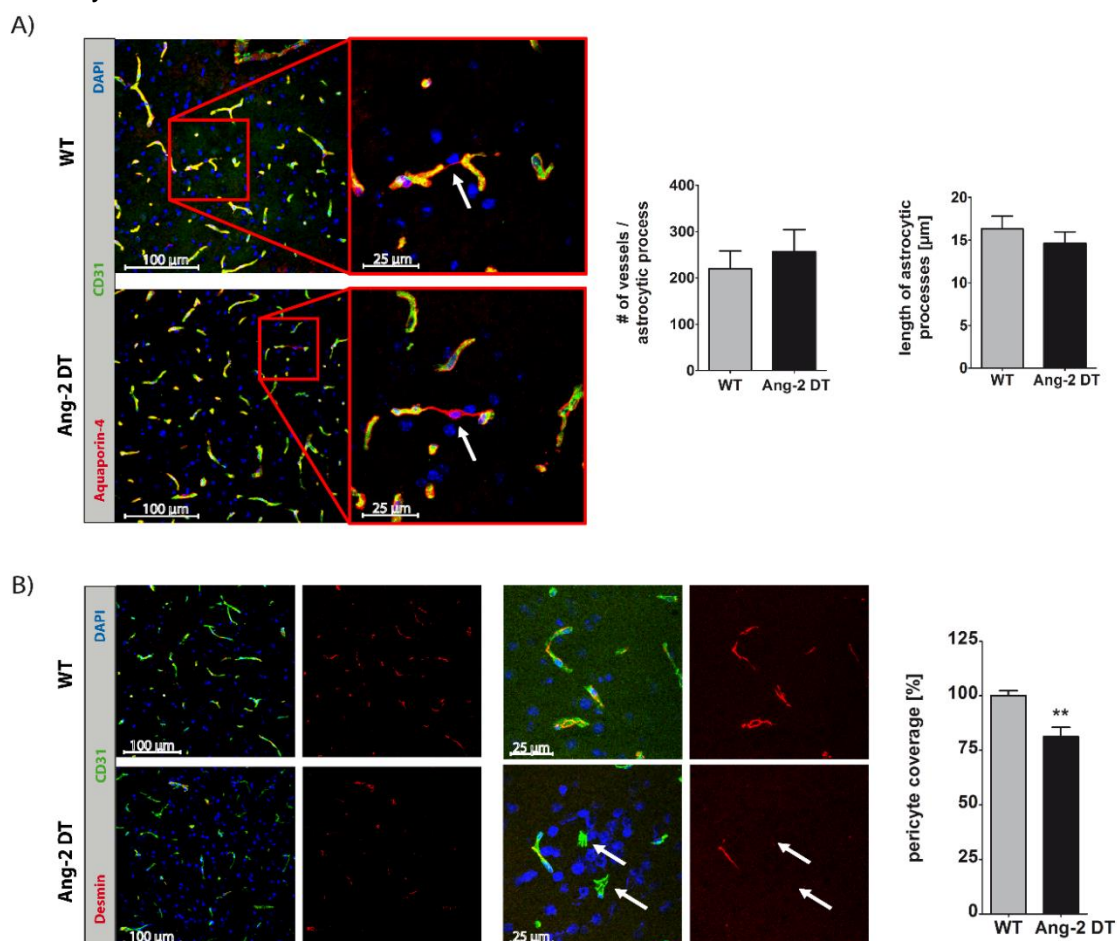


**Figure 3-5: Ang-2 overexpressing mice possess decreased number of pericytes in brain sections**

A) Brain sections of wild type and Ang-2 DT mice were stained with CD31 (vessel marker, green) and aquaporin-4 (astrocytic endfeet marker, red). There was no detectable difference between wild type and transgenic mice in the length of astrocytic endfeet or in the number of endfeet defects indicated by a loss of colocalization of CD31 and aquaporin-4 staining (for endfeet defects  $n = 6$  each; and for endfeet length  $n = 7$  each; 2-tailed unpaired t-test). B) Brain cryosections stained for CD31 (endothelial marker, green) and desmin (pericyte marker, red) revealed significantly less number of pericytes in the transgenic mice compared to wild type ( $n = 8$ ; 2-tailed unpaired t-test).

Quantitation of the numbers of vessels with endfeet defects and also the length of the endfeet did not show any difference between wild type and Ang-2 DT conditions (Figure 3-5 A). Ang-2 promotes the detachment of pericytes in peripheral blood vessels, induces pericyte dropout in the retina and reduces the number of pericytes in the skin (Hammes

et al., 2004; Augustin et al., 2009; Scholz et al., 2011) which is still not investigated in the brain. The pericyte marker desmin and endothelial marker CD31 were therefore used to detect changes in pericyte coverage between wild type and Ang-2 DT mice. Significantly less numbers of pericytes in the brain were detected in transgenic mice compared to wild type littermates (Figure 3-5 B), which indicate an effect of Ang-2 on pericytes in the brain that explain partly the increased permeability in these mice as pericytes have been shown to regulate BBB permeability (Armulik 2010).

### 3.3.2 Ultrastructural analyses reveal permeability features in Ang-2 DT mice

As pericytes constitute a part of the NVU, which were decreased in the Ang-2 DT mice (Figure 3-5 B), detailed structural analysis of components of the NVU was undertaken. Electron microscopy of brain microvessels from Ang-2 DT mice revealed permeability features compared to wild type. Mice overexpressing Ang-2 exhibited edema formation in the tissue surrounding endothelial cells, suggesting astrocytic endfeet swelling (Figure 3-6 A), which could not be detected in cryosections by confocal analysis (Figure 3-5 A). Infrequently, some pericytes showed degenerating features indicated by the presence of swollen mitochondria, high number of lysosomes and pinocytotic vesicles at the cell membrane (Figure 3-6 B). The decrease of pericyte numbers in immunohistochemistry stainings in Ang-2 DT mice (Figure 3-5 B) supports the increase in transcytosis via the caveolae pathway as shown previously in pericyte deficient mice (Armulik et al., 2010). Additionally, ultrastructural images revealed more pinocytotic vesicles in the luminal and basal membrane of Ang-2 DT mice compared to wild type, implying an upregulation of the transcellular transport (Figure 3-6 C). Furthermore, gaps between adjacent endothelial cells were prominent in Ang-2 overexpressing mice (Figure 3-6 D). This finding suggests disturbed junctional arrangement between endothelial cells forming the BBB.

Changes of the glycocalyx were also evaluated as they have been shown to be associated with BBB permeability (Henry and Duling, 1999; Vink et al., 2000). The glycocalyx is a specialized matrix located on the luminal side of endothelial cells and consists of soluble plasma components which are connected to each other by proteoglycans and / or glycosaminoglycans (Reitsma et al., 2007). Staining for glycocalyx in blood vessels was performed with lanthanum nitrate, which binds to the negatively charged proteoglycans and hence could be detected by electron microscopy.

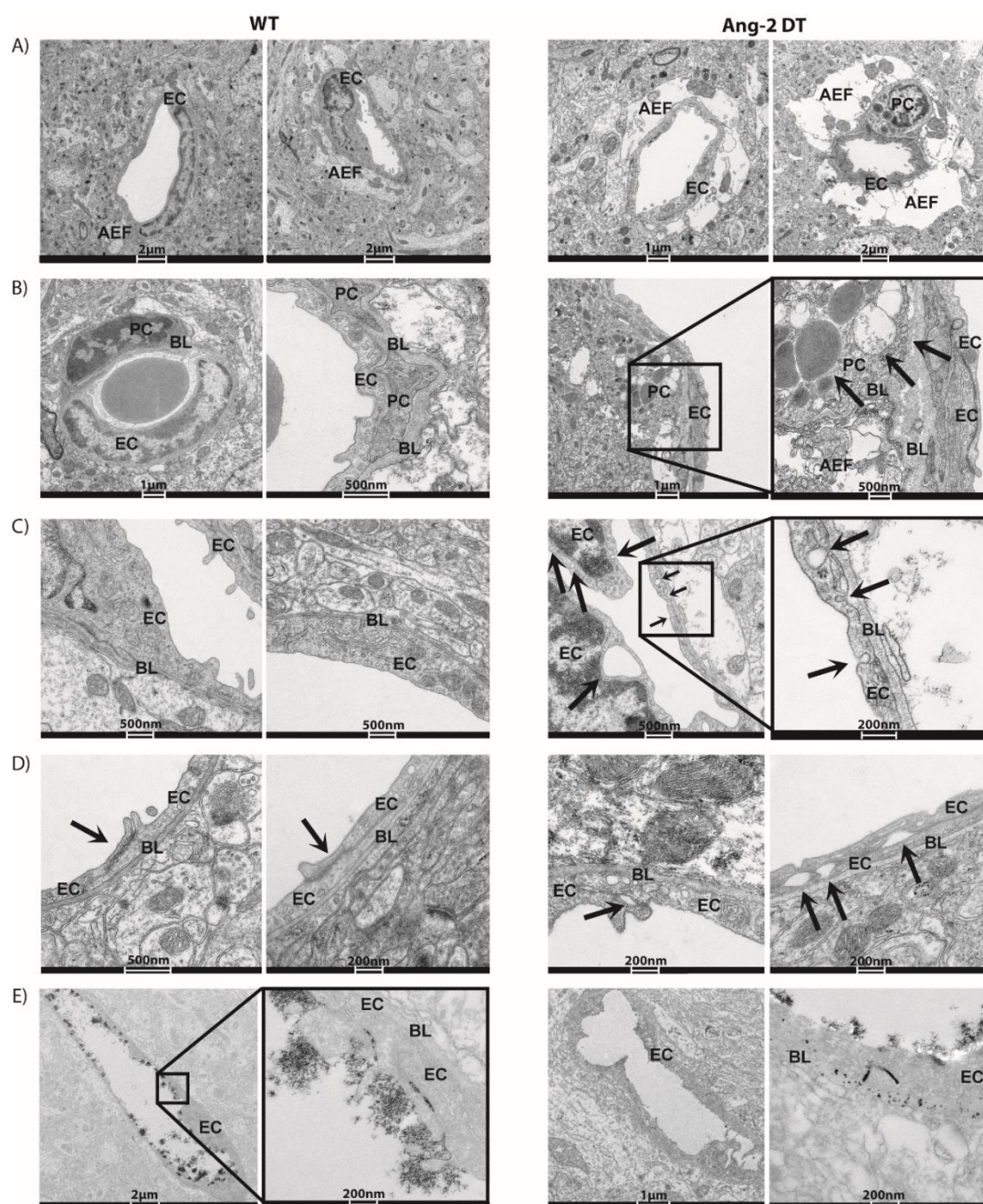


**Figure 3-6: Ultrastructural analysis demonstrate permeability features in Ang-2 DT mice**

Representative images of neurovascular changes are shown in the figure (n = 3 mice each in wild type and Ang-2 DT groups were investigated). AEF = astrocytic endfeet; BL = basal lamina; EC = endothelial cell; PC = pericyte. A) EM (electron microscopy) analysis revealed astrocytic swelling in Ang-2 DT mice. B) left arrow: swollen mitochondria; middle arrow: lysosomes; right arrow: pinocytic vesicles; C) big arrows in the left panel: vesicles in and gaps between ECs; upper arrow in the right panel: vesicle; middle arrow in the right panel: a gap between endothelial cells; lower arrow in the right panel: vesicle formation D) arrows in WT: normal junction formation between endothelial cells; arrows in Ang-2 DT: gaps between endothelial cells; E) lanthanum nitrate stains for the glycocalyx showing reduced glycocalyx thickness in Ang-2 DT mice compared to wild type.

---

Ang-2 DT brains showed significantly decreased glycocalyx thickness from 300 nm to approximately 100 nm. Particles of lanthanum nitrate were also detectable within the endothelium and in the basal lamina (Figure 3-6 E), suggesting a transcytotic transport from the luminal to the abluminal side of endothelial cells. These features could only be detected in Ang-2 overexpressing mice albeit not in all microvessels. The ultrastructural analysis indicated defined changes in the endothelium and in the surrounding brain tissue of Ang-2 DT mice, all of which support the increased neurovascular permeability in the Ang-2 transgenic mice compared to the wild types.

### 3.3.3 The expression of junctional molecules and components of the transcytotic pathway are modified by the overexpression of Ang-2

Tight and adherens junctions are major components of the BBB which result in intercellular tightening of endothelial cells in the brain. They regulate the BBB in combination with transcellular transporters which were further analyzed in the following experiments. MBMVs were isolated from wild type and Ang-2 DT brains to verify the increase in transcellular transport by caveolae expression and investigate changes in junctional proteins which would lead to an increase in paracellular transport.

Immunohistochemical analysis of wild type and Ang-2 DT brains revealed no obvious changes in structure, organization or expression of VE-cadherin, Claudin-5 or ZO-1 (Figure 3-7 B). Therefore a more sensitive method using MBMVs isolated from wild type and transgenic mice was used for investigating the expression of BBB permeability related proteins. Similar to immunohistochemical analysis the mRNA expression of several tight and adherens junctions were not affected except for Claudin-3 which was significantly downregulated in Ang-2 overexpressing mice compared to wild type (Figure 3-7 A). However in Western Blot analysis, the adherens junction marker VE-Cadherin and the tight junction marker Claudin-5 were downregulated in Ang-2 DT mice whereas  $\beta$ -Catenin was not affected (Figure 3-7 C). Next we proceeded to study alterations in transport systems which could also increase permeability via transcellular pathways. Between wild type and mice overexpressing Ang-2, Caveolin-1 expression analysis revealed an increase in Ang-2 DT mice. Caveolin-1 is known as a protein marker for caveolae formation which increases vascular transport via vesicles (Li et al., 1998). This data goes in line with the observed increase in vesicular formations in EM analysis in Ang-2 overexpressing mice (Figure 3-7 C) thus indicating that increased permeability by Ang-2 partly is a result of caveolae mediated transcytosis. The glucose transporter-1 (Glut-1) was however not altered. Thus the paracellular effects of Ang-2 via



downregulation of VE-Cadherin, Claudin-5 and Claudin-3 together with caveolae mediated transcytosis modulate the permeability of the BBB.

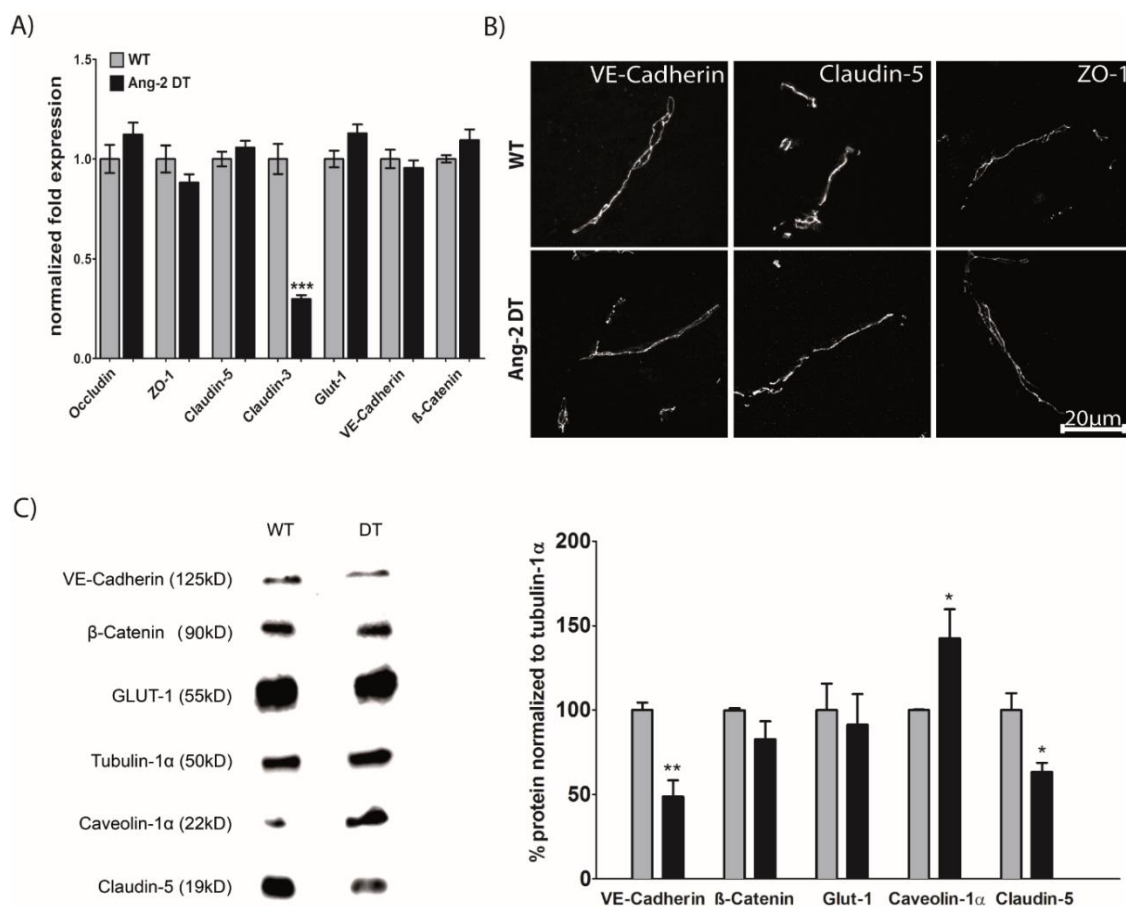


**Figure 3-7: Junction proteins and a transcellular transport protein show different expression level in Ang-2 DT mice**

A) qPCR analysis of isolated MBMVs (2 brains per genotype) revealed a significant decrease in Claudin-3 expression in Ang-2 DT mice compared to wild type ( $n = 3$ ; 2-tailed unpaired t-test; \*\*\*  $p < 0.001$ ). B) Representative images of VE-Cadherin, Claudin-5 and ZO-1 showed no structural or expressional changes in brain sections of Ang-2 overexpressing mice compared to wild type. C) Isolated MBMVs in Western Blot analysis revealed decreased expression of VE-Cadherin and Claudin-5 whereas Caveolin-1 $\alpha$  was upregulated in Ang-2 DT mice. 7 brains of each group were pooled together in each preparation. Wild type expression was set to 100 % ( $n = 3$  preparations; \*  $p < 0.05$ ; \*\*  $p < 0.01$ ; 2-tailed unpaired t-test).

### 3.3.4 Number of infiltrating macrophages increases in Ang-2 DT mice

It has already been demonstrated in a previous publication that Ang-2 is associated with myeloid cell infiltration. In different organs significantly more macrophages could be identified in mice overexpressing Ang-2 associated with an increase of permeability in peripheral blood vessels (Scholz et al., 2011). Therefore we proceeded to investigate a potential leukocyte infiltration in the brain mediated by Ang-2. FACS analysis revealed

an increase in the number of macrophages and neutrophils (Figure 3-8 B). How the macrophages in Ang-2 overexpressing mice enter the BBB to the CNS still needs to be investigated.

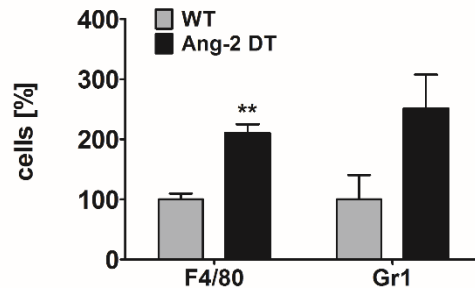


**Figure 3-8: Macrophages and myeloid derived suppressor cells infiltrate into brain tissue of Ang-2 DT mice**

FACS analysis of WT and Ang-2 DT brains revealed significantly higher number of macrophages (F4/80) (n = 3; \* p < 0.05; \*\* p < 0.01; 2-tailed unpaired t-test), Gr1 = neutrophils.

### 3.3.5 Ang-2 mediated brain permeability does not result in gross edema formation

Passage of small molecules (0.45 kD) through the BBB endothelium could alter the fluid and electrolyte balance resulting in accumulation of water from blood in the surrounding brain tissue, known as edema formation. Ultrastructural microscopy revealed swollen astrocytes in Ang-2 DT mice, which was not detected in wild type littermates (Figure 3-6 A). The overall edema was therefore assessed. The brain water content was obtained as a ratio of wet brains (right after sacrificing the mice) to that of dried brains (6 days in a 62 °C incubator).

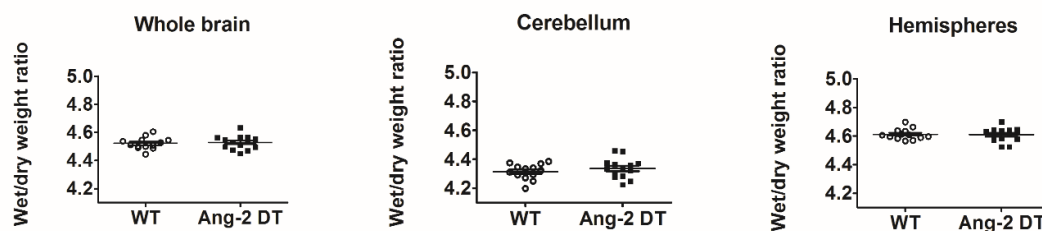


**Figure 3-9: No edema formation in mice overexpressing Ang-2**

After sacrificing mice the brain weight was measured followed by incubation in a 62 °C incubator for 6 days. The ratio of dried brain weight to the wet brain weight right after sacrificing was obtained as a measure of edema, which was distinguished between the whole brain, cerebellum and the hemispheres. No increase in water content was observed in Ang-2 DT brains compared to the WT littermates (WT n = 13; Ang-2 DT n = 14; 2-tailed unpaired t-test).

Analysis was performed for the whole brain, the cerebellum, and the cortical hemispheres for localized analysis. No measurable differences were detectable between the genotypes, indicating a lack of edema formation in mice overexpressing Ang-2 (Figure 3-9). This goes with the behavioral analysis of Ang-2 overexpressing mice, which do not exhibit obvious changes in movement or ingestion behavior.

### 3.4 Continuous Ang-2 expression does not interfere with intrinsic Ang-1 levels

As the permeability effects of Ang-2 overexpression were only limited to small molecules in Ang-2 DT mice, potential compensatory effects of Ang-1 (the described agonist of the Tie2 receptor (section 1.3.2)) on Ang-2 mediated permeability were therefore assessed. To this end, brain samples of wild type and Ang-2 transgenic mice were evaluated for expression levels of Ang-1. Immunohistochemical stainings, quantitative expression analysis by Western blot and expression pattern from blood serum revealed no changes in expression levels of Ang-1 indicating no compensatory effect of Ang-1 in Ang-2 DT mice from 8 to 12 weeks (Figure 3-10).

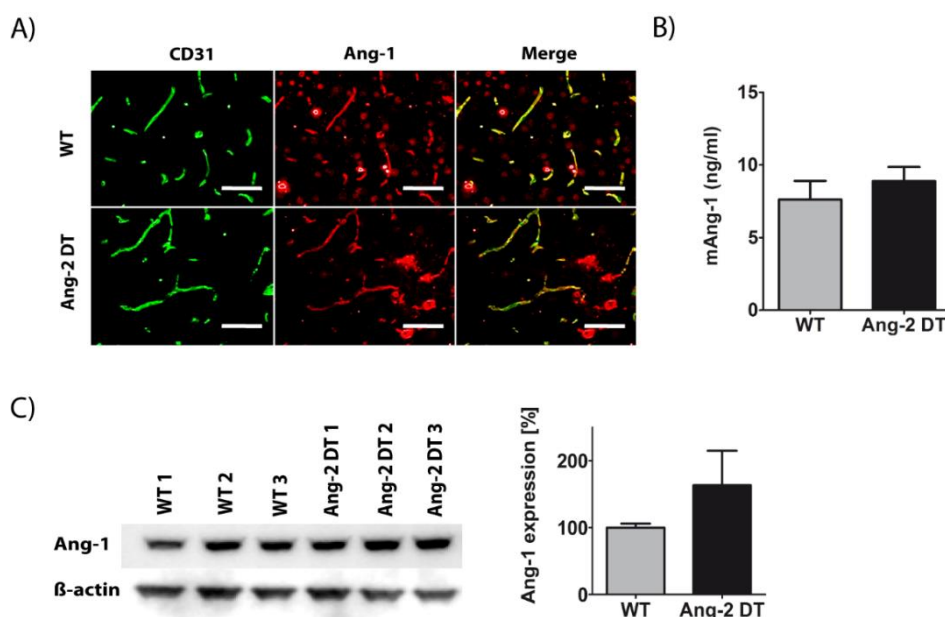


**Figure 3-10: No compensatory effect of endogenous Ang-1 detectable in Ang-2 DT mice**

A) Representative images of wild type and Ang-2 DT brain samples stained with CD31 as a vessel marker (green) and Ang-1 (red) showing no difference in Ang-1 expression. B) ELISA analysis of mAng-1 expression in wild type and Ang-2 DT blood serum indicated no obvious differences ( $n = 4$ ; 2-tailed unpaired t-test). C) Ang-1 expression levels obtained by Western blot analysis of whole brain homogenates also did not indicate any difference between wild type and Ang-2 transgenic mice ( $n = 3$ ; 2-tailed unpaired t-test).

### 3.5 Tightening of the BBB upon long-term overexpression in Ang-2 DT mice

All the previous results are in experiments involving young adult mice overexpressing hAng-2 in an endothelial specific manner from birth for 8 to 12 weeks. The consequences in brain permeability of the long-term expression analysis of Ang-2 DT mice was expected to be more severe as a previous study analyzed a more dramatic pericyte dropout and more infiltrating myeloid cells up to 52 weeks in the skin (Scholz et al., 2011). Therefore the effects of long-term expression of Ang-2 in mice overexpressing hAng-2 for 6-12 months were investigated.

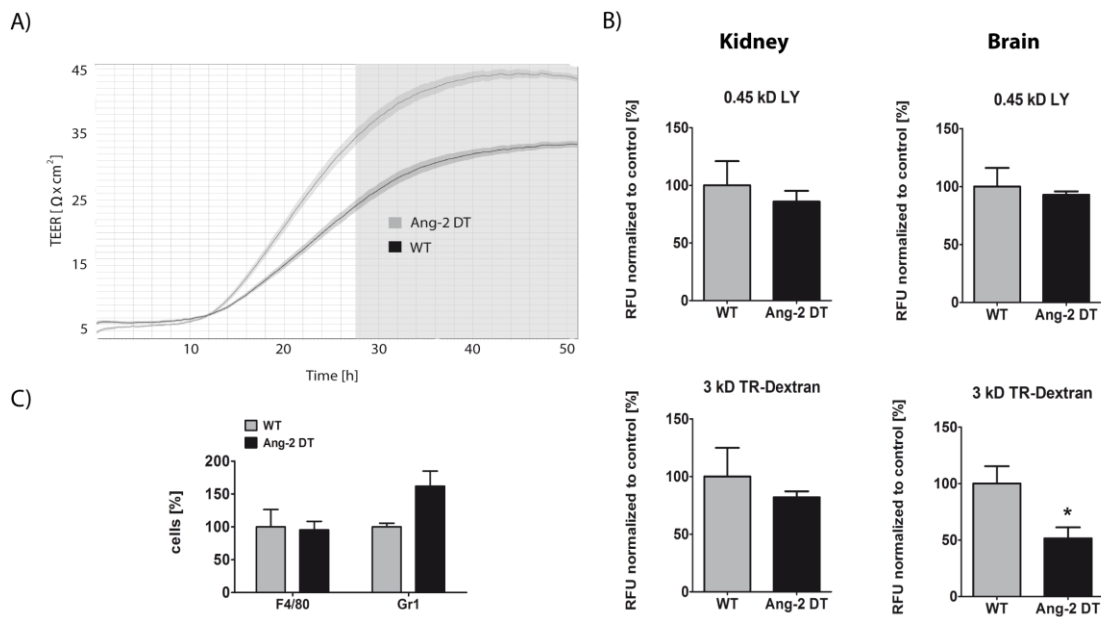


**Figure 3-11: Tightening effect of the BBB in 6-12 months old Ang-2 DT mice**

A) MBMECs isolated from 7 months old Ang-2 DT mice showed higher TEER values compared to WT cells in impedance analysis using cellZscope (n = 1 preparation from 6 mice/group). B) LuciferYellow and TexasRed (TR) 3kD-dextran were simultaneously injected into 6 months old wild type and Ang-2 DT littermates and circulated for 4-5 min. The fluorescence of brain supernatants revealed a significant decrease in TR 3 kD-dextran (WT n = 7; Ang-2 DT n = 6; \* p < 0.05; 2-tailed unpaired t-test). C) FACS analysis of 12 months old CD1 mice showed no significant changes in macrophage expression (F4/80) or neutrophils (Gr1); (n = 3; 2-tailed unpaired t-test).

Interestingly, isolated MBMECs from 7 months old Ang-2 DT mice did not depict a decrease in TEER observed in 8 weeks old mice but rather showed the opposite effect when compared to wild type littermates. Furthermore, the *in vivo* analysis using fluorescent tracers indicated lower permeability to TexasRed 3kD-dextran in the Ang-2 DT brains compared to wild types (Figure 3-11 A, B). This finding is in line with the examined numbers of infiltrating macrophages in brain tissues of 12 months old Ang-2 DT mice, which did not differ from the wild type mice by FACS analysis (Figure 3-11 C), whereas 8 to 12 weeks old Ang-2 DT mice possessed increased infiltrating leukocytes

(Figure 3-8 B). These findings suggest a tightening effect of the BBB upon long-term expression of Ang-2, which could potentially be a compensatory effect or aging related protective effect and hence needs further investigation.

### **3.6 Ang-2 overexpression leads to increased stroke sizes and increased permeability in infarct areas, effects partly reversed in therapeutic treatments targeting the Tie2 signaling pathway**

Modifications of the Ang-2 / Tie2 signaling pathway occur in conjunction with the VEGF pathway during tumor angiogenesis. Transcription levels of Ang-2 are considerably upregulated in the endothelium of tumors, in inflammatory conditions like sepsis or in stroke (Scholz et al., 2015). Therefore, the effects of Ang-2 were investigated in pathology focusing on stroke as a cerebrovascular disease model. We examined human stroke samples and experimental stroke models (MCAO) in wild type and Ang-2 overexpressing mice to investigate the consequences of the Ang-2 expression in stroke and BBB permeability therein.

#### **3.6.1 Ang-2 levels correlate with stroke stages in human patients**

Samples from human stroke cases were used to determine hAng-2 expression in different stroke stages. The classification of infarct stages was performed according to the 3-stage stroke classification frequently used in neuropathological diagnostics, first described in detail by Hugo Spatz in 1939 (Spatz, 1939) and modified over the years (Ellison 2004). Histopathologically, the lesions were classified into stage I (acute), stage II (subacute), and stage III (chronic). The expression of hAng-2 significantly correlated with stroke stages. Almost no hAng-2 could be detected in the normal brain whereas highest hAng-2 expression was discovered in subacute stages (Figure 3-12 A). Furthermore, serum levels taken from patients 2-15 days after stroke showed highest hAng-2 expression in territorial stroke patients compared to control patients who never had stroke (Figure 3-12 B). Taken together, brain Ang-2 expression correlates with stroke grade and is also detectable in the blood days after the stroke incidence thus implicating a role of Ang-2 in stroke.

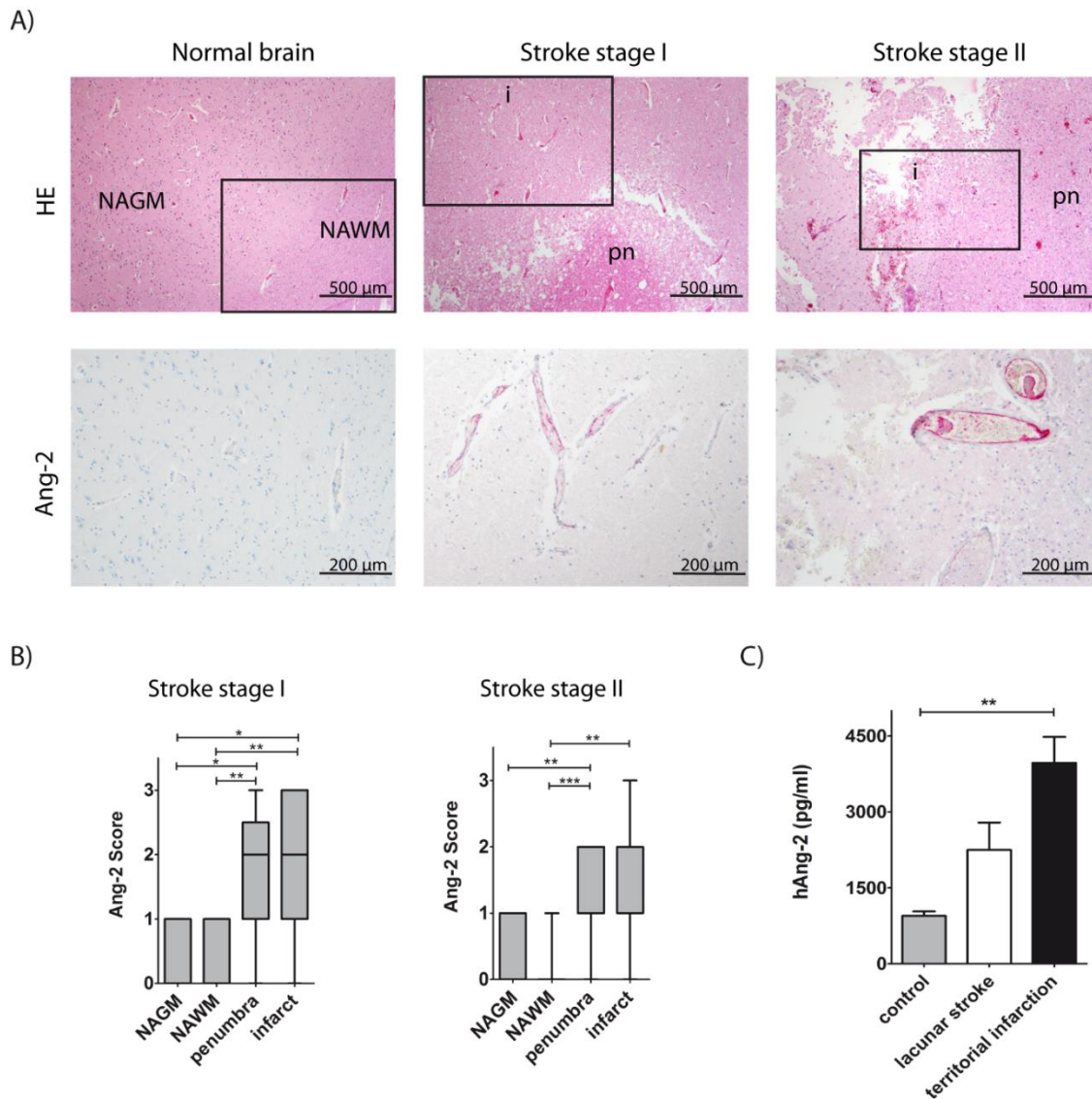


**Figure 3-12: Ang-2 expression increases in higher stroke grades**

A) H&E and Ang-2 staining was performed on human stroke samples from stage I and II compared to healthy brains. B) The Ang-2 expression was higher in the penumbra and infarct region after stroke; NAGM = normal appearing grey matter; NAWM = normal appearing white matter; pn = penumbra; I = infarct; (n = 13 cases, Whiskers plot 2.5-97.5 percentile, Kruskal-Wallis test with Dunn's multiple comparison test; \* p < 0.05; \*\* p < 0.01; \*\*\* p < 0.001). C) Serum hAng-2 expression was analyzed by ELISA on stroke patients 2-15 days after stroke. This revealed a significantly higher expression in territorial infarction cases compared to control healthy subjects (n = 4 for lacunar, n = 15 for territorial infarction and n = 4 for healthy subjects; One-way Anova followed by Dunnett's post-hoc test ; \*\* p < 0.01).

### 3.6.2 Overexpression of Ang-2 results in increased infarct size and permeability

To investigate whether Ang-2 is a risk factor for stroke, an experimental stroke model was utilized in which permanent middle cerebral artery occlusion (MCAO) was performed to elicit stroke. Mice overexpressing hAng-2 since birth for 8 to 14 weeks, revealed

significantly bigger infarct volumes compared to wild type animals 24 h and 72 h after stroke (Figure 3-13 A). An IgG staining of brain slices indicated an increase in permeability in Ang-2 DT mice in the infarct area 24 h after stroke (Figure 3-13 B).

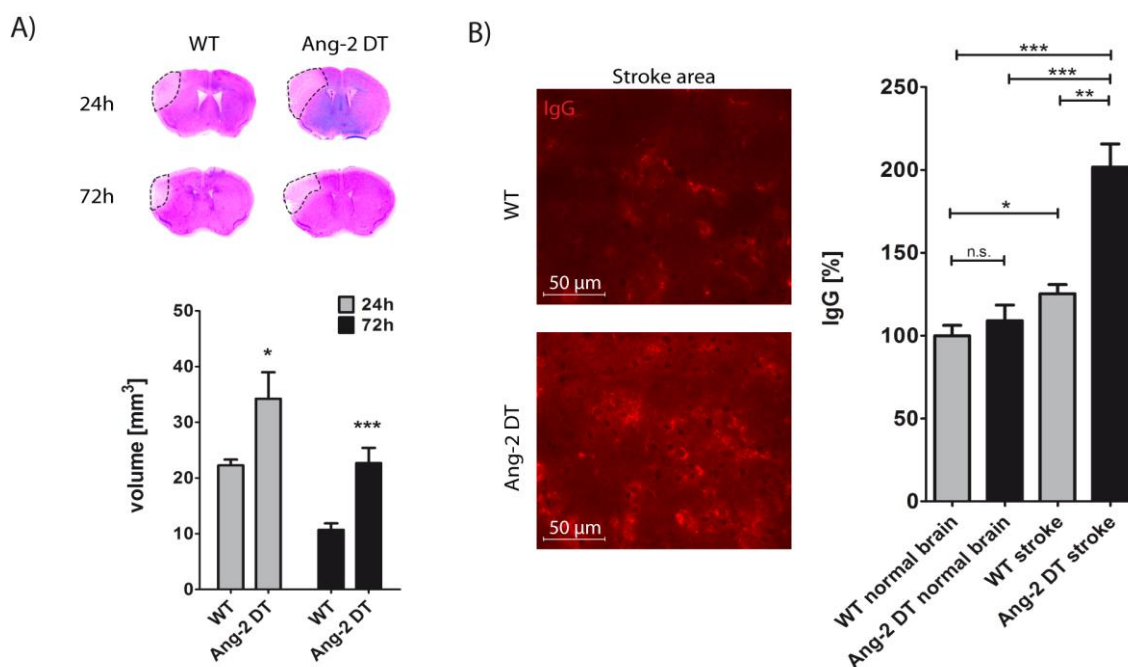


**Figure 3-13: Stroke size and permeability increase in Ang-2 DT mice subjected to permanent MCAO**

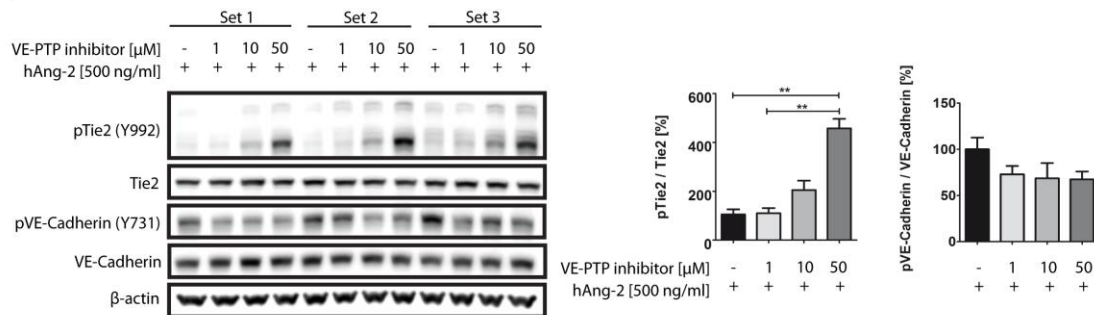
A) Giemsa staining and stroke volume measurements showed a significantly increased stroke size in Ang-2 DT mice at 24 h and 72 h after permanent MCAO (24 h,  $n = 4$  each; 72 h, WT  $n = 10$ ; DT  $n = 7$ , \*  $p < 0.05$ ; \*\*\*  $p < 0.001$ , 2-tailed unpaired t-test) compared to WT littermates. B) IgG staining demonstrates a significantly higher permeability to IgG in stroke areas in general with the permeability in stroke area being significantly higher in the Ang-2 DT mice compared to the WT (WT  $n = 4$ ; DT  $n = 6$ , \*  $p < 0.05$ ; \*\*  $p < 0.01$ , \*\*\*  $p < 0.001$ , 2-tailed unpaired t-test).

### 3.6.3 Therapeutics activating Tie2 signaling show improved outcome in infarct sizes and brain permeability

As ischemic stroke resulted in increased Ang-2 expression, bigger infarct volume and higher permeability (see 3.6.1 and 3.6.2), therapeutic targeting of the Angiotensin / Tie2 signaling pathway was performed to test the beneficial effects on stroke outcome. The transient MCAO mouse model, where the reperfusion after the occlusion is more comparable to stroke incidents in human, was used for therapeutic studies. A vascular endothelial protein tyrosine phosphatase (VE-PTP) inhibitor was tested in young adult male mice. A modified VE-PTP inhibitor was already used in previous studies and was demonstrated to inhibit the function of VE-PTP (Goel et al., 2013). On the one hand blocking of VE-PTP is associated with Tie2 phosphorylation and thus activation. On the

other hand it phosphorylates VE-Cadherin leading to increased permeability (Nottebaum et al., 2008; Shen et al., 2014).

A)



B)

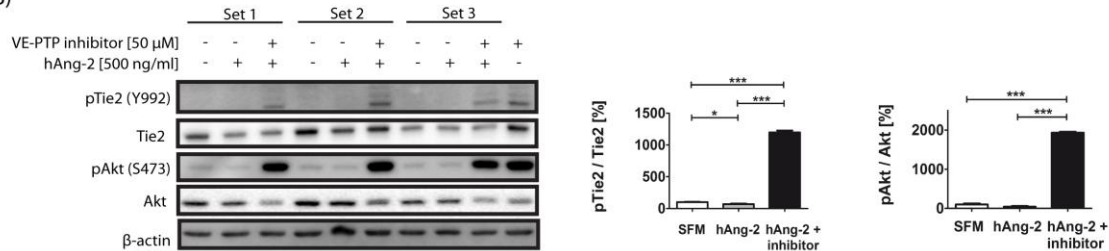


**Figure 3-14: The VE-PTP Inhibitor induces the activation of the Tie2 signaling pathway and decreases pVE-Cadherin *in vitro***

A) bEnd5 cells were treated for 16 h with hAng-2 (500 ng/ml) in serum-free conditions. The VE-PTP-Inhibitor drug was added to the cells for 10 min at different concentrations (1  $\mu$ M, 10  $\mu$ M and 50  $\mu$ M). Western blot analysis revealed an increase in pTie2 with 50  $\mu$ M of the inhibitor. pVE-Cadherin decreased in tendency but no dose dependency was observed. B) In three different preparations (3-4 mice each time) of isolated C57 / B16 MBMECs the VE-PTP inhibitor increased the activation of Tie2 at tyrosine 992. Moreover the drug increased pAkt levels indicating an activation of Akt pathway that is downstream of Tie2. All sets were compared with serum-free medium (SFM) control condition (n = 3; \* p < 0.05; \*\* p < 0.01; \*\*\* p < 0.001; 2-tailed unpaired t-test).

The mechanistic impact of the drug was therefore tested in bEnd5 cells and isolated MBMECs *in vitro*. A dose response study of the inhibitor from 1  $\mu$ M to 50  $\mu$ M was performed in bEnd5 cells pre-treated with recombinant hAng-2 for 16 h, a time point where permeability effects were observed in TEER analysis (Figure 3-3). A 10 min treatment with the VE-PTP inhibitor was then performed. The Western blots indicate a significant Tie2 activation in the cells that were treated with 50  $\mu$ M of the inhibitor. Additionally, the VE-Cadherin activation was decreased in tendency as measured by pVE-Cadherin. 50  $\mu$ M of the inhibitor showed the most effect in bEnd5 cells (Figure 3-14 A). This concentration was therefore used for further studies on isolated C57 / B16 MBMECs. In MBMECs pre-treated with recombinant hAng-2 for 16 h both Tie2 and downstream Akt activation was observed upon VE-PTP inhibitor treatment, confirming the data in bEND5 cells. On the other hand it decreased the phosphorylation of VE-



Cadherin in bEND5 cells suggesting more stabilized blood vessels with the application of the drug (Figure 3-14) which is in contradiction to the already described increase in pVE-Cadherin contributing to increased permeability (Nottebaum et al., 2008; Shen et al., 2014).

Therapeutic effects of the drug were then investigated in an experimental stroke model where Ang-2 levels were increased and overexpression of Ang-2 led to poor stroke outcome (Figure 3-12; Figure 3-13). Strokes were induced in mice by the transient MCAO, a model that is clinically similar to the human strokes. As the VE-PTP inhibitor is only stable for 12 h, it was subcutaneously injected into wild type CD1 male mice 14 h and 2 h before and 10 h after the MCAO. Control animals were injected with the same amount of dH<sub>2</sub>O (the vehicle for the VE-PTP inhibitor). The occlusion was performed for 30 min followed by sacrificing the mice after 24 h. Triphenyl tetrazolium chloride (TTC) of 2 mm brain slices distinguished stroke and normal brain area, with the normal area stained red due to mitochondrial activity whereas stroke area is unstained due to dead cells and hence appears whitish. Mice treated with the inhibitor exhibited significantly smaller stroke sizes compared to controls that were injected with the same volume dH<sub>2</sub>O (Figure 3-15 A). The IgG staining in mice treated with the drug showed a decrease in permeability in stroke areas (Figure 3-15 B). Neurological improvement after stroke incidence was also measured in this study by different parameters as described previously (Chen et al., 2001). Mice were scored 24 h after occlusion, right before sacrificing the mice. Higher scores were given for bigger neurological deficits tested on all parameters. The flexion was tested by raising the mouse holding the tail and the flexion of forelimb and hindlimb was assessed. The gait was scored by allowing the mouse to walk on an even surface. Subsequently the coordination was determined by allowing the mouse to walk on a raised stick. The treated mice showed improvement in all the parameters as indicated by lower scores compared to vehicle treated group, which was however not significant (Figure 3-15 C).

The mechanistic impact of the drug treatment that leads to better neurological outcome and decreased infarct areas was investigated by Western blotting. This analysis indicated that the action of the VE-PTP inhibitor was similar to that in MBMECS *in vitro*, where dramatic Akt activation was observed as indeed from higher levels of pAkt to Akt (Figure 3-16 A). Furthermore, Tie2 was also activated in stroke areas *in vivo* demonstrated by pTie2 staining (Figure 3-16 B). The action of the inhibitor drug appears to be very specific mediated by the activation of Tie2 pathway in stroke thus leading to a

reduction of infarct areas with significantly decreased permeability in stroke areas including a trend towards better neurological behavior (Figure 3-15).

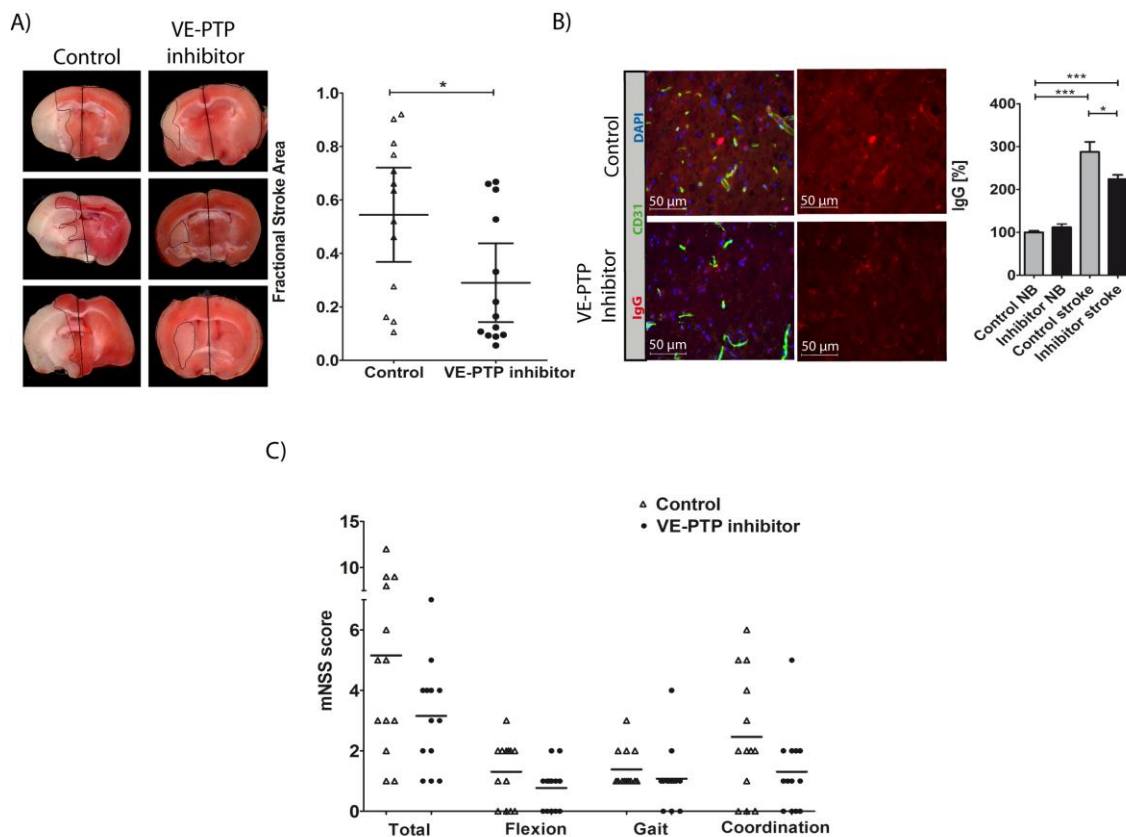


**Figure 3-15: The VE-PTP Inhibitor decreases stroke volumes and permeability in WT CD1 mice 24 h after occlusion**

A) This figure shows TTC stained sections from three different animals per group 24 h post MCAO. The animals treated with the inhibitor were injected with 30 mg/kg body weight of the drug at 14 h and 2 h before the surgery and 10 h after occlusion. The stroke size was obtained as a ratio of stroke area to that of the non-ischemic hemisphere area. The treated group exhibited decreased infarct sizes compared to control animals treated with the same volume of dH<sub>2</sub>O (n = 13; \* p < 0.05; 2-tailed unpaired t-test). B) Brain sections were stained with CD31 (blood vessel marker) and IgG to obtain the changes in permeability upon drug treatment. A decreased IgG staining in stroke areas was observed in VE-PTP inhibitor samples compared to stroke areas in control groups (NB = normal brain; n = 6; \* p < 0.05; \*\*\* p < 0.001; 2-tailed unpaired t-test). C) Behavioral scoring was also performed 24 h after MCAO on the treated mice comparing them to untreated group. The flexion of the fore- and hindlimb was tested by raising the mouse by the tail (worst 3 points). The gait was tested by allowing the mouse to walk on an even surface (worst 4 points) and the coordination was investigated by letting the mouse balancing on a round beam (worst 6 points). In the total measurement a sensory function is included which was tested by corneal and pinna reflex (worst 2 points). The single sensory function is not listed here because all of the mice showed those reflexes. The mice treated with the inhibitor showed improvement in all neurological scores, which was however not significant (n = 13; 2-tailed unpaired non-parametric Mann-Whitney test).

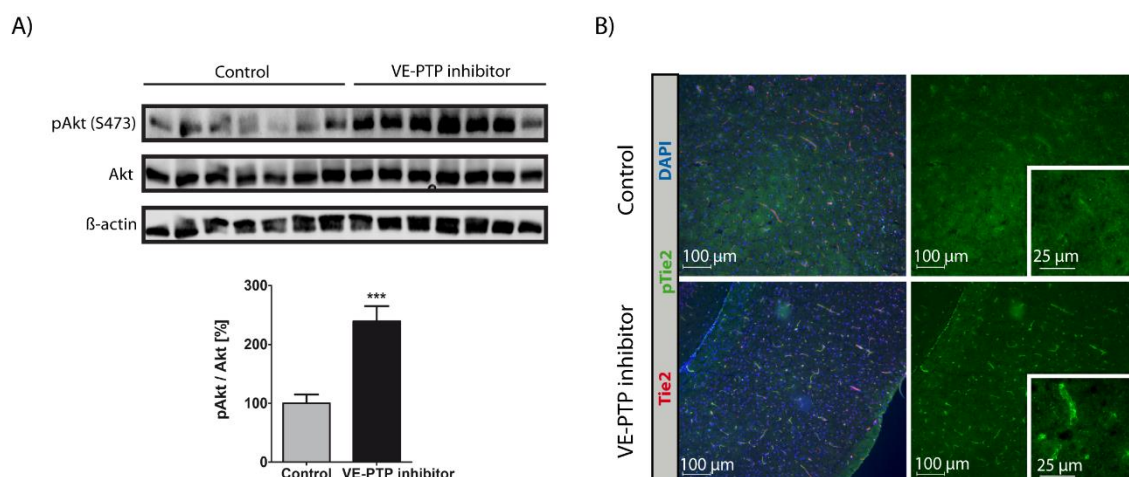


**Figure 3-16: The inhibitor of VE-PTP induces the Akt and Tie2 activation also *in vivo***

A) Western Blot analysis of control and inhibitor treated samples of the transient stroke hemisphere revealed increased pAkt activation ( $n = 7$ ;  $*** p < 0.001$ ; 2-tailed unpaired t-test) indicating the drug action *in vivo*. B) One representative image of a Tie2 (red) and pTie2 (green) staining of the stroke hemisphere demonstrated increased pTie2 staining in samples treated with VE-PTP inhibitor compared to controls also confirming the Western blot data for drug action *in vivo*.

## 4. DISCUSSION

The BBB is highly regulated and stringently controls the extracellular environment for proper CNS function. The BBB is at least in part disturbed in several neurological disorders that lead to cerebrovascular leakage, resulting in brain edema and intracranial pressure that may eventually lead to brain death. The breakdown of the BBB is associated with dysregulation and degeneration of neurons due to changes of the NVU. Modulation of tight junctions, changes in specific transporter systems, increased transcytosis and increase in leukocyte infiltration accompany BBB breakdown (Obermeier et al., 2013; Daneman and Prat, 2015).

Ang-2 has been reported to be highly upregulated in inflamed brains (Scholz et al., 2011) and in stroke areas (Beck et al., 2000; Zhang et al., 2002), suggesting a role for Ang-2 in the breakdown of the BBB. The current work defines Ang-2 as an inducer for opening the BBB under physiological conditions during continuous overexpression of Ang-2 *in vivo* and *in vitro* in primary cultured brain endothelial cells. Ang-2 expression correlated with stroke grades in human patients and Ang-2 overexpression led to increased stroke size and increased permeability in the stroke areas in an experimental mouse MCAO model. This demonstrates Ang-2 as one of the risk factors for stroke. Therapeutic activation of the Tie2 pathway in mice subjected to MCAO with a VE-PTP inhibitor decreased stroke size and permeability indicating the beneficial effects of therapeutic strategies targeting the Angiotensin / Tie2 pathway.

### 4.1 Ang-2 increases the permeability of brain endothelial cells *in vitro*

As an initial step to determine whether Ang-2 induces brain permeability, primary cultured mouse brain microvascular endothelial cells (MBMECs) from wild type and Ang-2 overexpressing littermates were isolated for *in vitro* analysis. MBMECs were used for *in vitro* permeability analysis as overexpression of Ang-2 for 8 weeks showed a high mRNA expression of hAng-2 in brain microvessels (Figure 3-2). The transendothelial electrical resistance (TEER) reflecting barrier tightness was measured on isolated brain endothelial cells in a continuous fashion using the cellZscope device. The resistance of MBMECs upon endothelial-specific overexpression of Ang-2 or upon recombinant human Ang-2 treatment significantly decreased (Figure 3-3 A-C), indicating a barrier opening effect of Ang-2. In addition, experiments in bEnd5 cells, an immortalized brain endothelial line exhibited the same trend in the reduction of TEER with treatment of

recombinant hAng-2 (Fig. 3-3 D). This observation is in line with the already described effect of Ang-2 on human pulmonary microvascular endothelial cells. There it was demonstrated that Ang-2 sensitizes the initial thrombin-induced permeability (van der Heijden et al., 2011). However, as TEER is indicative of permeability to ions, permeability to other solutes of different sizes was evaluated upon Ang-2 treatment of MBMECs (Czupalla et al., 2014). For this analysis, a transwell tracer assay with fluorescently labeled dextrans (3 kD, 20 kD, and 70 kD) and Lucifer Yellow (0.45 kD) was performed. For these experiments the C57 / Bl6 mouse strain was used to preclude that Ang-2-mediated permeability was strain specific to the CD1 mice that were used throughout the study. Ang-2 treatment resulted in an increase in permeability to all different sized tracers although the degree was lowest in Lucifer Yellow (0.45 kD) tracer (50 %) that is the smallest of all, which can be explained from the relatively high basal permeability of MBMECs monolayers to this tracer compared to the other tracers (Figure 3-3 E). Higher basal permeability of MBMECs to smaller solutes is also reflected in the TEER data where the Ang-2 mediated increase in flux to ions that are even smaller than Lucifer Yellow tracer resulted in a decrease in TEER of just about 20 %. Dextran permeability as well as the TEER data indicate a direct effect of Ang-2 on brain endothelial cells that potentially affects intercellular junctions as both the assays measure primarily paracellular transport. This was shown in different mouse strains and brain endothelial cell lines.

The role of Ang-2 *in vivo* on brain permeability was elaborated in CD1 mice overexpressing hAng-2 in an endothelial specific manner by withdrawal of doxycycline from food. There was already a significantly increase in hAng-2 expression after one day and that increased over time and which could be reversed by addition of doxycycline back to food (Figure 3-1 A). Mice that overexpressed Ang-2 for 8 to 12 weeks from birth that showed a significantly higher expression of hAng-2 compared to wild type (Figure 3-1 B) were utilized to investigate the effect of Ang-2 on brain permeability via fluorescent tracer assays. Initially, the leakage of the Evans blue dye that binds to serum albumin (hence of 70 kD molecular weight) was tested. The dye was circulated for 2 h before perfusing the mice to obtain absorbance based brain permeability to Evans blue. There was no difference in the absorbance of Evans blue permeability between wild type and Ang-2 overexpressing mice (Figure 3-4 A-C) indicating that the barrier opening effects of Ang-2 *in vivo* to higher molecular weight tracers was lower than that *in vitro* where FITC 70 kD-dextran permeability was increased about 2 times. This is in contrast to already described Ang-2 mediated peripheral endothelial permeability, where Evans blue

and other higher molecular weight tracers were shown to be increased by Ang-2 or decreased in Ang-2 knockout mice (Benest et al., 2013; Ziegler et al., 2013), which is probably due to a tighter barrier complex in the brain compared to peripheral blood vessels. However, the permeability to the fluorescent tracer Lucifer Yellow (0.45 kD) was significantly increased also *in vivo* in Ang-2 overexpressing mice compared to wild type but only in trend for TexasRed 3kD-dextran (Figure 3-4 E). These results indicate that Ang-2 increases endothelial permeability also *in vivo* although the size based permeability increase is different compared to the *in vitro* set-up. This is owing to the extremely tight barrier *in vivo*, which is comprised of other components of the NVU compared to the *in vitro* monolayer culture conditions. The effects of Ang-2 on NVU components was therefore investigated.

#### **4.2 Modifications of the neurovascular unit mediated by Ang-2**

In a previous work from our laboratory it has been demonstrated that Ang-2 overexpression reduces the number of pericytes upon time in the peripheral vessels (Scholz et al., 2011). This was also observed in other studies, which showed an increase in endothelial permeability in non-brain endothelial cells (Benest et al., 2013; Ziegler et al., 2013). With the established role of pericytes in regulating the permeability of BBB that is formed by the brain capillary endothelium (Armulik et al., 2010), changes in the NVU due to observed Ang-2 mediated BBB permeability was therefore investigated.

Parts of the NVU were analyzed by immunohistochemistry (IHC) and ultrastructural analysis via electron microscopy (EM). One component of the NVU are astrocytes which are linkers between neurons and endothelial cells (Abbott et al., 2006). Astrocytic endfeet coverage has an essential role in barrier permeability which was reported in several previous studies that demonstrate a tight BBB *in vitro* upon co-culture experiments with astrocytes (Jeliazkova-Mecheva and Bobilya, 2003; Ma et al., 2005; Li et al., 2010). In IHC analysis no obvious changes in the astrocytic endfeet processes of Ang-2 overexpressing endothelial cells in the brain were observed with the staining for endfeet marker aquaporin-4 (Figure 3-5 A). However, the EM ultrastructural analysis identified astrocytic endfeet swelling in mice overexpressing Ang-2 (Figure 3-6 A) potentially by water uptake via aquaporin-4 channels (Zador et al., 2009), which cannot be detected by IHC. This raised the question whether mice that overexpressed Ang-2 acquired detectable brain edema. Because BBB breakdown is often associated with edema effects, the brain water content of Ang-2 overexpressing mice and wild type littermates were determined by wet to dry brain weight ratio method. There was no significant

difference in the water content (Figure 3-9), however this method is not very sensitive and thus only detects differences in severe conditions.

Ultrastructural analysis revealed infrequent pericyte degeneration (Figure 3-6 B), which could be confirmed with IHC staining using desmin as a pericyte marker. Brain sections of Ang-2 overexpressing mice demonstrated a significant reduction of pericyte numbers compared to wild type littermates. This indicates that pericyte reduction is one reason for the observed increased permeability due to Ang-2. Moreover, pericytes have a protective effect on endothelial cells and provide a survival benefit to the endothelium (Franco et al., 2011), which could also be affected in the Ang-2 overexpressing mice. Recently it was shown that pericytes are also essential for maintaining and regulating BBB permeability by preventing caveolae-mediated transcytosis in pericyte retention mice that did not have any alterations in the intercellular tight or adherens junctions (Armulik et al., 2010). EM analysis of the Ang-2 overexpressing mice indeed showed increased flask shaped plasmalemmal vesicles in Ang-2 transgenic mice reminiscent of caveolae (Figure 3-6 C), a sub set of the lipid rafts that are responsible for higher endothelial permeability of peripheral vascular endothelium (Chen et al., 2002). In addition to that, Western blot expression analysis from wild type and Ang-2 transgenic littermates demonstrated an increase in caveolin-1 expression (Figure 3-7 C), a scaffolding protein essential for caveolae formation (Tuma and Hubbard, 2003) in the Ang-2 overexpressing mice, supporting the EM analysis. Furthermore, particles of lanthanum nitrate that stains luminal glycocalyx were found deposited on the abluminal side in the basement membrane, which were occasionally found in intracellular vesicles suggesting increased transcytosis in the Ang-2 overexpressing mice (Figure 3-6 E).

As it is known that glycocalyx influences vascular permeability via its binding to plasma proteins (Vink et al., 2000), the luminal glycocalyx length between Ang-2 transgenic and wild type mice was analyzed by EM. The glycocalyx normally limits the access of certain macromolecules (Reitsma et al., 2007). It was previously shown that in perfused heart models the endothelial barrier function is impaired after glycocalyx degradation (Jacob et al., 2006). Using lanthanum nitrate, a cation that binds to negatively charged glycoproteins forming the glycocalyx, a decrease in the length of the glycocalyx in Ang-2 transgenic mice was observed from about 300nm - 400 nm to about 100 nm (Figure 3-6 E). Interestingly, Ang-1 has been reported to increase the depth of the glycocalyx and reduce vascular permeability supporting the shedding of the glycocalyx mediated by

---

Ang-2, the antagonist of Ang-1 (Salmon et al., 2009). However, it is currently unclear how Angiopoetins modulate the glycocalyx.

Further, ultrastructural analysis revealed decreased length and complexity of the inter endothelial junctions with prevalent gaps indicative of increases in paracellular permeability mediated by Ang-2 (Figure 3-6 D) as presumed from *in vitro* permeability assays in primary cultured brain endothelial cells from Ang-2 transgenic mice. Although IHC stainings of tight or adherens junctions did not display conspicuous changes in the arrangement or expression pattern (Figure 3-7 B), the quantitative expression analysis via Western blotting confirmed the reduction and disassembly of junctional proteins deduced from EM analysis. Ang-2 induced junctional changes were also observed in human brain microvascular endothelial cells in a previous publication. Researchers reported a downregulation of Claudin-5 mediated by Ang-2 which verifies our observed data by Western blot analysis (Avraham et al., 2014). Expression at the mRNA level demonstrated in this work highly diminished Claudin-3 transcript, which could not be verified in protein analysis due to unavailability of specific antibodies (Figure 3-7 A). Other junctional proteins however did not reveal any changes at the mRNA level although Claudin-5 and VE-Cadherin were significantly downregulated in Western Blot analysis (Figure 3-7 C) implying a diminished expression in translation for both proteins.

#### **4.3 Inflammatory response due to Ang-2 mediated permeability**

As astrocytic swelling that could be a result of inflammatory response was detectable in Ang-2 overexpressing mice, leukocyte trafficking was investigated to elaborate whether Ang-2 mediated permeability caused a secondary inflammatory response. Therefore brains of wild type and Ang-2 transgenic mice were assessed for leukocyte infiltration using markers for macrophages (F4/80) and neutrophils (Gr1). F4/80 were significantly increased in Ang-2 DT mice, whereas neutrophils were increased in tendency (Figure 3-8 B). This result confirms that the infiltration of macrophages also occurs in the brain similar to the periphery in Ang-2 overexpressing mice (Scholz et al., 2011). This is in line with the observed decrease in the length and thickness of the glycocalyx in Ang-2 DT mice, which is reported for increased leukocyte adhesion (Henry and Duling, 2000; Constantinescu et al., 2003). An intact glycocalyx surface in the blood lumen serves as a barrier for leukocyte recruitment and subsequently their transfer across the endothelium (Rehm et al., 2007; Bruegger et al., 2009).



*In vivo* permeability studies on different sized tracers indicated that only Lucifer Yellow (0.45 kD) but not the higher molecular tracers was significantly increased in the brains of Ang-2 overexpressing mice (Figure 3-4). However, an increase in the number of macrophages whose size is much bigger (160 kD) was detected. This contradiction in the size-based permeability can be explained from the paracellular route preferred by the tracers whereas the infiltrating leukocytes might preferentially migrate transcellularly (Engelhardt and Wolburg, 2004).

Taken together, Ang-2 at the BBB increases permeability by effecting the expression of both, paracellular junctions and transcellular vesicular transport systems and the endothelial glycocalyx membrane. Additionally resulting in astrocytic endfeet swelling, pericyte loss, and leukocyte infiltration.

#### **4.4 Angiopoietins and Wnt / Sonic hedgehog pathways**

The observation that Ang-2 signaling plays a role in brain vascular permeability opens up the question whether Angiopoietin / Tie2 signaling acts independently or in conjunction with other signaling pathways mediating BBB properties.

The BBB permeability was shown to be regulated by canonical Wnt /  $\beta$ -Catenin signaling effecting brain vascular development and maintenance of barrier properties (Liebner et al., 2008; Daneman et al., 2009). More recently sonic hedgehog signaling has been shown to contribute to barrier maturation (Alvarez et al., 2011). However, it is unclear if the Wnt / sonic pathways act alone or interact with other pathways in controlling the BBB function. With regard to interplay between Angiopoietin / Tie2 pathway and Wnt /  $\beta$ -Catenin signaling, it was very recently demonstrated that shear stress increased Ang-2 expression via the activation of canonical Wnt pathway in aortic endothelial cells. This effect was reversed with Wnt inhibition and also *in vivo* vascular repair in zebrafish (Li et al., 2014). However, the authors do not assess the role of Ang-2 in inhibiting Ang-1 mediated Tie2 signaling which has an established role in maintaining vessel integrity (Thurston et al., 2000), thus making it difficult to assess the independent effects of Angiopoietins and Wnts and their interplay. Such a role for Ang-2 in vascular repair is supported by studies showing vascular regression in the absence of VEGF (Holash et al., 1999). The role of sonic hedgehog (shh) pathway in regulating Angiopoietins has been reported *in vitro* in NIH 3T3 cells that do not express shh protein (Lee et al., 2007). It was demonstrated using recombinant shh that resulted in activation of target gene Gli1 also lead to the upregulation of Ang-1 mRNA and a decrease in the levels of Ang-2

mRNA. This effect was reversed in loss of function experiments using cyclopamine, a specific inhibitor of shh signaling pathway. These findings suggest a role of Angiopoetins downstream to the sonic pathway. The above role of shh in regulating Ang-1 / Ang-2 is well supported by the established vessel maturation and barrier maintenance of shh pathway (Alvarez et al., 2011).

#### **4.5 The impact of Ang-2 in pathophysiology**

Stroke is a severe neurologic disorder, which leads to breakdown of the BBB with increased edema into the neurologic brain tissue. Ang-2 has been shown to be associated with BBB disruption and apoptosis (Beck et al., 2000; Nag et al., 2005), with its overexpression in the early phase of BBB breakdown in qRT-PCR analysis after a rat cortical cold-injury model whereas Ang-1 and Tie2 protein expression decreased (Nourhaghighi et al., 2003). However, the authors did not elaborate the direct effects of Ang-2 on BBB permeability. A similar observation was made with human stroke patients in this work. Ang-2 expression pattern correlated with human stroke grades (Figure 3-12 A) suggesting a role for Ang-2 during BBB disruption. Ang-2 was detectable from 2 up to 15 days after stroke incidence in the blood of patients with territorial stroke cases possessing the most Ang-2 expression in ELISA studies (Figure 3-12 B). Ang-2 was demonstrated as a risk factor for stroke in the current work in a permanent MCAO model, in which the Ang-2 overexpressing mice had bigger strokes and increased permeability in the stroke areas (Figure 3-13 A, B).

#### **4.6 Therapeutic targeting of Tie2 signaling in stroke**

With Ang-2 as a risk factor for stroke, an inhibitor of vascular endothelial protein tyrosine phosphatase (VE-PTP) was tested as a therapeutic target. VE-PTP is known to be upregulated in hypoxic cells where it negatively regulates the Tie2 activation (Shen et al., 2014). VE-PTP also associates with VE-Cadherin where it supports the adhesive activity of VE-Cadherin and therefore the integrity of endothelial cell connections (Nottebaum et al., 2008; Broermann et al., 2011). It has been reported that the inhibitor of VE-PTP slows down the growth of micrometastasis and prevents the extravasation of tumor cells by activation of eNOS in a zebrafish model (Goel et al., 2013). This prompted us to test the effect of this inhibitor in a transient stroke mouse model whereby activation of Tie2 and its downstream signaling cascades could lead to a decrease in permeability and induce vessel integrity and potentially improvement in stroke sizes. To determine the mechanism of action of the VE-PTP Inhibitor at the BBB, *in vitro* analysis was

---

performed in MBMECs from C57 / Bl6 mice and its downstream signaling was elaborated. Cells were pre-treated with recombinant hAng-2, comparable with the situation in stroke conditions where Ang-2 expression is high, followed by treatment with the VE-PTP inhibitor. Both pTie2 and pAkt were upregulated whereas VE-Cadherin was in tendency decreased (Figure 3-14 A, B). Thus the inhibitor is able to rescue the effects of Ang-2 mediated decrease in Tie-2 signaling. These findings demonstrate that the VE-PTP inhibitor activates Tie2 signaling at the BBB over the activation of VE-Cadherin indicated by a decrease in its phosphorylation. It has been demonstrated that the dissociation or inhibition of VE-PTP and VE-Cadherin complex is important for the VEGF-induced permeability (Broermann et al., 2011).

Therapeutic effects of the inhibitor were therefore evaluated in a transient MCAO stroke model that is more comparable with the situation in human patients. Wild type CD1 mice were pre-treated twice with VE-PTP inhibitor and once after MCAO, as its half-life in the mice is about 12 h. The therapeutic effects of the inhibitor were assessed after 24 h of MCAO where a diminished stroke size compared to control groups was observed (Figure 3-15 A, B). This was accompanied by a decrease in permeability in the stroke area of treated animals. Moreover, the behavioral evaluation revealed that mice treated with the VE-PTP inhibitor had a neurological improvement after stroke (Figure 3-15 C). Western blot analysis of the stroke samples treated with the inhibitor revealed an activation of Akt (Figure 3-15 D) as observed *in vitro* in MBMECs. This was further supported by an increase in pTie2 staining in VE-PTP inhibitor mouse brains by IHC (Figure 3-15 E). This analysis demonstrates that specific effects of the VE-PTP inhibitor in improving stroke outcome are mediated by activated Tie2 signaling.

Therapeutic approaches to minimize brain damage after stroke were tested in this study with the VE-PTP inhibitor. A similar approach to the VE-PTP inhibitor is Ang-1 treatment, which also induces the activation of Tie2 and diminishes the phosphorylation of VE-Cadherin, sequestering Src from mDia (London et al., 2009), which is in line with the observed effects with the VE-PTP inhibitor. Ang-1 antagonizes VEGF, which induces permeability and matrix metalloprotease-9 activity, and therefore could be used early in BBB breakdown to diminish the disruption effect and induce the formation of mature vessels (Matyszak and Perry, 1996). Ang-1 expression in patients who suffered from stroke was 3-fold lower compared to healthy subjects. Patients with severe disability or those who died after ischemic stroke possessed even lower Ang-1 levels suggesting a particular role of Ang-1 / Tie2 pathway for recovery after stroke (Golledge et al., 2014).

Additionally, the application of recombinant Ang-1 inhibited the vascular permeability induced by VEGF and also decreased the infarct size (Zhang et al., 2002). It has been shown that increased expression of Ang-1 and decreased expression of Ang-2 contributed to vascular remodeling after stroke (Ye et al., 2011).

Microglia and peripheral macrophages produce inflammatory cytokines after stroke, which are harmful to the surrounding tissue (Perry et al., 2010). Depletion of macrophages has been shown to improve the artery structure and endothelial function after stroke (Pires et al., 2013). Ang-2 induces myeloid cell infiltration (Scholz et al., 2011), which contribute to the production of inflammatory mediators that cause collateral damage to the brain. Therefore it still needs to be investigated whether the reactivation of Tie2 via the VE-PTP inhibitor decreases the infiltration of myeloid cells and blood-derived macrophages in stroke samples, which could be one of the reasons for the decreased stroke size observed in this work. Moreover, a second peak of Ang-2 induction appears days after stroke, which causes microvessel degradation (Lin et al., 2000), which could also be potentially blocked by treatment with the VE-PTP inhibitor. Angiogenesis occurs after stroke, which is also associated with increase in macrophages (Manoonkitiwongsa et al., 2001). A previous work demonstrates Ang-2 as a mediator that interacts with macrophages inducing cell death. It is suggested that Ang-2 activates the expression of Wnt7b, a ligand for the Wnt /  $\beta$ -Catenin pathway promoting the cell cycle entry. This is accompanied by a decrease in Akt activation inducing apoptotic mediators like Foxo and Bad (Rao et al., 2007). Thus the activation of Tie2 would potentially lead to decreased cell death in the surrounding tissue. Therefore, combination treatments activating Tie2 for diminishing BBB permeability at the early stages along with treatments inhibiting leukocyte infiltration and diminishing pro-inflammatory macrophages at later stages could have a stronger effect in reducing the infarct size including the penumbra area.

Thus, Ang-2 contributes to permeability and increased stroke size by inhibiting Tie2 signaling, effects that could partially be rescued by a VE-PTP inhibitor that activates Tie2 and reduces the phosphorylation of VE-Cadherin for stabilization of adjacent endothelial cells at the BBB.

#### **4.7 A potential role of Ang-2 in aging**

Interestingly, endothelial-specific overexpression of Ang-2 for 6 to 12 months resulted in decreased permeability in Ang-2 DT MBMECs compared to wild type measured by TEER

(Figure 3-11 A). This was confirmed by tracer studies *in vivo* showing decreased TexasRed 3kD-dextran permeability in 7 month old Ang-2 DT mice compared to wild type (Figure 3-11 B). Furthermore, infiltrating macrophages were not increased in Ang-2 overexpressing mice compared to wild type (Figure 3-11 C), an effect that was prominent in young animals. These data suggest a tightening effect of Ang-2 on brain microvessels upon long-term expression, which could potentially be a compensatory effect as young Ang-2 DT mice exhibited a breakdown of the BBB. This compensatory effect was not observed in peripheral blood vessels where Ang-2 expression up to 52 weeks resulted in strong myeloid cell infiltration in different organs (Scholz et al., 2011). Ang-1 expression was analyzed in young Ang-2 DT mice to determine the presence of Ang-1 mediated compensatory effects. No differences could be observed between wild type and Ang-2 overexpressing mice (Figure 3-10), this however is yet to be investigated in older Ang-2 DT animals.

Aging studies of Ang-2 in human corpus cavernosum from young and aged healthy probands revealed marginal increase in mRNA expression of Ang-2 in aged persons whereas the Ang-1 / Tie2 ratio decreased six times compared to young patients (Figueiredo et al., 2011). Moreover, it is known that Ang-2 is overexpressed in human Alzheimer's disease (AD) patients (Thirumangalakudi et al., 2006), an age-related disorder, whereas Ang-1 serum levels are also significantly higher in AD patients. Additionally, the degree of cognitive impairment correlated with Ang-1 serum levels. The study however did not investigate an association of high Ang-2 expression with cognitive impairment (Schreitmüller et al., 2012). Ang-2 is probably upregulated due to hypoperfusion and hypoxia events in AD patients whereas Ang-1 levels might be high due to compensatory effects of long-term high Ang-2 expression which leads to the cognitive impairment. These studies open the question whether Ang-2 in age-related disorders exhibit a more dramatic impact on brain permeability in longer-term expressions, whereas the discovered compensatory response (in 6-12 months Ang-2 overexpressing mice) in this study based on potentially increased Ang-1 expression was only time-dependently resulting in tightening of the BBB. This needs to be further investigated.

#### **4.8 Conclusion and perspectives**

In the current work, I was able to demonstrate that Ang-2 mediates brain vascular permeability in primary cells and in a genetic mouse model overexpressing Ang-2 in the endothelium. Ang-2 decreases the expression of Claudin-5, Claudin-3 and VE-Cadherin

leading to increased paracellular permeability. The increase in transcellular transport visualized by EM analysis and quantified by Western blot analysis via the upregulation of Caveolin-1 expression could be a consequence of reduced pericyte coverage (Armulik et al., 2010). This results in infiltrating macrophages in the Ang-2 overexpressing mice, which could also be secondary to decreased glycocalyx formation that is known to prevent leukocyte infiltration (Figure 4-1 A). In a disease model it was shown that Ang-2 is a risk factor that contributes to bigger strokes and higher permeability in stroke areas compared to control groups, effects that could be rescued by activation of Tie2 signaling using a VE-PTP inhibitor. Activation of Tie2 and decreased phosphorylation of the adherens junction VE-Cadherin leading to a diminished infarct size and reduced permeability after stroke demonstrate the specific effects of the VE-PTP inhibitor (Figure 4-2 B).

It is however unclear whether the Ang / Tie signaling pathway acts in conjunction with the Wnt- and / or Sonic hedgehog pathway or whether Tie signaling independently influences BBB properties. Previous work (Lee et al., 2007; Li et al., 2014) suggests a link to both pathways, which however needs to be investigated in detail at the BBB.

Macrophages play certain roles during stroke development and Ang-2 has been shown to be associated with myeloid cell infiltration (Scholz et al., 2011). Combination treatments targeting infiltrating macrophages which harm the surrounding tissue of infarct area along with those activating Tie2 might result in even greater decrease in stroke volumes and potentially better neurologic activity.

Interestingly, older Ang-2 overexpressing mice acquire improved BBB properties as demonstrated by TEER measurement and tracer analysis. In line with this, numbers of macrophages do not change in long-term overexpression of Ang-2 (Figure 4-1 C). These data suggest a compensatory effect, which was not investigated in this work. Additional analyses of the brain in ultrastructure or by immunohistochemistry stainings need to be performed to elaborate the compensatory effects of Ang-2 expression. Further analysis should concentrate on potential proteins, which could be regulated in this mouse system leading to a tighter barrier in the brain. This could be analyzed by an RNA screening of microvessels from the brain for detection of regulated proteins. It is still not clear whether Ang-2 expression levels alter during aging. There is an interesting link between Angiopoietins and AD, an age-related disorder. Future studies of Angiopoietins in AD could yield more information about their role in aging.

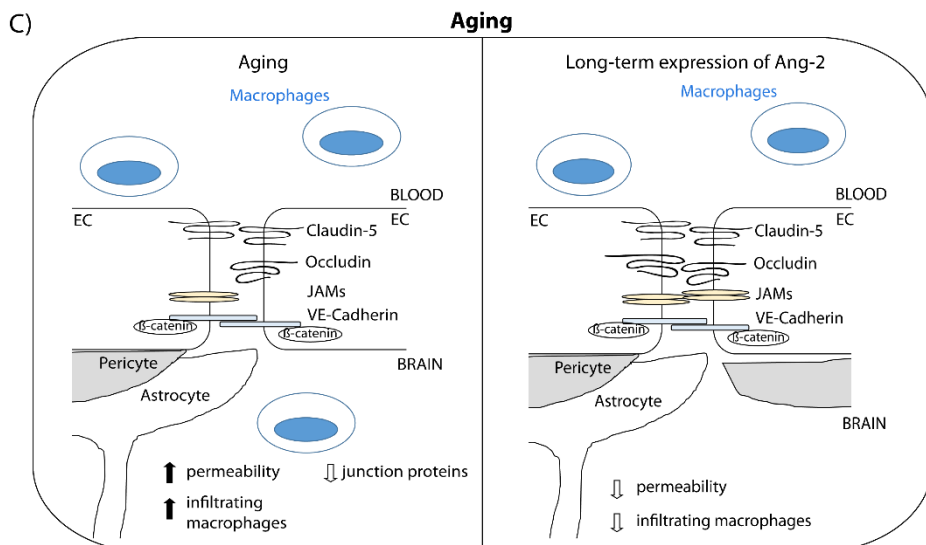
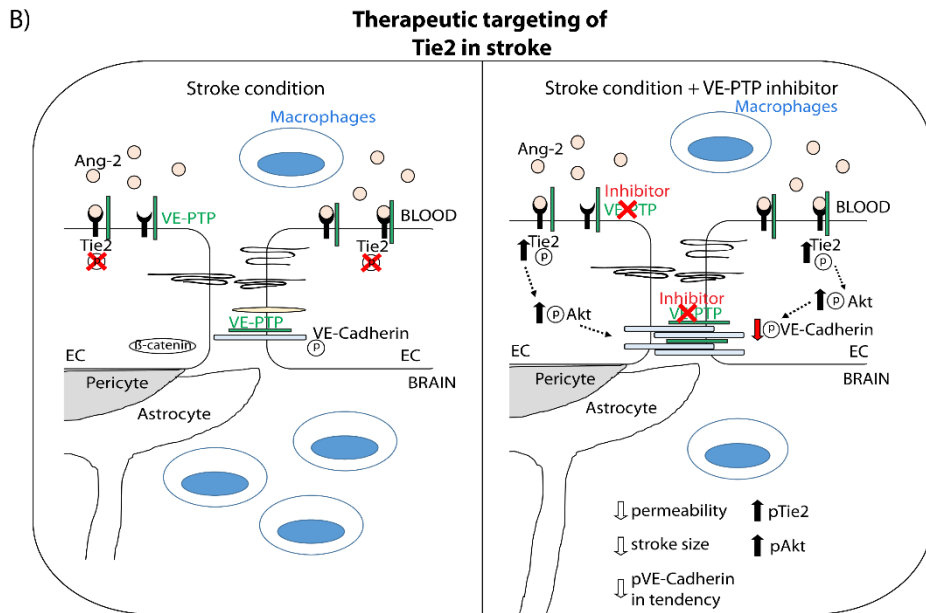
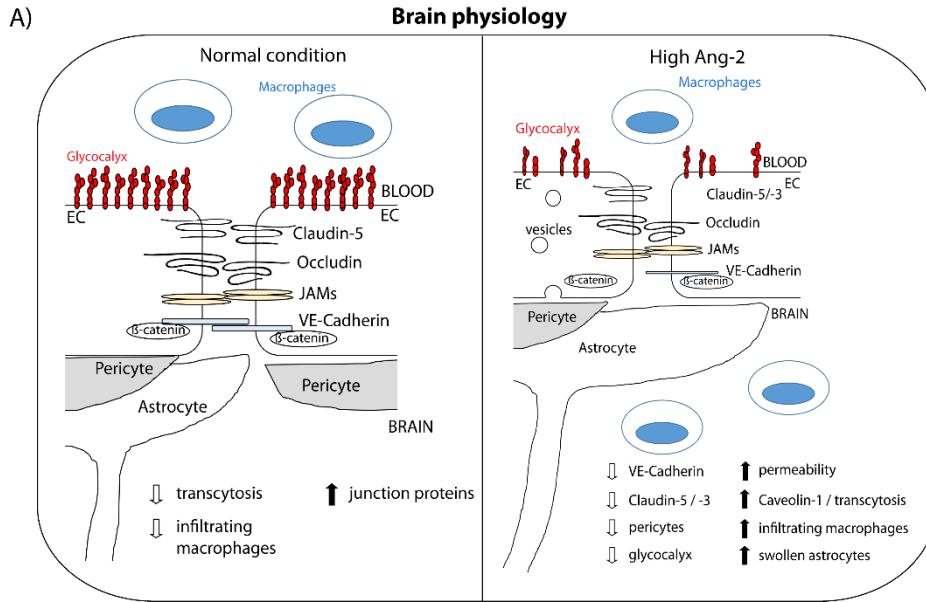


**Figure 4-1: The influence of Ang-2 on brain permeability**

Ang-2 influences brain permeability in physiologic conditions, in cerebrovascular diseases and potentially in aging. A) In brain physiology high Ang-2 expression contributes to reduced junction proteins such as VE-Cadherin and Claudin-5 / -3 which raises paracellular permeability. At the same time number of pericytes decreases which leads to elevated transcytosis rates. This is in line with increased Caveolin-1 expression. High Ang-2 rates also promote the infiltration of macrophages also due to diminished diameter of the glycocalyx at the luminal side. B) In stroke conditions high Ang-2 levels are accompanied with high brain permeability. The VE-PTP inhibitor induces the activation of Tie2 and Akt during high levels in stroke conditions which leads to decreased brain permeability and stroke sizes by limiting the pVE-Cadherin expression in tendency. C) During aging the BBB becomes affected by downregulation of junction proteins which increases rates of infiltrating macrophages and permeability. Long-term expression of Ang-2 results in tightening effects demonstrated by decreased permeability and low amounts of infiltrating macrophages.

In conclusion, Ang-2 is a novel regulator of blood-brain barrier permeability. Investigating its interaction with other signaling cascades will lead to a better understanding of the permeability regulation at the BBB. Targeting the Angiopoietin / Tie2 signaling pathway could lead to novel therapeutics that either can transiently open the BBB for CNS drug delivery or tighten the BBB in neurological disorders that are associated with increased vascular leakage and brain edema.



## 5. REFERENCES

- Abadier M, Haghayegh Jahromi N, Cardoso Alves L, Boscacci R, Vestweber D, Barnum S, Deutsch U, Engelhardt B, Lyck R (2015) Cell surface levels of endothelial ICAM-1 influence the transcellular or paracellular T-cell diapedesis across the blood-brain barrier. *Eur J Immunol* 45:1043–1058.
- Abbott NJ, Rönnbäck L, Hansson E (2006) Astrocyte-endothelial interactions at the blood-brain barrier. *Nat Rev Neurosci* 7:41–53.
- Adams RH, Alitalo K (2007) Molecular regulation of angiogenesis and lymphangiogenesis. *Nat Rev Mol Cell Biol* 8:464–478.
- Agrawal S, Anderson P, Durbeej M, van Rooijen N, Ivars F, Opdenakker G, Sorokin LM (2006) Dystroglycan is selectively cleaved at the parenchymal basement membrane at sites of leukocyte extravasation in experimental autoimmune encephalomyelitis. *J Exp Med* 203:1007–1019.
- Alvarez JI, Dodelet-Devillers A, Kebir H, Ifergan I, Fabre PJ, Terouz S, Sabbagh M, Wosik K, Bourbonniere L, Bernard M, van Horssen J, de Vries HE, Charron F, Prat A (2011) The Hedgehog Pathway Promotes Blood-Brain Barrier Integrity and CNS Immune Quiescence. *Science* 334:1727–1731.
- Arai F, Hirao A, Ohmura M, Sato H, Matsuoka S, Takubo K, Ito K, Koh GY, Suda T (2004) Tie2/angiopoietin-1 signaling regulates hematopoietic stem cell quiescence in the bone marrow niche. *Cell* 118:149–161.
- Argaw AT, Gurfein BT, Zhang Y, Zameer A, John GR (2009) VEGF-mediated disruption of endothelial CLN-5 promotes blood-brain barrier breakdown. *Proc Natl Acad Sci U S A* 106:1977–1982.
- Arisaka T, Mitsumata M, Kawasumi M, Tohjima T, Hirose S, Yoshida Y (1995) Effects of shear stress on glycosaminoglycan synthesis in vascular endothelial cells. *Ann N Y Acad Sci* 748:543–554.
- Armulik A, Genové G, Betsholtz C (2011) Pericytes: developmental, physiological, and pathological perspectives, problems, and promises. *Dev Cell* 21:193–215.
- Armulik A, Genové G, Mäe M, Nisancioglu MH, Wallgard E, Niaudet C, He L, Norlin J, Lindblom P, Strittmatter K, Johansson BR, Betsholtz C (2010) Pericytes regulate the blood-brain barrier. *Nature* 468:557–561.
- Asahi M, Asahi K, Jung JC, del Zoppo GJ, Fini ME, Lo EH (2000) Role for matrix metalloproteinase 9 after focal cerebral ischemia: effects of gene knockout and enzyme inhibition with BB-94. *J Cereb Blood Flow Metab* 20:1681–1689.
- Attwell D, Buchan AM, Charpak S, Lauritzen M, Macvicar BA, Newman EA (2010) Glial and neuronal control of brain blood flow. *Nature* 468:232–243.
- Augustin HG, Koh GY, Thurston G, Alitalo K (2009) Control of vascular morphogenesis and homeostasis through the angiopoietin-Tie system. *Nat Rev Mol Cell Biol* 10:165–177.

- Avraham HK, Jiang S, Fu Y, Nakshatri H, Ovadia H, Avraham S (2014) Angiopoietin-2 mediates blood-brain barrier impairment and colonization of triple-negative breast cancer cells in brain. *J Pathol* 232:369–381.
- Ayata C, Ropper AH (2002) Ischaemic brain oedema. *J Clin Neurosci* 9:113–124.
- Barton WA, Tzvetkova-Robev D, Miranda EP, Kolev M V, Rajashankar KR, Himanen JP, Nikolov DB (2006) Crystal structures of the Tie2 receptor ectodomain and the angiopoietin-2-Tie2 complex. *Nat Struct Mol Biol* 13:524–532.
- Bazzoni G, Dejana E (2004) Endothelial cell-to-cell junctions: molecular organization and role in vascular homeostasis. *Physiol Rev* 84:869–901.
- Beck H, Acker T, Wiessner C, Allegrini PR, Plate KH (2000) Expression of angiopoietin-1, angiopoietin-2, and tie receptors after middle cerebral artery occlusion in the rat. *Am J Pathol* 157:1473–1483.
- Beck H, Plate KH (2009) Angiogenesis after cerebral ischemia. *Acta Neuropathol* 117:481–496.
- Belayev L, Busto R, Zhao W, Ginsberg MD (1996) Quantitative evaluation of blood-brain barrier permeability following middle cerebral artery occlusion in rats. *Brain Res* 739:88–96.
- Benest A V, Kruse K, Savant S, Thomas M, Laib AM, Loos EK, Fiedler U, Augustin HG (2013) Angiopoietin-2 is critical for cytokine-induced vascular leakage. *PLoS One* 8:e70459.
- Betz AL, Goldstein GW (1978) Polarity of the blood-brain barrier: neutral amino acid transport into isolated brain capillaries. *Science* 202:225–227.
- Betz AL, Iannotti F, Hoff JT (1989) Brain edema: a classification based on blood-brain barrier integrity. *Cerebrovasc Brain Metab Rev* 1:133–154.
- Bogdanovic E, Nguyen VPKH, Dumont DJ (2006) Activation of Tie2 by angiopoietin-1 and angiopoietin-2 results in their release and receptor internalization. *J Cell Sci* 119:3551–3560.
- Breier G, Risau W (1996) The role of vascular endothelial growth factor in blood vessel formation. *Trends Cell Biol* 6:454–456.
- Brieher W (2013) Mechanisms of actin disassembly. *Mol Biol Cell* 24:2299–2302.
- Broermann A, Winderlich M, Block H, Frye M, Rossaint J, Zarbock A, Cagna G, Linnepe R, Schulte D, Nottebaum AF, Vestweber D (2011) Dissociation of VE-PTP from VE-cadherin is required for leukocyte extravasation and for VEGF-induced vascular permeability in vivo. *J Exp Med* 208:2393–2401.
- Broughton S, Partridge L (2009) Insulin/IGF-like signalling, the central nervous system and aging. *Biochem J* 418:1–12.

- Bruegger D, Rehm M, Abicht J, Paul JO, Stoeckelhuber M, Pfirrmann M, Reichart B, Becker BF, Christ F (2009) Shedding of the endothelial glycocalyx during cardiac surgery: on-pump versus off-pump coronary artery bypass graft surgery. *J Thorac Cardiovasc Surg* 138:1445–1447.
- Cai J, Kehoe O, Smith GM, Hykin P, Boulton ME (2008) The angiopoietin/Tie-2 system regulates pericyte survival and recruitment in diabetic retinopathy. *Invest Ophthalmol Vis Sci* 49:2163–2171.
- Candelario-Jalil E, Yang Y, Rosenberg GA (2009) Diverse roles of matrix metalloproteinases and tissue inhibitors of metalloproteinases in neuroinflammation and cerebral ischemia. *Neuroscience* 158:983–994.
- Cao Y, Sonveaux P, Liu S, Zhao Y, Mi J, Clary BM, Li C-Y, Kontos CD, Dewhirst MW (2007) Systemic overexpression of angiopoietin-2 promotes tumor microvessel regression and inhibits angiogenesis and tumor growth. *Cancer Res* 67:3835–3844.
- Carlson TR, Feng Y, Maisonpierre PC, Mrksich M, Morla AO (2001) Direct cell adhesion to the angiopoietins mediated by integrins. *J Biol Chem* 276:26516–26525.
- Carmeliet P, Ferreira V, Breier G, Pollefeyt S, Kieckens L, Gertsenstein M, Fahrig M, Vandenhoeck A, Harpal K, Eberhardt C, Declercq C, Pawling J, Moons L, Collen D, Risau W, Nagy A (1996) Abnormal blood vessel development and lethality in embryos lacking a single VEGF allele. *Nature* 380:435–439.
- Cascone I, Napione L, Maniero F, Serini G, Bussolino F (2005) Stable interaction between alpha5beta1 integrin and Tie2 tyrosine kinase receptor regulates endothelial cell response to Ang-1. *J Cell Biol* 170:993–1004.
- Chen J, Braet F, Brodsky S, Weinstein T, Romanov V, Noiri E, Goligorsky MS (2002) VEGF-induced mobilization of caveolae and increase in permeability of endothelial cells. *Am J Physiol Cell Physiol* 282:C1053–C1063.
- Chen J, Sanberg PR, Li Y, Wang L, Lu M, Willing AE, Sanchez-Ramos J, Chopp M (2001) Intravenous administration of human umbilical cord blood reduces behavioral deficits after stroke in rats. *Stroke* 32:2682–2688.
- Chen J, Yu H, Sun K, Song W, Bai Y, Yang T, Song Y, Zhang Y, Hui R (2010) Promoter variant of angiopoietin-2 and plasma angiopoietin-2 are associated with risk of stroke recurrence in lacunar infarct patients. *Biochem Biophys Res Commun* 398:212–216.
- Coffelt SB, Tal AO, Scholz A, De Palma M, Patel S, Urbich C, Biswas SK, Murdoch C, Plate KH, Reiss Y, Lewis CE (2010) Angiopoietin-2 regulates gene expression in TIE2-expressing monocytes and augments their inherent proangiogenic functions. *Cancer Res* 70:5270–5280.
- Coffin JD, Poole TJ (1991) Endothelial cell origin and migration in embryonic heart and cranial blood vessel development. *Anat Rec* 231:383–395.

- Constantinescu AA, Vink H, Spaan JAE (2003) Endothelial cell glycocalyx modulates immobilization of leukocytes at the endothelial surface. *Arterioscler Thromb Vasc Biol* 23:1541–1547.
- Coomber BL, Stewart PA (1985) Morphometric analysis of CNS microvascular endothelium. *Microvasc Res* 30:99–115.
- Cornford EM, Hyman S, Swartz BE (1994) The human brain GLUT1 glucose transporter: ultrastructural localization to the blood-brain barrier endothelia. *J Cereb Blood Flow Metab* 14:106–112.
- Correale J, Villa A (2007) The blood-brain-barrier in multiple sclerosis: functional roles and therapeutic targeting. *Autoimmunity* 40:148–160.
- Curry FE, Adamson RH (2012) Endothelial glycocalyx: permeability barrier and mechanosensor. *Ann Biomed Eng* 40:828–839.
- Czapalla CJ, Liebner S, Devraj K (2014) In vitro models of the blood-brain barrier. *Methods Mol Biol* 1135:415–437.
- Dallabrida SM, Ismail N, Oberle JR, Himes BE, Rupnick MA (2005) Angiotensin-1 promotes cardiac and skeletal myocyte survival through integrins. *Circ Res* 96:e8–e24.
- Daly C, Pasnikowski E, Burova E, Wong V, Aldrich TH, Griffiths J, Ioffe E, Daly TJ, Fandl JP, Papadopoulos N, McDonald DM, Thurston G, Yancopoulos GD, Rudge JS (2006) Angiotensin-2 functions as an autocrine protective factor in stressed endothelial cells. *Proc Natl Acad Sci U S A* 103:15491–15496.
- Daly C, Wong V, Burova E, Wei Y, Zabski S, Griffiths J, Lai KM, Lin HC, Ioffe E, Yancopoulos GD, Rudge JS (2004) Angiotensin-1 modulates endothelial cell function and gene expression via the transcription factor FKHR (FOXO1). *Genes Dev* 18:1060–1071.
- Daneman R (2012) The blood-brain barrier in health and disease. *Ann Neurol* 72:648–672.
- Daneman R, Agalliu D, Zhou L, Kuhnert F, Kuo CJ, Barres BA (2009) Wnt/beta-catenin signaling is required for CNS, but not non-CNS, angiogenesis. *Proc Natl Acad Sci U S A* 106:641–646.
- Daneman R, Prat A (2015) The Blood-Brain Barrier. *Cold Spring Harb Perspect Biol* 7:a020412 – .
- Daneman R, Zhou L, Agalliu D, Cahoy JD, Kaushal A, Barres BA (2010a) The mouse blood-brain barrier transcriptome: a new resource for understanding the development and function of brain endothelial cells. *PLoS One* 5:e13741.
- Daneman R, Zhou L, Kebede A a, Barres B a (2010b) Pericytes are required for blood-brain barrier integrity during embryogenesis. *Nature* 468:562–566.
- Davis S et al. (2003) Angiotensins have distinct modular domains essential for receptor binding, dimerization and superclustering. *Nat Struct Biol* 10:38–44.

- Davis S, Aldrich TH, Jones PF, Acheson A, Compton DL, Jain V, Ryan TE, Bruno J, Radziejewski C, Maisonpierre PC, Yancopoulos GD (1996) Isolation of angiopoietin-1, a ligand for the TIE2 receptor, by secretion-trap expression cloning. *Cell* 87:1161–1169.
- De Palma M, Venneri MA, Galli R, Sergi L, Politi LS, Sampaolesi M, Naldini L (2005) Tie2 identifies a hematopoietic lineage of proangiogenic monocytes required for tumor vessel formation and a mesenchymal population of pericyte progenitors. *Cancer Cell* 8:211–226.
- De Vivo DC, Leary L, Wang D (2002) Glucose transporter 1 deficiency syndrome and other glycolytic defects. *J Child Neurol* 17 Suppl 3:3S15–S23; discussion 3S24–S25.
- DeBusk LM, Hallahan DE, Lin PC (2004) Akt is a major angiogenic mediator downstream of the Ang1/Tie2 signaling pathway. *Exp Cell Res* 298:167–177.
- Del Maschio A, De Luigi A, Martin-Padura I, Brockhaus M, Bartfai T, Fruscella P, Adorini L, Martino G, Furlan R, De Simoni MG, Dejana E (1999) Leukocyte Recruitment in the Cerebrospinal Fluid of Mice with Experimental Meningitis Is Inhibited by an Antibody to Junctional Adhesion Molecule (Jam). *J Exp Med* 190:1351–1356.
- Del Zoppo GJ, Milner R, Mabuchi T, Hung S, Wang X, Koziol JA (2006) Vascular matrix adhesion and the blood-brain barrier. *Biochem Soc Trans* 34:1261–1266.
- Dumont DJ, Gradwohl G, Fong GH, Puri MC, Gertsenstein M, Auerbach A, Breitman ML (1994) Dominant-negative and targeted null mutations in the endothelial receptor tyrosine kinase, tek, reveal a critical role in vasculogenesis of the embryo. *Genes Dev* 8:1897–1909.
- Dumont DJ, Yamaguchi TP, Conlon RA, Rossant J, Breitman ML (1992) tek, a novel tyrosine kinase gene located on mouse chromosome 4, is expressed in endothelial cells and their presumptive precursors. *Oncogene* 7:1471–1480.
- Ellison D, Love S, Chimelli L, et al. Pathologic reactions in the CNS. *Neuropathology: a reference text of CNS pathology* 3-25
- Eklund L, Saharinen P (2013) Angiopoietin signaling in the vasculature. *Exp Cell Res* 319:1271–1280.
- Engelhardt B, Wolburg H (2004) Mini-review: Transendothelial migration of leukocytes: through the front door or around the side of the house? *Eur J Immunol* 34:2955–2963.
- Felcht M et al. (2012) Angiopoietin-2 differentially regulates angiogenesis through TIE2 and integrin signaling. *J Clin Invest* 122:1991–2005.
- Ferrara N (1996) Vascular endothelial growth factor. *Eur J Cancer* 32A:2413–2422.

- Fiedler U, Krissl T, Koidl S, Weiss C, Koblizek T, Deutsch U, Martiny-Baron G, Marmé D, Augustin HG (2003) Angiopoietin-1 and angiopoietin-2 share the same binding domains in the Tie-2 receptor involving the first Ig-like loop and the epidermal growth factor-like repeats. *J Biol Chem* 278:1721–1727.
- Fiedler U, Reiss Y, Scharpfenecker M, Grunow V, Koidl S, Thurston G, Gale NW, Witzenzath M, Rosseau S, Suttrop N, Sobke A, Herrmann M, Preissner KT, Vajkoczy P, Augustin HG (2006) Angiopoietin-2 sensitizes endothelial cells to TNF-alpha and has a crucial role in the induction of inflammation. *Nat Med* 12:235–239.
- Fiedler U, Scharpfenecker M, Koidl S, Hegen A, Grunow V, Schmidt JM, Kriz W, Thurston G, Augustin HG (2004) The Tie-2 ligand angiopoietin-2 is stored in and rapidly released upon stimulation from endothelial cell Weibel-Palade bodies. *Blood* 103:4150–4156.
- Figueiredo A, Cordeiro AL, Tomada N, Tomada I, Rodrigues A, Gouveia A, Neves D (2011) Real-time PCR study of Ang1, Ang2, Tie-2, VEGF, and KDR expression in human erectile tissue during aging. *J Sex Med* 8:1341–1351.
- Flamme I, Risau W (1992) Induction of vasculogenesis and hematopoiesis in vitro. *Development* 116:435–439.
- Franco M, Roswall P, Cortez E, Hanahan D, Pietras K (2011) Pericytes promote endothelial cell survival through induction of autocrine VEGF-A signaling and Bcl-w expression. *Blood* 118:2906–2917.
- Gale NW, Thurston G, Hackett SF, Renard R, Wang Q, McClain J, Martin C, Witte C, Witte MH, Jackson D, Suri C, Campochiaro PA, Wiegand SJ, Yancopoulos GD (2002) Angiopoietin-2 is required for postnatal angiogenesis and lymphatic patterning, and only the latter role is rescued by Angiopoietin-1. *Dev Cell* 3:411–423.
- Gerhardt H (2008) VEGF and endothelial guidance in angiogenic sprouting SC ND Introduction RIB ND ES SC. :241–246.
- Gerhardt H, Golding M, Fruttiger M, Ruhrberg C, Lundkvist A, Abramsson A, Jeltsch M, Mitchell C, Alitalo K, Shima D, Betsholtz C (2003) VEGF guides angiogenic sprouting utilizing endothelial tip cell filopodia. *J Cell Biol* 161:1163–1177.
- Goel S, Gupta N, Walcott BP, Snuderl M, Kesler CT, Kirkpatrick ND, Heishi T, Huang Y, Martin JD, Ager E, Samuel R, Wang S, Yazbek J, Vakoc BJ, Peterson RT, Padera TP, Duda DG, Fukumura D, Jain RK (2013) Effects of vascular-endothelial protein tyrosine phosphatase inhibition on breast cancer vasculature and metastatic progression. *J Natl Cancer Inst* 105:1188–1201.
- Golledge J, Clancy P, Maguire J, Lincz L, Koblar S, McEvoy M, Attia J, Levi C, Sturm J, Almeida OP, Yeap BB, Flicker L, Norman PE, Hankey GJ (2014) Plasma angiopoietin-1 is lower after ischemic stroke and associated with major disability but not stroke incidence. *Stroke* 45:1064–1068.
- Gordon GRJ, Howarth C, MacVicar BA (2011) Bidirectional control of arteriole diameter by astrocytes. *Exp Physiol* 96:393–399.

- Gu Y, Zheng G, Xu M, Li Y, Chen X, Zhu W, Tong Y, Chung SK, Liu KJ, Shen J (2012) Caveolin-1 regulates nitric oxide-mediated matrix metalloproteinases activity and blood-brain barrier permeability in focal cerebral ischemia and reperfusion injury. *J Neurochem* 120:147–156.
- Ha SN, Hochman J, Sheridan RP (2007) Mini review on molecular modeling of P-glycoprotein (Pgp). *Curr Top Med Chem* 7:1525–1529.
- Hackett SF, Wiegand S, Yancopoulos G, Campochiaro PA (2002) Angiopoietin-2 plays an important role in retinal angiogenesis. *J Cell Physiol* 192:182–187.
- Hamel E (2006) Perivascular nerves and the regulation of cerebrovascular tone. *J Appl Physiol* 100:1059–1064.
- Hammes H-P, Lin J, Wagner P, Feng Y, Vom Hagen F, Krzizok T, Renner O, Breier G, Brownlee M, Deutsch U (2004) Angiopoietin-2 causes pericyte dropout in the normal retina: evidence for involvement in diabetic retinopathy. *Diabetes* 53:1104–1110.
- Hansen TM, Moss AJ, Brindle NPJ (2008) Vascular endothelial growth factor and angiopoietins in neurovascular regeneration and protection following stroke. *Curr Neurovasc Res* 5:236–245.
- Harfouche R, Hussain SNA (2006) Signaling and regulation of endothelial cell survival by angiopoietin-2. *Am J Physiol Heart Circ Physiol* 291:H1635–H1645.
- Hawkins BT, Davis TP (2005) The blood-brain barrier/neurovascular unit in health and disease. *Pharmacol Rev* 57:173–185.
- Hayashi Y, Nomura M, Yamagishi S, Harada S, Yamashita J, Yamamoto H (1997) Induction of various blood-brain barrier properties in non-neural endothelial cells by close apposition to co-cultured astrocytes. *Glia* 19:13–26.
- Heinke J, Patterson C, Moser M (2012) Life is a pattern: vascular assembly within the embryo. *Front Biosci (Elite Ed)* 4:2269–2288.
- Hellström M, Gerhardt H, Kalén M, Li X, Eriksson U, Wolburg H, Betsholtz C (2001) Lack of pericytes leads to endothelial hyperplasia and abnormal vascular morphogenesis. *J Cell Biol* 153:543–553.
- Hellström M, Phng L-K, Hofmann JJ, Wallgard E, Coultas L, Lindblom P, Alva J, Nilsson A-K, Karlsson L, Gaiano N, Yoon K, Rossant J, Iruela-Arispe ML, Kalén M, Gerhardt H, Betsholtz C (2007) Dll4 signalling through Notch1 regulates formation of tip cells during angiogenesis. *Nature* 445:776–780.
- Henninger DD, Panés J, Eppihimer M, Russell J, Gerritsen M, Anderson DC, Granger DN (1997) Cytokine-induced VCAM-1 and ICAM-1 expression in different organs of the mouse. *J Immunol* 158:1825–1832.
- Henry CB, Duling BR (1999) Permeation of the luminal capillary glycocalyx is determined by hyaluronan. *Am J Physiol* 277:H508–H514.

- Henry CB, Duling BR (2000) TNF-alpha increases entry of macromolecules into luminal endothelial cell glycocalyx. *Am J Physiol Heart Circ Physiol* 279:H2815–H2823.
- Heo JH, Han SW, Lee SK (2005) Free radicals as triggers of brain edema formation after stroke. *Free Radic Biol Med* 39:51–70.
- Holash J, Maisonpierre PC, Compton D, Boland P, Alexander CR, Zagzag D, Yancopoulos GD, Wiegand SJ (1999) Vessel cooption, regression, and growth in tumors mediated by angiopoietins and VEGF. *Science* 284:1994–1998.
- Hu B, Jarzynka MJ, Guo P, Imanishi Y, Schlaepfer DD, Cheng S-Y (2006) Angiopoietin 2 induces glioma cell invasion by stimulating matrix metalloprotease 2 expression through the  $\alpha$ v $\beta$ 1 integrin and focal adhesion kinase signaling pathway. *Cancer Res* 66:775–783.
- Huang Y (2006) Molecular and cellular mechanisms of apolipoprotein E4 neurotoxicity and potential therapeutic strategies. *Curr Opin Drug Discov Devel* 9:627–641.
- Huang ZG, Xue D, Preston E, Karbalai H, Buchan AM (1999) Biphasic opening of the blood-brain barrier following transient focal ischemia: effects of hypothermia. *Can J Neurol Sci* 26:298–304.
- Iadecola C (1998) Neurogenic control of the cerebral microcirculation: is dopamine minding the store? *1*:263–265.
- Iivanainen E, Nelimarkka L, Elenius V, Heikkinen S-M, Junttila TT, Sihombing L, Sundvall M, Maatta JA, Laine VJO, Yla-Herttuala S, Higashiyama S, Alitalo K, Elenius K (2003) Angiopoietin-regulated recruitment of vascular smooth muscle cells by endothelial-derived heparin binding EGF-like growth factor. *FASEB J* 17:1609–1621.
- Imanishi Y, Hu B, Jarzynka MJ, Guo P, Elishaev E, Bar-Joseph I, Cheng S-Y (2007) Angiopoietin-2 Stimulates Breast Cancer Metastasis through the  $\alpha$ 5 $\beta$ 1 Integrin-Mediated Pathway. *Cancer Res* 67:4254–4263.
- Jacob M, Bruegger D, Rehm M, Welsch U, Conzen P, Becker BF (2006) Contrasting effects of colloid and crystalloid resuscitation fluids on cardiac vascular permeability. *Anesthesiology* 104:1223–1231.
- Jeliazkova-Mecheva V V., Bobilya DJ (2003) A porcine astrocyte/endothelial cell coculture model of the blood-brain barrier. *Brain Res Protoc* 12:91–98.
- Jeon BH, Khanday F, Deshpande S, Haile A, Ozaki M, Irani K (2003) Tie-ing the antiinflammatory effect of angiopoietin-1 to inhibition of NF-kappaB. *Circ Res* 92:586–588.
- Johnson-Léger CA, Aurrand-Lions M, Beltraminelli N, Fasel N, Imhof BA (2002) Junctional adhesion molecule-2 (JAM-2) promotes lymphocyte transendothelial migration. *Blood* 100:2479–2486.
- Jones N, Dumont DJ (1998) The Tek/Tie2 receptor signals through a novel Dok-related docking protein, Dok-R. *Oncogene* 17:1097–1108.



- Jones N, Ijtin K, Dumont DJ, Alitalo K (2001) Tie receptors: new modulators of angiogenic and lymphangiogenic responses. *Nat Rev Mol Cell Biol* 2:257–267.
- Kermode AG, Tofts PS, Thompson AJ, MacManus DG, Rudge P, Kendall BE, Kingsley DP, Moseley IF, du Boulay EP, McDonald WI (1990) Heterogeneity of blood-brain barrier changes in multiple sclerosis: an MRI study with gadolinium-DTPA enhancement. *Neurology* 40:229–235.
- Kim I, Kim HG, So JN, Kim JH, Kwak HJ, Koh GY (2000) Angiopoietin-1 regulates endothelial cell survival through the phosphatidylinositol 3'-Kinase/Akt signal transduction pathway. *Circ Res* 86:24–29.
- Kim K-T, Choi H-H, Steinmetz MO, Maco B, Kammerer RA, Ahn SY, Kim H-Z, Lee GM, Koh GY (2005) Oligomerization and multimerization are critical for angiopoietin-1 to bind and phosphorylate Tie2. *J Biol Chem* 280:20126–20131.
- Klagsbrun M, D'Amore PA (1996) Vascular endothelial growth factor and its receptors. *Cytokine Growth Factor Rev* 7:259–270.
- Kleffner I, Bungeoth M, Schiffbauer H, Schäbitz W-R, Ringelstein EB, Kühlenbäumer G (2008) The role of aquaporin-4 polymorphisms in the development of brain edema after middle cerebral artery occlusion. *Stroke* 39:1333–1335.
- Knowland D, Arac A, Sekiguchi KJ, Hsu M, Lutz SE, Perrino J, Steinberg GK, Barres BA, Nimmerjahn A, Agalliu D (2014) Stepwise recruitment of transcellular and paracellular pathways underlies blood-brain barrier breakdown in stroke. *Neuron* 82:603–617.
- Kobayashi H, DeBusk LM, Babichev YO, Dumont DJ, Lin PC (2006) Hepatocyte growth factor mediates angiopoietin-induced smooth muscle cell recruitment. *Blood* 108:1260–1266.
- Koehler RC, Gebremedhin D, Harder DR (2006) Role of astrocytes in cerebrovascular regulation. *J Appl Physiol* 100:307–317.
- Kontos CD, Cha EH, York JD, Peters KG (2002) The endothelial receptor tyrosine kinase Tie1 activates phosphatidylinositol 3-kinase and Akt to inhibit apoptosis. *Mol Cell Biol* 22:1704–1713.
- Korhonen J, Partanen J, Armstrong E, Vaahtokari A, Elenius K, Jalkanen M, Alitalo K (1992) Enhanced expression of the tie receptor tyrosine kinase in endothelial cells during neovascularization. *Blood* 80:2548–2555.
- Korhonen J, Polvi A, Partanen J, Alitalo K (1994) The mouse tie receptor tyrosine kinase gene: expression during embryonic angiogenesis. *Oncogene* 9:395–403.
- Lee S-W, Kim WJ, Choi YK, Song HS, Son MJ, Gelman IH, Kim Y-J, Kim K-W (2003) SSeCKS regulates angiogenesis and tight junction formation in blood-brain barrier. *Nat Med* 9:900–906.
- Lee SW, Moskowitz MA, Sims JR (2007) Sonic hedgehog inversely regulates the expression of angiopoietin-1 and angiopoietin-2 in fibroblasts. *Int J Mol Med* 19:445–451.

- Li G, Simon MJ, Cancel LM, Shi ZD, Ji X, Tarbell JM, Morrison B, Fu BM (2010) Permeability of endothelial and astrocyte cocultures: In vitro Blood-brain barrier models for drug delivery studies. *Ann Biomed Eng* 38:2499–2511.
- Li R, Beebe T, Jen N, Yu F, Takabe W, Harrison M, Cao H, Lee J, Yang H, Han P, Wang K, Shimizu H, Chen J, Lien CL, Chi NC, Hsiai TK (2014) Shear stress-activated WNT-angiopoietin-2 signaling recapitulated vascular repair in zebrafish embryos. *Arterioscler Thromb Vasc Biol* 10:2268-22675.
- Li S, Galbiati F, Volonte' D, Sargiacomo M, Engelman JA, Das K, Scherer PE, Lisanti MP (1998) Mutational analysis of caveolin-induced vesicle formation. *FEBS Lett* 434:127–134.
- Liebner S, Corada M, Bangsow T, Babbage J, Taddei A, Czapalla CJ, Reis M, Felici A, Wolburg H, Fruttiger M, Taketo MM, von Melchner H, Plate KH, Gerhardt H, Dejana E (2008) Wnt/beta-catenin signaling controls development of the blood-brain barrier. *J Cell Biol* 183:409–417.
- Liebner S, Czapalla CJ, Wolburg H (2011) Current concepts of blood-brain barrier development. *Int J Dev Biol* 55:467–476.
- Liebner S, Fischmann A, Rascher G, Duffner F, Grote EH, Kalbacher H, Wolburg H (2000) Claudin-1 and claudin-5 expression and tight junction morphology are altered in blood vessels of human glioblastoma multiforme. *Acta Neuropathol* 100:323–331.
- Lin TN, Wang CK, Cheung WM, Hsu CY (2000) Induction of angiopoietin and Tie receptor mRNA expression after cerebral ischemia-reperfusion. *J Cereb Blood Flow Metab* 20:387–395.
- Lindahl P, Johansson BR, Levéen P, Betsholtz C (1997) Pericyte loss and microaneurysm formation in PDGF-B-deficient mice. *Science* 277:242–245.
- Lippoldt A, Kniesel U, Liebner S, Kalbacher H, Kirsch T, Wolburg H, Haller H (2000) Structural alterations of tight junctions are associated with loss of polarity in stroke-prone spontaneously hypertensive rat blood-brain barrier endothelial cells. *Brain Res* 885:251–261.
- Lobov IB, Brooks PC, Lang RA (2002) Angiopoietin-2 displays VEGF-dependent modulation of capillary structure and endothelial cell survival in vivo. *Proc Natl Acad Sci U S A* 99:11205–11210.
- Lobov IB, Renard RA, Papadopoulos N, Gale NW, Thurston G, Yancopoulos GD, Wiegand SJ (2007) Delta-like ligand 4 (Dll4) is induced by VEGF as a negative regulator of angiogenic sprouting. *Proc Natl Acad Sci U S A* 104:3219–3224.
- Logan CY, Nusse R (2004) The Wnt signaling pathway in development and disease. *Annu Rev Cell Dev Biol* 20:781–810.
- London NR, Whitehead KJ, Li DY (2009) Endogenous endothelial cell signaling systems maintain vascular stability. *Angiogenesis* 12:149–158.

- Löscher W, Potschka H (2005) Drug resistance in brain diseases and the role of drug efflux transporters. *Nat Rev Neurosci* 6:591–602.
- Ludwig RJ, Zollner TM, Santoso S, Hardt K, Gille J, Baatz H, Johann PS, Pfeffer J, Radeke HH, Schön MP, Kaufmann R, Boehncke W-H, Podda M (2005) Junctional adhesion molecules (JAM)-B and -C contribute to leukocyte extravasation to the skin and mediate cutaneous inflammation. *J Invest Dermatol* 125:969–976.
- Ma SH, Lepak LA, Hussain RJ, Shain W, Shuler ML (2005) An endothelial and astrocyte co-culture model of the blood-brain barrier utilizing an ultra-thin, nanofabricated silicon nitride membrane. *Lab Chip* 5:74–85.
- Machein MR, Knedla A, Knoth R, Wagner S, Neuschl E, Plate KH (2004) Angiopoietin-1 promotes tumor angiogenesis in a rat glioma model. *Am J Pathol* 165:1557–1570.
- Maisonpierre PC, Suri C, Jones PF, Bartunkova S, Wiegand SJ, Radziejewski C, Compton D, McClain J, Aldrich TH, Papadopoulos N, Daly TJ, Davis S, Sato TN, Yancopoulos GD (1997) Angiopoietin-2, a natural antagonist for Tie2 that disrupts in vivo angiogenesis. *Science* 277:55–60.
- Mandriota SJ, Pyke C, Di Sanza C, Quinodoz P, Pittet B, Pepper MS (2000) Hypoxia-inducible angiopoietin-2 expression is mimicked by iodonium compounds and occurs in the rat brain and skin in response to systemic hypoxia and tissue ischemia. *Am J Pathol* 156:2077–2089.
- Manoonkitiwongsa PS, Jackson-Friedman C, McMillan PJ, Schultz RL, Lyden PD (2001) Angiogenesis After Stroke Is Correlated With Increased Numbers of Macrophages: The Clean-up Hypothesis. *J Cereb Blood Flow Metab* 21:1223–1231.
- Marchi N, Hallene KL, Kight KM, Cucullo L, Moddel G, Bingaman W, Dini G, Vezzani A, Janigro D (2004) Significance of MDR1 and multiple drug resistance in refractory human epileptic brain. *BMC Med* 2:37.
- Marron MB, Singh H, Tahir TA, Kavumkal J, Kim H-Z, Koh GY, Brindle NPJ (2007) Regulated proteolytic processing of Tie1 modulates ligand responsiveness of the receptor-tyrosine kinase Tie2. *J Biol Chem* 282:30509–30517.
- Matyszak MK, Perry VH (1996) A comparison of leucocyte responses to heat-killed bacillus Calmette-Guérin in different CNS compartments. *Neuropathol Appl Neurobiol* 22:44–53.
- McCarthy MJ, Crowther M, Bell PR, Brindle NP (1998) The endothelial receptor tyrosine kinase tie-1 is upregulated by hypoxia and vascular endothelial growth factor. *FEBS Lett* 423:334–338.
- Mittapalli RK, Manda VK, Adkins CE, Geldenhuys WJ, Lockman PR (2010) Exploiting nutrient transporters at the blood-brain barrier to improve brain distribution of small molecules. *Ther Deliv* 1:775–784.
- Mulivor AW, Lipowsky HH (2004) Inflammation- and ischemia-induced shedding of venular glycocalyx. *Am J Physiol Heart Circ Physiol* 286:H1672–H1680.

- Nag S, Manias JL, Stewart DJ (2009) Pathology and new players in the pathogenesis of brain edema. *Acta Neuropathol* 118:197–217.
- Nag S, Papneja T, Venugopalan R, Stewart DJ (2005) Increased angiopoietin2 expression is associated with endothelial apoptosis and blood-brain barrier breakdown. *Lab Invest* 85:1189–1198.
- Neuhaus J (1990) Orthogonal arrays of particles in astroglial cells: quantitative analysis of their density, size, and correlation with intramembranous particles. *Glia* 3:241–251.
- Nitta T, Hata M, Gotoh S, Seo Y, Sasaki H, Hashimoto N, Furuse M, Tsukita S (2003) Size-selective loosening of the blood-brain barrier in claudin-5-deficient mice. *J Cell Biol* 161:653–660.
- Nottebaum AF, Cagna G, Winderlich M, Gamp AC, Linnepe R, Polaschegg C, Filippova K, Lyck R, Engelhardt B, Kamenyeva O, Bixel MG, Butz S, Vestweber D (2008) VE-PTP maintains the endothelial barrier via plakoglobin and becomes dissociated from VE-cadherin by leukocytes and by VEGF. *J Exp Med* 205:2929–2945.
- Nourhaghighi N, Teichert-Kuliszewska K, Davis J, Stewart DJ, Nag S (2003) Altered expression of angiopoietins during blood-brain barrier breakdown and angiogenesis. *Lab Invest* 83:1211–1222.
- Nusse R (2005) Wnt signaling in disease and in development. *Cell Res* 15:28–32.
- Obermeier B, Daneman R, Ransohoff RM (2013) Development, maintenance and disruption of the blood-brain barrier. *Nat Med* 19:1584–1596.
- Oby E, Janigro D (2006) The blood-brain barrier and epilepsy. *Epilepsia* 47:1761–1774.
- Oh H, Takagi H, Suzuma K, Otani A, Matsumura M, Honda Y (1999) Hypoxia and Vascular Endothelial Growth Factor Selectively Up-regulate Angiopoietin-2 in Bovine Microvascular Endothelial Cells. *J Biol Chem* 274:15732–15739.
- Ohgaki H, Kleihues P (2005) Epidemiology and etiology of gliomas. *Acta Neuropathol* 109:93–108.
- Oldendorf WH, Cornford ME, Brown WJ (1977) The large apparent work capability of the blood-brain barrier: a study of the mitochondrial content of capillary endothelial cells in brain and other tissues of the rat. *Ann Neurol* 1:409–417.
- Oliner J et al. (2004) Suppression of angiogenesis and tumor growth by selective inhibition of angiopoietin-2. *Cancer Cell* 6:507–516.
- Paka L, Kako Y, Obunike JC, Pillarisetti S (1999) Apolipoprotein E containing high density lipoprotein stimulates endothelial production of heparan sulfate rich in biologically active heparin-like domains. A potential mechanism for the anti-atherogenic actions of vascular apolipoprotein e. *J Biol Chem* 274:4816–4823.

- Papapetropoulos A, Fulton D, Mahboubi K, Kalb RG, O'Connor DS, Li F, Altieri DC, Sessa WC (2000) Angiopoietin-1 inhibits endothelial cell apoptosis via the Akt/survivin pathway. *J Biol Chem* 275:9102–9105.
- Parmar KM, Larman HB, Dai G, Zhang Y, Wang ET, Moorthy SN, Kratz JR, Lin Z, Jain MK, Gimbrone MA, García-Cardena G (2006) Integration of flow-dependent endothelial phenotypes by Kruppel-like factor 2. *J Clin Invest* 116:49–58.
- Patan S (1998) TIE1 and TIE2 receptor tyrosine kinases inversely regulate embryonic angiogenesis by the mechanism of intussusceptive microvascular growth. *Microvasc Res* 56:1–21.
- Perry VH, Nicoll JAR, Holmes C (2010) Microglia in neurodegenerative disease. *Nat Rev Neurol* 6:193–201.
- Peters KG, Coogan A, Berry D, Marks J, Iglehart JD, Kontos CD, Rao P, Sankar S, Trogan E (1998) Expression of Tie2/Tek in breast tumour vasculature provides a new marker for evaluation of tumour angiogenesis. *Br J Cancer* 77:51–56.
- Pfrieger FW, Barres BA (1997) Synaptic efficacy enhanced by glial cells in vitro. *Science* 277:1684–1687.
- Pires PW, Girgla SS, McClain JL, Kaminski NE, van Rooijen N, Dorrance AM (2013) Improvement in middle cerebral artery structure and endothelial function in stroke-prone spontaneously hypertensive rats after macrophage depletion. *Microcirculation* 20:650–661.
- Plate KH, Beck H, Danner S, Allegrini PR, Wiessner C (1999) Cell type specific upregulation of vascular endothelial growth factor in an MCA-occlusion model of cerebral infarct. *J Neuropathol Exp Neurol* 58:654–666.
- Poole TJ, Coffin JD (1989) Vasculogenesis and angiogenesis: two distinct morphogenetic mechanisms establish embryonic vascular pattern. *J Exp Zool* 251:224–231.
- Prat A, Biernacki K, Wosik K, Antel JP (2001) Glial cell influence on the human blood-brain barrier. *Glia* 36:145–155.
- Procopio WN, Pelavin PI, Lee WM, Yeilding NM (1999) Angiopoietin-1 and -2 coiled coil domains mediate distinct homo-oligomerization patterns, but fibrinogen-like domains mediate ligand activity. *J Biol Chem* 274:30196–30201.
- Pun PBL, Lu J, Moochhala S (2009) Involvement of ROS in BBB dysfunction. *Free Radic Res* 43:348–364.
- Puri MC, Partanen J, Rossant J, Bernstein A (1999) Interaction of the TEK and TIE receptor tyrosine kinases during cardiovascular development. *Development* 126:4569–4580.
- Rao S, Lobov IB, Vallance JE, Tsujikawa K, Shiojima I, Akunuru S, Walsh K, Benjamin LE, Lang RA (2007) Obligatory participation of macrophages in an angiopoietin 2-mediated cell death switch. *Development* 134:4449–4458.

- Rehm M, Bruegger D, Christ F, Conzen P, Thiel M, Jacob M, Chappell D, Stoeckelhuber M, Welsch U, Reichart B, Peter K, Becker BF (2007) Shedding of the endothelial glycocalyx in patients undergoing major vascular surgery with global and regional ischemia. *Circulation* 116:1896–1906.
- Reiss Y, Scholz A, Plate KH (2015) The Angiopoietin - Tie system: Common signaling pathways for angiogenesis, cancer and inflammation. Springer 2015, *Vascular Signaling in Health and Disease*. Chapter 13, in press
- Reiss Y (2010) Angiopoietins. *Recent Results Cancer Res* 180:3–13.
- Reiss Y, Droste J, Heil M, Tribulova S, Schmidt MHH, Schaper W, Dumont DJ, Plate KH (2007) Angiopoietin-2 impairs revascularization after limb ischemia. *Circ Res* 101:88–96.
- Reitsma S, Slaaf DW, Vink H, van Zandvoort MAMJ, oude Egbrink MGA (2007) The endothelial glycocalyx: composition, functions, and visualization. *Pflugers Arch* 454:345–359.
- Risau W (1997) Mechanisms of angiogenesis. *Nature* 386:671–674.
- Rodewald HR, Sato TN (1996) Tie1, a receptor tyrosine kinase essential for vascular endothelial cell integrity, is not critical for the development of hematopoietic cells. *Oncogene* 12:397–404.
- Saharinen P, Eklund L, Miettinen J, Wirkkala R, Anisimov A, Winderlich M, Nottebaum A, Vestweber D, Deutsch U, Koh GY, Olsen BR, Alitalo K (2008) Angiopoietins assemble distinct Tie2 signalling complexes in endothelial cell-cell and cell-matrix contacts. *Nat Cell Biol* 10:527–537.
- Saitou M, Furuse M, Sasaki H, Schulzke JD, Fromm M, Takano H, Noda T, Tsukita S (2000) Complex phenotype of mice lacking occludin, a component of tight junction strands. *Mol Biol Cell* 11:4131–4142.
- Salmon AHJ, Neal CR, Sage LM, Glass CA, Harper SJ, Bates DO (2009) Angiopoietin-1 alters microvascular permeability coefficients in vivo via modification of endothelial glycocalyx. *Cardiovasc Res* 83:24–33.
- Sandoval KE, Witt KA (2008) Blood-brain barrier tight junction permeability and ischemic stroke. *Neurobiol Dis* 32:200–219.
- Sato TN, Tozawa Y, Deutsch U, Wolburg-Buchholz K, Fujiwara Y, Gendron-Maguire M, Gridley T, Wolburg H, Risau W, Qin Y (1995) Distinct roles of the receptor tyrosine kinases Tie-1 and Tie-2 in blood vessel formation. *Nature* 376:70–74.
- Scharpfenecker M, Fiedler U, Reiss Y, Augustin HG (2005) The Tie-2 ligand angiopoietin-2 destabilizes quiescent endothelium through an internal autocrine loop mechanism. *J Cell Sci* 118:771–780.
- Schmidt T, Carmeliet P (2010) Blood-vessel formation: Bridges that guide and unite. *Nature* 465:697–699.

- Schnürch H, Risau W (1993) Expression of tie-2, a member of a novel family of receptor tyrosine kinases, in the endothelial cell lineage. *Development* 119:957–968.
- Scholz A, Lang V, Henschler R, Czabanka M, Vajkoczy P, Chavakis E, Drynski J, Harter PN, Mittelbronn M, Dumont DJ, Plate KH, Reiss Y (2011) Angiopoietin-2 promotes myeloid cell infiltration in a  $\beta_2$ -integrin-dependent manner. *Blood* 118:5050–5059.
- Scholz A, Plate KH, Reiss Y (2015) Angiopoietin-2: a multifaceted cytokine that functions in both angiogenesis and inflammation. *Ann N Y Acad Sci*.
- Schreibelt G, van Horssen J, van Rossum S, Dijkstra CD, Drukarch B, de Vries HE (2007) Therapeutic potential and biological role of endogenous antioxidant enzymes in multiple sclerosis pathology. *Brain Res Rev* 56:322–330.
- Schreitmüller B, Leyhe T, Stransky E, Köhler N, Laske C (2012) Elevated Angiopoietin-1 Serum Levels in Patients with Alzheimer's Disease. *Int J Alzheimers Dis* 2012:1–5.
- Shalaby F, Rossant J, Yamaguchi TP, Gertsenstein M, Wu XF, Breitman ML, Schuh AC (1995) Failure of blood-island formation and vasculogenesis in Flk-1-deficient mice. *Nature* 376:62–66.
- Shen F, Walker EJ, Jiang L, Degos V, Li J, Sun B, Heriyanto F, Young WL, Su H (2011) Coexpression of angiopoietin-1 with VEGF increases the structural integrity of the blood-brain barrier and reduces atrophy volume. *J Cereb Blood Flow Metab* 31:2343–2351.
- Shen J, Frye M, Lee BL, Reinardy JL, McClung JM, Ding K, Kojima M, Xia H, Seidel C, Lima e Silva R, Dong A, Hackett SF, Wang J, Howard BW, Vestweber D, Kontos CD, Peters KG, Campochiaro PA (2014) Targeting VE-PTP activates TIE2 and stabilizes the ocular vasculature. *J Clin Invest* 124:4564–4576.
- Shepro D, Morel NM (1993) Pericyte physiology. *FASEB J* 7:1031–1038.
- Sims DE (1986) The pericyte--a review. *Tissue Cell* 18:153–174.
- Sorokin L (2010) The impact of the extracellular matrix on inflammation. *Nat Rev Immunol* 10:712–723.
- Spatz H (1939) Pathologische Anatomie der Kreislaufstörungen des Gehirns. *Zeitschrift für die gesamte Neurol und Psychiatr* 167:301–351.
- Spengos K, Tsivgoulis G, Zakopoulos N (2006) Blood pressure management in acute stroke: a long-standing debate. *Eur Neurol* 55:123–135.
- Sperandio M, Gleissner CA, Ley K (2009) Glycosylation in immune cell trafficking. *Immunol Rev* 230:97–113.
- Stamatovic SM, Dimitrijevic OB, Keep RF, Andjelkovic A V (2006) Inflammation and brain edema: new insights into the role of chemokines and their receptors. *Acta Neurochir Suppl* 96:444–450.

- Stenman JM, Rajagopal J, Carroll TJ, Ishibashi M, McMahon J, McMahon AP (2008) Canonical Wnt signaling regulates organ-specific assembly and differentiation of CNS vasculature. *Science* 322:1247–1250.
- Stratmann A, Risau W, Plate KH (1998) Cell type-specific expression of angiopoietin-1 and angiopoietin-2 suggests a role in glioblastoma angiogenesis. *Am J Pathol* 153:1459–1466.
- Strbian D, Durukan A, Pitkonen M, Marinkovic I, Tatlisumak E, Pedrono E, Abo-Ramadan U, Tatlisumak T (2008) The blood-brain barrier is continuously open for several weeks following transient focal cerebral ischemia. *Neuroscience* 153:175–181.
- Suri C, Jones PF, Patan S, Bartunkova S, Maisonpierre PC, Davis S, Sato TN, Yancopoulos GD (1996) Requisite role of angiopoietin-1, a ligand for the TIE2 receptor, during embryonic angiogenesis. *Cell* 87:1171–1180.
- Suri C, McClain J, Thurston G, McDonald DM, Zhou H, Oldmixon EH, Sato TN, Yancopoulos GD (1998) Increased vascularization in mice overexpressing angiopoietin-1. *Science* 282:468–471.
- Swift MR, Weinstein BM (2009) Arterial-venous specification during development. *Circ Res* 104:576–588.
- Tadros A, Hughes DP, Dunmore BJ, Brindle NPJ (2003) ABIN-2 protects endothelial cells from death and has a role in the antiapoptotic effect of angiopoietin-1. *Blood* 102:4407–4409.
- Takakura N, Huang XL, Naruse T, Hamaguchi I, Dumont DJ, Yancopoulos GD, Suda T (1998) Critical role of the TIE2 endothelial cell receptor in the development of definitive hematopoiesis. *Immunity* 9:677–686.
- Thirumangalakudi L, Samany PG, Owoso A, Wiskar B, Grammas P (2006) Angiogenic proteins are expressed by brain blood vessels in Alzheimer's disease. *J Alzheimers Dis* 10:111–118.
- Thomas M, Augustin HG (2009) The role of the Angiopoietins in vascular morphogenesis. *Angiogenesis* 12:125–137.
- Thurston G (1999) Leakage-Resistant Blood Vessels in Mice Transgenically Overexpressing Angiopoietin-1. *Science* 286:2511–2514.
- Thurston G, Rudge JS, Ioffe E, Zhou H, Ross L, Croll SD, Glazer N, Holash J, McDonald DM, Yancopoulos GD (2000) Angiopoietin-1 protects the adult vasculature against plasma leakage. *Nat Med* 6:460–463.
- Tournaire R, Simon M-P, Noble F le, Eichmann A, England P, Pouyssegur J (2004) A short synthetic peptide inhibits signal transduction, migration and angiogenesis mediated by Tie2 receptor. *EMBO Rep* 5:262–267.
- Tsiamis AC, Morris PN, Marron MB, Brindle NPJ (2002) Vascular endothelial growth factor modulates the Tie-2:Tie-1 receptor complex. *Microvasc Res* 63:149–158.



- Tuma PL, Hubbard AL (2003) Transcytosis: crossing cellular barriers. *Physiol Rev* 83:871–932.
- Ueda A, Shimomura M, Ikeda M, Yamaguchi R, Tanishita K (2004) Effect of glycocalyx on shear-dependent albumin uptake in endothelial cells. *Am J Physiol Heart Circ Physiol* 287:H2287–H2294.
- Uemura A, Ogawa M, Hirashima M, Fujiwara T, Koyama S, Takagi H, Honda Y, Wiegand SJ, Yancopoulos GD, Nishikawa S-I (2002) Recombinant angiopoietin-1 restores higher-order architecture of growing blood vessels in mice in the absence of mural cells. *J Clin Invest* 110:1619–1628.
- Ullian EM, Sapperstein SK, Christopherson KS, Barres BA (2001) Control of synapse number by glia. *Science* 291:657–661.
- Vajkoczy P, Laschinger M, Engelhardt B (2001) Alpha4-integrin-VCAM-1 binding mediates G protein-independent capture of encephalitogenic T cell blasts to CNS white matter microvessels. *J Clin Invest* 108:557–565.
- Valable S, Bellail A, Lesné S, Liot G, Mackenzie ET, Vivien D, Bernaudin M, Petit E (2003) Angiopoietin-1-induced PI3-kinase activation prevents neuronal apoptosis. *FASEB J* 17:443–445.
- Valable S, Montaner J, Bellail A, Berezowski V, Brillault J, Cecchelli R, Divoux D, Mackenzie ET, Bernaudin M, Roussel S, Petit E (2005) VEGF-induced BBB permeability is associated with an MMP-9 activity increase in cerebral ischemia: both effects decreased by Ang-1. *J Cereb Blood Flow Metab* 25:1491–1504.
- Valenzuela DM, Griffiths JA, Rojas J, Aldrich TH, Jones PF, Zhou H, McClain J, Copeland NG, Gilbert DJ, Jenkins NA, Huang T, Papadopoulos N, Maisonpierre PC, Davis S, Yancopoulos GD (1999) Angiopoietins 3 and 4: diverging gene counterparts in mice and humans. *Proc Natl Acad Sci U S A* 96:1904–1909.
- Van den Berg BM, Vink H, Spaan JAE (2003) The endothelial glycocalyx protects against myocardial edema. *Circ Res* 92:592–594.
- Van der Heijden M, van Nieuw Amerongen GP, van Bezu J, Paul MA, Groeneveld ABJ, van Hinsbergh VWM (2011) Opposing effects of the angiopoietins on the thrombin-induced permeability of human pulmonary microvascular endothelial cells. *PLoS One* 6:e23448.
- Van Haaren PMA, VanBavel E, Vink H, Spaan JAE (2003) Localization of the permeability barrier to solutes in isolated arteries by confocal microscopy. *Am J Physiol Heart Circ Physiol* 285:H2848–H2856.
- Van Itallie CM, Anderson JM (2013) Claudin interactions in and out of the tight junction. *Tissue barriers* 1:e25247.
- Vink H, Constantinescu AA, Spaan JA (2000) Oxidized lipoproteins degrade the endothelial surface layer : implications for platelet-endothelial cell adhesion. *Circulation* 101:1500–1502.

- Wang Y, Imitola J, Rasmussen S, O'Connor KC, Khoury SJ (2008) Paradoxical dysregulation of the neural stem cell pathway sonic hedgehog-Gli1 in autoimmune encephalomyelitis and multiple sclerosis. *Ann Neurol* 64:417–427.
- Wang Y, Rattner A, Zhou Y, Williams J, Smallwood PM, Nathans J (2012) Norrin/Frizzled4 signaling in retinal vascular development and blood brain barrier plasticity. *Cell* 151:1332–1344.
- Wang Y, Tasevski V, Wallace EM, Gallery ED, Morris JM (2007) Reduced maternal serum concentrations of angiopoietin-2 in the first trimester precede intrauterine growth restriction associated with placental insufficiency. *BJOG* 114:1427–1431.
- Ward NL, Van Slyke P, Sturk C, Cruz M, Dumont DJ (2004) Angiopoietin 1 expression levels in the myocardium direct coronary vessel development. *Dev Dyn* 229:500–509.
- Warth A, Kröger S, Wolburg H (2004) Redistribution of aquaporin-4 in human glioblastoma correlates with loss of agrin immunoreactivity from brain capillary basal laminae. *Acta Neuropathol* 107:311–318.
- Weber CC, Cai H, Ehrbar M, Kubota H, Martiny-Baron G, Weber W, Djonov V, Weber E, Mallik AS, Fussenegger M, Frei K, Hubbell JA, Zisch AH (2005) Effects of protein and gene transfer of the angiopoietin-1 fibrinogen-like receptor-binding domain on endothelial and vessel organization. *J Biol Chem* 280:22445–22453.
- Witt KA, Mark KS, Sandoval KE, Davis TP (2008) Reoxygenation stress on blood-brain barrier paracellular permeability and edema in the rat. *Microvasc Res* 75:91–96.
- Witzenbichler B, Westermann D, Knueppel S, Schultheiss H-P, Tschöpe C (2005) Protective role of angiopoietin-1 in endotoxic shock. *Circulation* 111:97–105.
- Wolburg H, Noell S, Fallier-Becker P, Mack AF, Wolburg-Buchholz K The disturbed blood-brain barrier in human glioblastoma. *Mol Aspects Med* 33:579–589.
- Wolburg H, Wolburg-Buchholz K, Kraus J, Rascher-Eggstein G, Liebner S, Hamm S, Duffner F, Grote E-H, Risau W, Engelhardt B (2003) Localization of claudin-3 in tight junctions of the blood-brain barrier is selectively lost during experimental autoimmune encephalomyelitis and human glioblastoma multiforme. *Acta Neuropathol* 105:586–592.
- Wu C, Ivars F, Anderson P, Hallmann R, Vestweber D, Nilsson P, Robenek H, Tryggvason K, Song J, Korpos E, Loser K, Beissert S, Georges-Labouesse E, Sorokin LM (2009) Endothelial basement membrane laminin alpha5 selectively inhibits T lymphocyte extravasation into the brain. *Nat Med* 15:519–527.
- Xu Q, Wang Y, Dabdoub A, Smallwood PM, Williams J, Woods C, Kelley MW, Jiang L, Tasman W, Zhang K, Nathans J (2004) Vascular development in the retina and inner ear: control by Norrin and Frizzled-4, a high-affinity ligand-receptor pair. *Cell* 116:883–895.
- Xu Y, Yu Q (2001) Angiopoietin-1, unlike angiopoietin-2, is incorporated into the extracellular matrix via its linker peptide region. *J Biol Chem* 276:34990–34998.

- Yabkowitz R, Meyer S, Black T, Elliott G, Merewether LA, Yamane HK (1999) Inflammatory cytokines and vascular endothelial growth factor stimulate the release of soluble tie receptor from human endothelial cells via metalloprotease activation. *Blood* 93:1969–1979.
- Ye X, Chopp M, Cui X, Zacharek A, Cui Y, Yan T, Shehadah A, Roberts C, Liu X, Lu M, Chen J (2011) Niaspan enhances vascular remodeling after stroke in type 1 diabetic rats. *Exp Neurol* 232:299–308.
- Yu X, Seegar TCM, Dalton AC, Tzvetkova-Robev D, Goldgur Y, Rajashankar KR, Nikolov DB, Barton WA (2013) Structural basis for angiotensin-1-mediated signaling initiation. *Proc Natl Acad Sci U S A* 110:7205–7210.
- Yuan HT, Khankin E V, Karumanchi SA, Parikh SM (2009) Angiotensin 2 is a partial agonist/antagonist of Tie2 signaling in the endothelium. *Mol Cell Biol* 29:2011–2022.
- Zador Z, Stiver S, Wang V, Manley GT (2009) Role of aquaporin-4 in cerebral edema and stroke. *Handb Exp Pharmacol*:159–170.
- Zagzag D, Hooper A, Friedlander DR, Chan W, Holash J, Wiegand SJ, Yancopoulos GD, Grumet M (1999) In situ expression of angiotensins in astrocytomas identifies angiotensin-2 as an early marker of tumor angiogenesis. *Exp Neurol* 159:391–400.
- Zhang L, Yang N, Park J-W, Katsaros D, Fracchioli S, Cao G, O'Brien-Jenkins A, Randall TC, Rubin SC, Coukos G (2003) Tumor-derived vascular endothelial growth factor up-regulates angiotensin-2 in host endothelium and destabilizes host vasculature, supporting angiogenesis in ovarian cancer. *Cancer Res* 63:3403–3412.
- Zhang ZG, Zhang L, Jiang Q, Zhang R, Davies K, Powers C, Bruggen N van, Chopp M (2000) VEGF enhances angiogenesis and promotes blood-brain barrier leakage in the ischemic brain. *J Clin Invest* 106:829–838.
- Zhang ZG, Zhang L, Tsang W, Soltanian-Zadeh H, Morris D, Zhang R, Goussev A, Powers C, Yeich T, Chopp M (2002) Correlation of VEGF and angiotensin expression with disruption of blood-brain barrier and angiogenesis after focal cerebral ischemia. *J Cereb Blood Flow Metab* 22:379–392.
- Zhao L, Yang Z, Liu Y, Ying H, Zhang H, Xue Y (2011) Vascular endothelial growth factor increases permeability of the blood-tumor barrier via caveolae-mediated transcellular pathway. *J Mol Neurosci* 44:122–129.
- Ziegler T et al. (2013) Angiotensin 2 mediates microvascular and hemodynamic alterations in sepsis. *J Clin Invest* 123.
- Zlokovic B V. (2008) The Blood-Brain Barrier in Health and Chronic Neurodegenerative Disorders. *Neuron* 57:178–201.

## 6. APPENDIX

### 6.1 Instruments

Device	Instrument name	Company
Centrifuge	Labofuge 400	Heraeus instruments
Centrifuge	5415 D	eppendorf
Centrifuge	Labofuge 400 R	Heraeus instruments
Confocal laser scanning microscope	Eclipse TE-2000E	Nikon
Electrophoresis chamber	Wide Mini-Sub cell GT	Bio-Rad
Eppendorf research	Pipettes	Eppendorf
FACS	FACS Canto II	BD
Fluorescence microscope	Eclipse 80i	Nikon
Gel documentation station	Multi Image Light Cabinet	Alpha innotech
Heating plate	Drying plate 12895	Medax
Incubator	Hera Cell 150	Thermo Electron Corporation
Membrane documentation	Odyssey 2800	LI-COR
Microtome	HM550	Microm
PCR machine	RoboCycler Gradient 96	Stratagene
pH meter	pH 720	WTW InoLab
Plate reader	Tecan reader infinite M200	Tecan
Power supply for gel electrophoresis and Western blot	PowerPac HC	Bio-Rad
qPCR machine	CFX 96 Real-Time System	Bio-Rad
Rocking shaker	Duomax 1030	Heidolph
Safety Cabinet	Hera Safe KS Class II	Thermo Electron Corporation
Scale	Scout Pro 2000 g	Ohaus
Shaker	Promax 1020	Heidolph
Special accuracy weighing machine	TE 313S-DS	Sartorius
TEER measurement	CellZscope	nanoAnalytics
Thermomixer	Thermomixer compact	eppendorf
Vortexer	Vortex-Genie 2	Scientific Industries
Waterbath	TW12	Julabo
Minilys Homogenizer	Bertin technologies	PeQlab

**6.2 Reagents**

Name	Company	Ordering Number
Acrylamide	Roth	3029.1
Agarose	Sigma	A9539
APS	Roth	9592.3
Aqua PolyMount	Polysciences	18606
Bond breaker TCEP	Thermo Scientific	77720
Boric acid	MP	195074
Bovine Serum Albumin (BSA; Albumin Fraction V)	Applichem	A1391
Bromine phenol blue	Sigma	B5525
CaCl <sub>2</sub>	AppliChem	A3652
Collagenase II	Worthington	LS004174
Collagenase A	Roche	10103578001
Collagenase P	Roche	11213857001
Collagenase / Dispase	Roche	10269638001
Collagen Type I	Corning	354236
DAPI	AnaSpec	83210
DNase I (FACS)	Sigma	D5025
DNase I	Worthington	6333
DNase	Qiagen	79254
DMSO	Roth	4720.4
EDTA	AppliChem	A3553
Evans blue	Sigma	E2129
FBS	Biochrom	S0115
Fibronectin	Sigma	F4759
FITC 70 kD-dextran	Sigma	46945
Formamide	Sigma	F5786
Glycerol	Sigma	G7893
Glycine	Sigma	G7126
Halt™ Protease & Phosphatase Inhibitor Cocktail (100 x)	Thermo Scientific	1861281
HBSS	Gibco	14170-088
Heparin	Sigma	H4784
HEPES	Sigma	H3375

Name	Company	Ordering Number
H <sub>2</sub> O <sub>2</sub> 30 %	Roth	8070.1
KCl	Riedel-de Haen	31248
Ketavet	Pfizer	B1830-12
KH <sub>2</sub> PO <sub>4</sub>	Merck	A917973811
Lanthanum nitrate hexahydrate	Fluka	61520-F
L-Glutamine	Sigma	G7513
Lucifer Yellow	Sigma	L0259
MCDB131 medium	Gibco	10372-019
β-Mercaptoethanol	Sigma	M6250
MgCl <sub>2</sub>	Sigma	M8266
NaCl	Sigma	31434-R
Na <sub>2</sub> HPO <sub>4</sub>	Sigma	S3264
Natural goat serum	Sigma	G9023
NP-40	Sigma	21-3277
O.C.T. Compound	Sakura	4583
PBS	Gibco	10010.015
Penicillin / Streptavidin	Sigma	P4333
PFA	Merck	K33608805433
Protein A/G PLUS-Agarose beads	Santa Cruz	Sc-2003
Proteinase K	Roche	03115879001
RIPA buffer	Sigma	R0278
RNase H	Roche	10786349001
Rompun 2 %	Bayer	ICP06BW1
1x Roti-Block	Roth	A151.2
SDS	Roth	4360.1
sucrose	Fluka	84099
TEMED	Roth	2367.1
Texas Red 3 kD-dextran	Invitrogen	D-3328
TMR 20 kD-dextran	Sigma	73766
Tris ultrapure	AppliChem	A1086
Triton X-100	Sigma	T8787
Trypsin-EDTA (1 x)	Gibco	25300-062
Tween 20	AppliChem	A4974
UREA	Riedel de Haen	33247
Western Blotting luminal reagent	Santa Cruz	F2209

## 6.3 Buffers and solutions

### 6.3.1 Medium for cell culture

Table 6-1: MCDB131 medium

Ingredients	Volume [ml]
MCDB131 medium	37,5
FBS	10
L-Glutamine	0.5
Penicillin / Streptavidin	0.5
1 % Heparin	0.5
ECGS	0.5
NaHCO <sub>3</sub>	0.5

Stored at 4 °C.

### 6.3.2 Agarose gel electrophoresis

Table 6-2: Ingredients for TBE buffer (10 x)

Ingredients	Amount
Tris base	108 g
Boric acid	55 g
EDTA 0.5 M pH 8.0	40 ml
ad dH <sub>2</sub> O	1000 ml

Stored at RT.

Table 6-3: Preparation of Blue Juice (5 x)

Ingredients	Concentration
Sucrose	65 %
Tris HCl (pH 7.5)	10 mM
EDTA	10 mM
Bromine phenol blue	0.3 %

Stored at -20 °C.

Table 6-4: Tail lysis buffer (pH 8.0)

Ingredients	Concentration
KCl	50 mM
MgCl <sub>2</sub>	1.5 mM
Tris	10 mM
NP-40	0.15 %
Tween 20	0.45 %

Stored at 4 °C.

### 6.3.3 Buffers for MBMVs

Table 6-5: MVB buffer (1 x; pH 7.4)

Ingredients	Amount
10 x HEPES (150 mM; pH 7.4)	50 ml
10 x Salt solution	50 ml
BSA	2.5 g
Glucose	0.45 g
ad dH <sub>2</sub> O / DEPC-Water	500 ml

dH<sub>2</sub>O was used for Western Blot analysis, DEPC-Water was used for qPCR analysis.

Stored at 4 °C.



Table 6-6: Salt Solution (10 x)

Ingredients	Concentration
NaCl	1.47 M
KCl	40 mM
CaCl <sub>2</sub>	30 mM
MgCl <sub>2</sub>	12 mM

Stored at 4 °C.

Table 6-7: HES buffer

Ingredients	Concentration
HEPES	10 mM
EDTA	1 mM
Sucrose	250 mM

Stored at 4 °C.

Table 6-8: PBS for 25 % BSA

Ingredients	Concentration
NaCl	140 mM
CaCl <sub>2</sub>	0.2 mM
MgCl <sub>2</sub>	0.2 mM
Na <sub>2</sub> HPO <sub>4</sub>	10 mM
KH <sub>2</sub> PO <sub>4</sub>	10 mM

A 25 % BSA solution was prepared in PBS, filtered with a 0.45 µm membrane and stored at -20 °C.

## 6.3.4 Buffers for MBMECs

Table 6-9: Buffer A (pH 7.4)

Ingredients	Concentration
NaCl	153 mM
KCl	5.6 mM
CaCl <sub>2</sub>	1.7 mM
MgCl <sub>2</sub>	1.2 mM
HEPES	15 mM
BSA	10 g
ad dH <sub>2</sub> O	1000 ml

Buffer A was filtered through a 0.22 µm mesh and stored at 4 °C.

## 6.3.5 Buffers and solutions for SDS PAGE

Table 6-10: Final concentration of UREA / SDS buffer used for Western Blot analysis

Ingredients	Concentration
UREA	2.3 M
SDS	1.5 %
Tris pH 6.8	50 mM
TCEP	25 mM
Bromine phenol blue	0,01 %

Stored at -20 °C.

Table 6-11: 4 x Tris-Cl Upper buffer (pH 6.8)

Ingredients	Concentration
Tris-Cl	0.5 M
SDS	0.4 %

---

Stored at 4 °C.

Table 6-12: 4 x Tris-Cl Lower buffer (pH 8.8)

Ingredients	Concentration
Tris-Cl	1.5 M
SDS	0.4 %

Stored at 4 °C.

Table 6-13: Running buffer (10 x)

Ingredients	Amount
Tris	30 g
Glycine	144 g
SDS	10 g
ad H <sub>2</sub> O	1 l

Stored at RT.

Table 6-14: Transfer buffer (10 x)

Ingredients	Concentration
Tris	22.32 g
Glycine	105 g
ad H <sub>2</sub> O	1 l

Stored at RT.

Table 6-15: TBS (20 x; pH 7.6-7.7)

Ingredients	Concentration
Tris	24.37 g
NaCl	70 g
ad H <sub>2</sub> O	1 l

Stored at RT.

Table 6-16: Ingredients for stacking and separating gels

Ingredients	12 % separating gel	8 % separating gel	3,9 % stacking gel
ddH <sub>2</sub> O	6.75 ml	8.25 ml	3.4 ml
40 % Acrylamide / 1,5 % bisacrylamide	3 ml	3 ml	1.25 ml
4x Tris / SDS pH 8,8	3.75 ml	3.75 ml	-
4x Tris / SDS pH 6,8	-	-	1,25 ml
80 % Glycerol	1.5 ml	1.5 ml	-
10 % APS	75 µl	75 µl	37.5 µl
TEMED	15 µl	15 µl	7.5 µl

### 6.3.6 Buffers for Immunohistochemistry

Table 6-17: 4 % Paraformaldehyde in PBS (pH 7.4)

Ingredients	Amount
PFA	80 g
dH <sub>2</sub> O	1.5 l
PBS (20 x)	100 ml
ad dH <sub>2</sub> O	2 l

Stored at -20 °C.

Table 6-18: PBS (20 x)

Ingredients	Amount
NaCl	163.6 g
KCl	4 g
Na <sub>2</sub> HPO <sub>4</sub> (x 2 H <sub>2</sub> O)	35.6 g
KH <sub>2</sub> PO <sub>4</sub>	4.9 g
ad dH <sub>2</sub> O	1 l

Stored at RT.

Table 6-19: PBSA solution (pH 7.5):

Ingredients	Concentration
NaCl	150 mM
Na <sub>2</sub> HPO <sub>4</sub>	10 mM
KH <sub>2</sub> PO <sub>4</sub>	10 mM
BSA	1 %
Triton-X 100	0.1 %

Table 6-20: Antibody incubation buffer (pH 7.2)

Ingredients	Concentration
BSA	0.5 %
Triton-X 100	0.25 %
ad PBS	100 ml

Stored at 4 °C.

Table 6-21: Permeabilization / blocking buffer (pH 7.4-7.6):

Ingredients	Concentration
BSA	1 %
Triton-X 100	0.5 %
ad PBS	100 ml

Stored at 4 °C.

## 6.4 Primers

### 6.4.1 Primers for PCR

Primers	Sequence 5' – 3' sense	Sequence 5' – 3' antisense
mTie1	ctcactttgccccttagaa	gctgtacgcggacccttt
hAng-2	gggaatgaggcttactcattg	gctggtcggatcatcatggt

### 6.4.2 Primers for qPCR

Table 6-22: Primers used for qPCR analysis

Primers	Sequence 5' – 3' sense	Sequence 5' – 3' antisense
CD31	attcctcaggctcgggtcttc	ccgccttctgtcacctcctt
hAng-2	agaggctgcaagtgtggaga	ttgctccgctgtttggtca
Tie2	cctgggcctgtgagacgaat	ccaggcactttgatgttctgct
VE-Cadherin	gcccagccctacgaacctaaa	gggtgaagttgctgtcctcgt
ZO-1	tgcttctctgctggccctaa	gggtggcttcaactgaggttc
Claudin-3	cgtacaagacgagacggccaag	cacgtacaaccagctcccac
Claudin-5	tgctgtgcgtggtgcagagt	tgctaccgctgccttaactgg
Occludin	gtgaatggcaagcgatcatacc	tgctgaagtcacacactca
Glut-1	tcgtcgtggcatccttattg	gtagcagggtgggatgaaga
β-Catenin	gagcacatcaggacaccaac	ggtgtgaacgtcccagcaag

## 6.5 Antibodies

### 6.5.1 Primary antibodies

Table 6-23: Antibodies for immunohistochemical analysis

Name of antibody	Stains for	Company	Dilution factor	Catalog number
CD31	blood vessels	BD	1:100	550274
desmin	pericytes	Dako	1:200	M0760
aquaporin-4	astrocytes	Millipore	1:200	AB2218

Table 6-24: Antibodies for Western Blot analysis

Name of antibody	Company	Dilution factor	Catalog number
$\alpha$ -tubulin	Sigma-Aldrich	1:500	T6199
pVE-Cadherin	abcam	1:1000	ab27776
VE-Cadherin	Santa Cruz	1:1000	sc-6458
Claudin-5	Invitrogen	1:500	35-2500
$\beta$ -Catenin	BD	1:500	610154
pTie2	R&D	1:400	AF2720
Tie2	R&D	1:500	AF762
Caveolin-1	Santa Cruz	1:500	sc-894
$\beta$ -actin	Santa Cruz	1:1000	sc-69879
Ang-2	abcam	1:1000	155106
pAkt	Cell Signaling	1:1000	4060S
Akt	Cell Signaling	1:1000	9272S
Glut-1	See reference (Devraj 2011)	1:1000	not applicable

Table 6-25: Antibodies for FACS analysis

Name of antibody	Fluorescence	Company	Catalog number
F4/80	FITC	eBioscience	11-4801-82
Gr1	APC780	BD	557661

### 6.5.2 Secondary antibodies

Table 6-26: Secondary antibodies

Name of antibody	Source	Company	Application	Dilution factor	Catalog number
$\alpha$ -rat alexa fluor 488	goat	Invitrogen	IF	1:200	A11006
$\alpha$ -mouse alexa fluor 568	goat	Invitrogen	IF	1:200	A11031
$\alpha$ -rabbit alexa fluor 568	goat	Invitrogen	IF	1:200	A11036
$\alpha$ -rat biotin	goat	Dianova	IHC	1:200	712-065-153
$\alpha$ -mouse alexa fluor 568	donkey	Invitrogen	WB	1:2000	A10037
$\alpha$ -goat alexa fluor 800	donkey	LI-COR	WB	1:3000	925-32214
$\alpha$ -rabbit HRP	donkey	Santa Cruz	WB	1:3000	sc-2313
a-mouse alexa fluor 700	donkey	Biomol	WB	1:2000	610-730-002
a-mouse HRP	donkey	Santa Cruz	WB	1:3000	sc-2318

### 6.6 Recombinant proteins

Product	Company	Catalog Number
human Ang-1	R&D systems	923-AN
human Ang-2	R&D systems	623-AN



## 6.7 Kits

Table 6-27: Kits used during this study

Kit	Company	Catalog number
Peroxidase substrate Kit AEC	Vector Labs	SK4200
Vectastain ABC Kit	Vector Labs	PK6100
RNeasy Plus Micro Kit (50)	Qiagen	74034
RevertAid H Minus First Strand cDNA synthesis Kit	Thermo Scientific	K1632
Pierce BCA Protein Assay Kit	Thermo Scientific	23225
DC Protein Assay	Bio-Rad	500-0116
Murine Ang-1 ELISA	MyBioSource	MBS266570
Human Ang-2 ELISA	R&D systems	DANG20

## 6.8 Software

Table 6-28: Softwares which were used for analysis and quantitation

Software	Used for	Version	Company
NIS Elements	Images	4.10.01	Nikon
CFX Manager	qPCR	3.1	Bio-Rad
Image Studio	Western Blot analysis	3.1	LI-COR
GraphPad Prism	Graphs; statistical analysis	5.01	Prism
cellZscope	TEER measurement	2.2.2	NanoAnalytics
FlowJo	FACS analysis	8.8.7	FlowJo, LLC
ImageJ	Stroke area	1.48	-

## **DANKSAGUNG**

Da eine wissenschaftliche Arbeit nie von einer Person alleine ausgeführt wird, möchte ich an dieser Stelle die Gelegenheit nutzen, mich bei denjenigen zu bedanken, die zu dieser Dissertation beigetragen haben.

Zunächst bedanke ich mich beim Direktor des Edinger Instituts, Prof. Dr. Karl H. Plate, der mir die Möglichkeit gegeben hat an diesem spannenden Thema arbeiten zu können und mich bei der Ausführung des Manuskripts für eine Fachzeitschrift und für die Dissertation gefördert und unterstützt hat. Konstruktive und zielführende Diskussionen, zusammen mit meiner Betreuerin Dr. med. habil. Yvonne Reiss, haben zur erfolgreichen Ausarbeitung meiner Arbeit geführt.

Außerdem gilt ein großer Dank an Frau Prof. Dr. Anna-Starzinski-Powitz, die als interne Fach-Betreuerin der Goethe-Universität Frankfurt für die Begutachtung meiner Arbeit fungiert, obwohl sie als Prodekanin viel beschäftigt ist.

Bei meiner Gruppenleiterin Dr. med. habil. Yvonne Reiss möchte ich mich besonders für die freie Entfaltung innerhalb ihrer Arbeitsgruppe bedanken, die mich stets bei Planungen und Durchführungen von Experimenten unterstützt hat und Kollaborationen zu anderen Arbeitsgruppen vermittelte. Dadurch konnte ich an einem internationalen Meeting in den USA teilnehmen, das mir neue Blickpunkte für meine Arbeit aufzeigte.

Zu den Kollaborationspartnern gehört Dr. Kavi Devraj, dem ich verdanke, dass mit seinem wissenschaftlichen und thematischen Wissen viele Gedankengänge in die Arbeit eingeflossen sind.

Andere Kollaborationspartner trugen zur Ausarbeitung teils komplexer Versuche bei, bei denen ich mich recht herzlich bedanken möchte. Dazu gehören: Prof. Dr. Michel Mittelbronn für die Analyse der humanen Schlaganfall-Proben, Prof. Dr. Christian Förch für das zur Verfügung stellen von Blutserum Proben von Schlaganfall-Patienten, Julia Starke und Dr. Heike Beck für die Durchführung des permanenten Schlaganfall-Modells, wobei Julia Starke auch zur Auswertung der Daten beitrug, Dr. Maiko Yamaji für die Ausführung von Western Blots und den Austausch wissenschaftlicher Expertise, Jadranka Macas für die Erstellung und Erklärungen der elektronen-mikroskopischen Aufnahmen, Dr. Mariangela DiTacchio für FACS Analysen, sowie Rajkumar Vutukuri und

PD Dr. Waltraud Pfeilschifter für die Durchführung und Expertise des transienten Schlaganfalls.

Weiterhin möchte ich mich bei meinen Arbeitskollegen für die gute Zusammenarbeit und freundliche, sowie angenehme Atmosphäre während der Arbeit bedanken. Kathleen Sommer, unsere technische Assistentin, hat mich in den Anfängen meiner Doktorarbeit sehr gut unterstützt und darüber hinaus bei vielen Experimenten Hilfestellungen geleistet. Bei Stefanie Jesgarek möchte ich mich besonders für die Betreuung der Maustierlisten, sowie für die Durchführung von Genotypisierungen und immunhistochemischen Färbungen bedanken. Stephanie Gelhardt danke ich für die bedeutende Betreuung der Mausezucht in der Zentralen Forschungseinheit, Frankfurt. Burak Yalcin, Nicole Ziegler, Jenny Zinke und Sonja Thom standen mir bei zahlreichen Fragen zur Seite.

Ohne einen starken Rückhalt und Unterstützung meiner Familie wäre die Ausarbeitung dieser Arbeit gar nicht möglich gewesen. Besonderen Dank und Anerkennung möchte ich daher meinen Eltern, meinem Bruder und meinem geliebten Freund widmen. Sie haben dieses Werk in allen Phasen mit jeglicher Unterstützung bedacht.

## ERKLÄRUNG

Ich erkläre hiermit, dass ich mich bisher keiner Doktorprüfung im Mathematisch-Naturwissenschaftlichen Bereich unterzogen habe.

Frankfurt am Main, den .....

.....

(Unterschrift)

## VERSICHERUNG

Ich erkläre hiermit, dass ich die vorgelegte Dissertation über

**„Angiopoietin-2 induced blood-brain barrier compromise and increased stroke is rescued by targeting vascular endothelial protein tyrosine phosphatase“**

selbständig angefertigt und mich anderer Hilfsmittel als der in ihr angegebenen nicht bedient habe, insbesondere, dass alle Entlehnungen aus anderen Schriften mit Angabe der betreffenden Schrift gekennzeichnet sind.

Ich versichere, die Grundsätze der guten wissenschaftlichen Praxis beachtet, und nicht die Hilfe einer kommerziellen Promotionsvermittlung in Anspruch genommen zu haben.

Frankfurt am Main, den .....

.....

(Unterschrift)

## CURRICULUM VITAE

### PERSONAL DETAILS

Name: **Stefanie Gurnik**  
Date and place of birth: 19th June 1987 in  
Nürnberg, Germany  
Nationality: German  
Present position: PhD student  
Present address: Institute of Neurology / Edinger Institute  
Neuroscience Center, Building 89  
Goethe University, School of Medicine  
Heinrich-Hoffmann-Str. 7  
60528 Frankfurt, Germany  
Telephone No: +49 (0) 69 6301 84161  
Fax No: +49 (0) 69 6301 84149  
E-Mail: stefanie.gurnik@kgu.de



### EDUCATION

12/2011 - 2015 (expected) **Postgraduate Study in Biology**  
Goethe University, Frankfurt am Main, Germany  
10/2008 – 09/2011 **Degree in Biology – Diploma in molecular biology**  
**Graduation grade: 1.2**  
Study of Biology  
Goethe University, Frankfurt am Main, Germany  
Final examination: forensic biology, cell biology,  
genetics  
10/2006 – 07/2008 **Pre-Diploma**  
**Graduation grade: 2.2**  
Study of Biology  
Goethe University, Frankfurt am Main, Germany  
07/2006 **Abitur / A-Level**  
**Graduation grade: 2.3**  
Oswald-von-Nell-Breuning-Schule, Rödermark,  
Germany

## PROFESSIONAL EXPERIENCE

- 12/2011 - 2015 (expected)      **PhD Thesis**  
**Institute for Neurology (Edinger Institute)**  
Johann Wolfgang Goethe University Medical School  
Frankfurt am Main, Germany.  
Supervisor: Prof. Dr. Karl-Heinz Plate / Dr. med. habil.  
Yvonne Reiss, Prof. Dr. Anna Starzinski-Powitz  
Topic:  
  - *“Angiopoietin-2 induced blood-brain barrier compromise and increased stroke size is rescued by targeting vascular endothelial protein tyrosine phosphatase”*
- 01/2011 - 09/2011      **Diploma Thesis**  
**Chemotherapeutic Research Institute Georg-Speyer-House, Institute for Tumor Biology and Experimental Therapy**  
Frankfurt am Main, Germany  
Supervisor: PD Dr. Martin Zörnig, Prof. Dr. Enrico Schleiff  
Topic:  
  - *“Analysis of the role of the anti-apoptotic protein Aven in DNA damage response “*
- 01/2010 - 02/2010      **Genetics - Group of Prof. Dr. Anna Starzinski-Powitz,**  
**Institute for Cellular Biology and Genetics,**  
Frankfurt am Main, Germany
- 09/2009 - 10/2010      **Forensic Biology - Group of Dr. Richard Zehner,**  
**Center of Forensic Medicine, Entomology,**  
Frankfurt am Main, Germany
- 07/2009 - 08/2009      **Forensic Biology - Group of Dr. Esther Reuss,**  
**Center of Forensic Medicine, DNA analysis,**  
Frankfurt am Main, Germany
- 04/2009 - 05/2009      **Cell Biology - Group of Prof. Dr. Enrico Schleiff**  
**Institute of Molecular cell biology of plants**  
Frankfurt am Main, Germany

11/2008 - 12/2008                      **Immunology - Group of Dr. Zoe Waibler,  
Paul-Ehrlich-Institut (PEI) - Institution of the  
Federal Republic of Germany**  
Langen, Germany

**CONFERENCES / PRESENTATIONS**

5<sup>th</sup>.09/2014                              **6<sup>th</sup> UCT science day**  
Frankfurt University, Germany

15<sup>th</sup> – 20<sup>th</sup>.06/2014                      **Barriers of the CNS (GRS), Gordon Research  
Conference**  
New London, NH, United States  
Poster: “The interference of Angiopoietin signaling in  
Blood-brain barrier properties”

14<sup>th</sup> – 15<sup>th</sup>.06/2014                      **Barriers of the CNS (GRS), Gordon Research  
Seminar**  
New London, NH, United States  
Talk: “The interference of Angiopoietin signaling in  
Blood-brain barrier properties”

6<sup>th</sup>.09/2013                                **5<sup>th</sup> UCT science day**  
Frankfurt University, Germany

15<sup>th</sup> – 18<sup>th</sup>.09/2012                      **7<sup>th</sup> Kloster Seon Angiogenesis Meeting**  
Seebruck, Germany

02<sup>nd</sup> – 05<sup>th</sup>.06/2012                      **International Vascular Biology Meeting**  
Wiesbaden, Germany